Technical Report 243/91

SALTS

in

POROUS BUILDING MATERIALS

CARSTEN BREDAHL NIELSEN

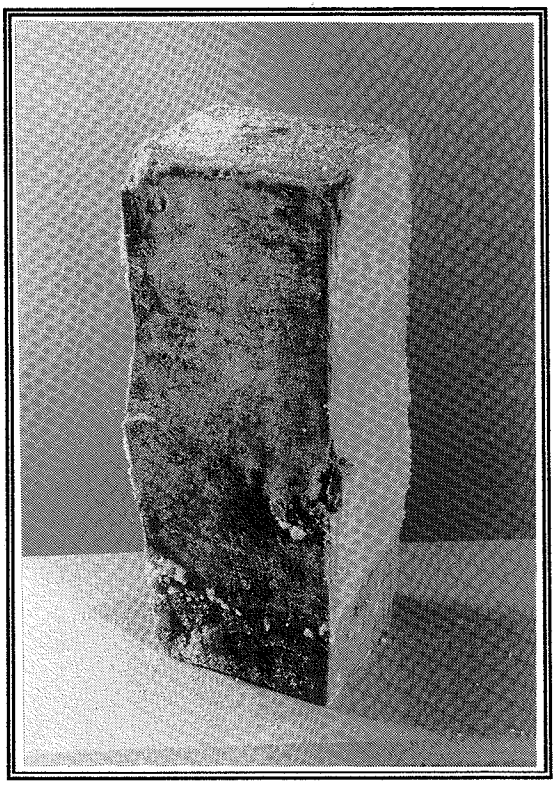

BUILDING MATERIALS LABORATORY
THE TECHNICAL UNIVERSITY OF DENMARK · 1991

Carsten Bredahl Nielsen
Salts in Porous Building Materials
August 1991
LBM, DTH, Technical Report 243/91

Front picture: NaCl-efflorescence on sandstone with crust

CONTENTS

PREFACE

Decay of stone in historic buildings and monuments seems to have accelerated in the latest fifty years and our cultural inheritance seems to crumble away. The main reason for this is the contents of salts in the porous material in connection with moisture and temperature changes. To stop or just retard deterioration it is necessary to know and understand the processes behind salt action so that the right preservation can be given.

This is the objective of the present work. From an engineering point of view it presents the results of three years work in this field by the author and contains theoretical and experimental work on moisture and salt transport, material structure, shrinkage and swelling and extraction of salts. Chapter 1, 2 and 3 presents the theoretical background. In chapter 4 structure investigations are described and in chapter 5 and 6 results from experimental work are presented and compared to the theoretical background.

This work serves as partial fulfilment of the requirements for obtaining the degree of Ph.D. at the Technical University of Denmark. The work was carried out at the Building Materials Laboratory at the Technical University of Denmark under the guidance of docent, tekn.dr. Anders Nielsen.

Copenhagen, August 1991

Carsten Bredahl Nielsen

SUMMARY

The present report deals with decay mechanisms in porous building materials due to salts. A new theory to estimate the effect of changing climate on saline structures is proposed and experimentally verified. The study is concentrated on three subjects

- Equilibrium state of salt and moisture in the pores
- Moisture and salt movement in structures
- Hygroscopic length changes of saline materials

Decay mechanisms are summarized. A short review of building stone and brick composition are given and moisture related properties of salts are described. Sorption isotherms and capillary suction are measured for saline materials. Extraction of salts from brick is carried out both in laboratory and on large-scale from church vaults. Accelerated weathering of small brick walls containing salt are compared to natural weathering.

The deliquescence point in a hygroscopic material with low salt content is below saturation humidity over a free salt solution, and moisture content in a saline material is higher than in a salt free material, even below the deliquescence point. Salts are observed to decrease capillary suction and evaporation in a porous material.

Theoretical models to calculate moisture and salt transport in structures and hygroscopic shrinkage and swelling of saline materials are proposed. Calculated transport of moisture and salt in brick and sandstone agree with observations from capillary suction experiments and large-scale extraction of chlorides in a brick church vault. Calculations give a reasonable estimate for strain in the hygroscopic range but seems to underestimate strain in the over hygroscopic range. The course of strain rather than the overall magnitude of strain is changed by salts.

Micro structure analysis using digital image processing on images of polished sections are carried out to determine pore size distributions for brick, sandstone and lime mortar. Although not complete comparable Mercury Intrusion Porosimetry and digital image processeing seems to complement each other, especially for materials with two distinct pore size ranges.

Decay of hygroscopic, porous materials by salts might be caused by differences in hygroscopic movement due to increased shrinkage at relative humidities close to the deliquescence point of the salt. The increase depends on hygroscopicity of the material. This might explain why a hygroscopic brick decay contrary to a less hygroscopic brick as observed in the vaults in Alslev church.

Measured chloride content in a vault in Odden church shows that approximately one fourth of the original chloride content is extracted in 6 months by a 35 mm lime mortar layer on top of the vault. Calculations indicate that salts are extracted much more efficiently by capillary suction from one side and collecting salts in a mortar layer on the other side of the vault. It seems possible to extract salts hygroscopically by maintaining a high relative humidity on one side of the vault and a low relative humidity on the other side.

SAMMENFATNING

Nærværende rapport behandler saltes forvitring af porøse bygningsmaterialer. En ny teori til vurdering af klimaets indvirkning på saltholdige materialer i konstruktioner foreslås og eftervises eksperimentelt. Rapporten er koncentreret om tre emner

- Ligevægts tilstanden for salt og fugt i porerne
- Fugt- og saltbevægelser i konstruktioner
- Hygroskopiske længdeændringer af saltholdige materialer

Nebrydningsmekanismerne beskrives. Der gives et kort sammendrag af tegls og naturstens opbygning, og saltes fugttekniske egenskaber beskrives. Sorptionsisotermer og kapillarsugning er målt for saltholdige materialer. Der er udført forsøg med udtrækning af salte i teglsten, både i laboratoriet og i fuldskala for kirkehvælvinger. Accelereret ældning af små teglmurværk med salt er sammenlignet med naturlig ældning.

Krystallisationspunktet i et hygroskopisk materiale med lavt saltindhold er lavere end mætningsdamptrykket over saltopløsningen, og fugtindholdet er højere end i et materiale uden salt, selv under krystallisationspunktet. Målinger viser, at salte formindsker kapillarsugning og fordampning i porøse materialer.

Der er opstillet teoretiske modeller til beregning af salt- og fugttransport i konstruktioner og til beregning af svind og svelning af saltholdige materialer. Beregnet fugt- og salttransport er i overensstemmelse med målinger ved kapillarsugning og ved udtrækning af salte i et kirkehvælv. Beregninger giver et rimeligt skøn for tøjninger i det hygroskopiske område, men undervurderer tøjninger i det over hygroskopiske område. Tøjningsforløbet snarere end størrelsen af tøjningen ændres af salte.

Der er foretaget strukturanalyser på planslib af tegl, sandsten og kalkmørtel med digital billedhehandling på billeder af planslib til bestemmelse af porestørrelsesfordelinger. Selv om metoderne ikke direkte kan sammenlignes, så supplerer kviksølv porøsimetri og digital billedbehandling hinanden, specielt for materialer med to adskilte porestørrelses intervaller.

Saltes forvitring af hygroskopiske, porøse materialer kan være forårsaget af forskelle i hygroskopiske bevægelser på grund af forøget svind ved relative fugtigheder tæt ved saltets krystallisationspunkt. Forøgelsen afhænger af, hvor hygroskopisk materialet er. Dette kan forklare, hvorfor en hygroskopisk teglsten forvitrer i modsætning til en mindre hygroskopisk teglsten, som det er iagttaget i kirkehvælvingerne i Alslev kirke.

Målinger af kloridindholdet i et hvælv i Odden kirke viser, at på 6 måneder er omkring en fjerdedel af det oprindelige kloridindhold blevet trukket ud i et 35 mm tykt kalkmørtellag på oversiden af hvælvet. Beregninger viser, at salte kan udtrækkes mere effektivt med kapillarsugning fra den ene side og opsamling af saltene i et mørtellag på den anden side af hvælvet. Ved at opretholde en høj relativ fugtighed på den ene side af hvælvet og en lav relativ fugtighed på den anden side ser det ud til, at salte kan udtrækkes hygroskopisk.

1. INTRODUCTION

1.1 SCOPE OF THE PRESENT REPORT

The scope of the present repport is to study the decay mechamisms of porous building materials by salts. This study includes

- structure and composition of porous materials
- properties of salts
- moisture and salt transport
- shrinkage and swelling of saline porous materials
- extraction of salts from porous materials

For this purpose a test program was set up

- to list moisture related salt properties
- to develop a theoretical model to calculate moisture and salt transport in porous materials
- to develop a theoretical model to calculate capillary shrinkage and swelling of porous materials
- to find a methodology to describe pore structure using digital image processing
- to test the influence of salts on adsorption and capillary suction of brick and sandstone
- to test large-scale salt extraction from a medieval brick church vault
- to test the influence of salts on shrinkage and swelling of brick and sandstone

1.2 DETERIORATION OF BUILDING MATERIALS

The presence of salts in porous building materials causes decay of the material. The decay is a result of various factors affecting the material; atmosphere (temperature, humidity, pollutants), rainwater, plants, bacteria, animals, humans. The decay is closely related to the geologic process of rock weathering. The process of weathering is merely the adjustment, or readjustment of minerals and rocks to conditions at the earth's surface, by conversion of existing minerals to minerals of higher stability towards the asmosphere. The presence of oxygen leads to oxidation, the presence of moisture to hydration or to solution and simultaneous with frost moisture leads to rupture of the stone.

Decay is a complex interaction of different mechanisms, and therefore in each case it is difficult to establish which is the most important. Often in a scientific test programme it is not possible to distinguish between decay by frost and decay by salt, which makes the interpretation of the results difficult. Therefore in this work only decay by salts is regarded and temperatures below zero are avoided.

It seems, that decay is accelerating strongly these years. The weathering damage the first 300-500 years of a certain material may be relatively mild compared with that in the last 50 years. This can bee seen as a natural accelerating decaying progress regarding it as the course of nature without any possibility for man to intervene. Depending on the structure of the material the decaying process may be slow as a geological process, but it may be rapid enough to cause damage in less than a generation. A speciel problem arises when the original material is poor and therefore not suitable for building constructions. The urban atmosphere of the twentieth century creates special environmental problems to exposed stone surfaces and can accelerate the process of weathering to many times that of natural rural environs. But trying to understand the decay mechanisms it may be possible to prolong lifetime of materials particularly in special exposed places and in places where it may be impossible to re-create the structural element as for statues and ornamental elements.

Below is given a survey of the existing theories of salt decay. It is a review from litterature among others given by Winkler (1973), Knöfel et al (1987) and Kiessl (1989). It may not be complete, but represents what the author regards as important.

Weathering agents

The atmosphere is a reservoir of aggressive impurities such as H_2O, SO_2, SO_3, NO_2, CO_2, Cl_2 etc. These eventually settle out on the stone surface as aerosols and react with stone in aqueous solution. Aerosols comprise sizes ranging from molecules to raindrops. Some of the ingredients, e.g. the sulfate and the chloride, may be added from vast natural sources, the oceans and salt flats. The intensity of air pollution is reflected in the quantity of suspended matter which settles as soot or dust, or remains in suspension as aerosoles. The chemical attack on stone is due largely to the solvent action of water and its dissolved impurities, including carbon dioxide and sulfates.

The composition of rainwater is closely related to the composition of the atmosphere. The strong corrosive action is based on the ions which are picked up during the travel through the atmosphere but there are contributions from local dust sources as well. The supply of chloride and sulfate is extensive near the sea shores and over industrial areas.

Devitofrancesco et al. (1987) has made observations on deposition velocities of aerosol particles on the surface of marble samples in laboratory experiments. They find that the aerosols of urban atmospheres are very hygroscopic because of the high content of substances like sulphuric acid, sulphates, nitrates, etc. The microdrops (2-20 μm) easily adhere to the material surface. The consequence of this is the formation of a light humid layer, which facilitates the subsequent adhesion of the substances dissolved in the microdrops. The

adsorption-condensation and the desorption-evaporation cycles are the chief cause of the decay of monuments and structures exposed to urban atmospheres. They find that the rain (liquid aerosol size 2-3 mm) action has to be considered nonexistent or quite negligible, except in the case of floor or horizontal surfaces, where it is possible the water remains for extended time.

Impurities in atmosphere and rainwater is carried into the material where they are accumulated throughout the years. Deterioration therefore may be caused by accumulated salts from previous air pollution. Even if air pollution was eliminated now, deterioration would still increase if no preservation was carried out.

Besides moisture from the atmosphere and rainwater, moisture is carried into the structure from ground water, leaking pipes and gutters, from the use of the building (kitchen and bathroom, moisture from humans) and construction moisture from new materials (repairs).

Disruptive effect of pure water

Winkler (1973) states that stone may be damaged by the disruptive force of pure water generated by the expansion by heating and he ascribes the spalling and surface flaking to the expansive action of pure water. In most cases it is hard to distinguish between this effect and frost damage. The disruption of stone by alternate wetting and drying *without change* of temperatures is long known and from experiments by Griggs, Winkler states, that it is the capillary moisture in the stone which causes flaking and bursting.

Crystallization pressure

When salts crystallize the solution has to be saturated or supersaturated. Due to equilibrium thermodynamics a pressure will be formed in the supersaturated solution. The crystallization pressure mainly depends on the degree of supersaturation. To obtain a pressure sufficient to disrupt building stone for most salts a degree of supersaturation of 10 is needed. In the pore system of a porous material the presence of supersaturation greater than two is unusual so the salt crystallization pressure is very low and may not cause decay of stone.

Hydration pressure

Some salts hydrate and dehydrate with changes in relative humidity. By the absorption of water the molar volume of the salt increases and the hydration pressure acting against the pore walls can be calculated. Hydration pressures sufficient to disrupt building stone can be calculated for Na_2SO_4 and $MgSO_4$, and the hydration pressure is used to explain the destruction of materials in the Na_2SO_4 test. The transformation from an anhydrous state into a hydrated state lasts only some minutes for the two salts, and therefore they are very aggressive. But these calculations are theoretical under idealized conditions of closed-pore systems and a full evaluation of the behaviour of salts in very narrow capillaries is very

difficult. Konow (1989) states that the assumptions for the salt crystallization and hydration theory is not valid in practice, and concludes that theese theories are not a satisfactory explanation of the decay of materials. The author agrees with her.

Humidity dependent salt recrystallization pressure

Pühringer (1983) has observed that particular salts vary their crystal shape depending on the relative humidity. These observations are in aggrement with what is found by Arnold and Zehnder (1988) and Konow (1989). These changes may exert a stress on the pore walls but, as for crystallization pressure and hydration pressure, it is very difficult to evaluate the behaviour in very narrow capillaries. Konow (1989) states that salt decay is a surface phenomenon as the deterioration always starts from the surface. She observed that the salt structure on the surface changed with relative humidity and that shrinkage and expansion of the salt structure tore small pieces of brick from the surface.

Thermal expansion

Deterioration of stone may take place due to differences in thermal expansion of entrapped crystallized salt and the surrounding porous material. Larsen and Nielsen (1990) found that thermal expansion coefficient was increased by 16% for dry brick with a NaCl content of 2 wt%. Differences in salt content through a porous material may give rise to shear forces between the exposed surface and the interior of the material.

Hygric expansion

Water vapour sorption and the uptake of capillary water cause swelling of a porous material. In bricks the swelling is influenced by the mineral composition. Salts influence the water uptake and swelling and differences in salt- and moisture content through the material may give rise to shear forces between the exposed surface and the interior of the material.

Clay mineral swelling

Mineral grains of especially sandstones can be coated with a thin layer of clay minerals. Knöffel et al. (1987) states that the swelling of clays is mainly caused by montmorillonites. These clay particles have a very small grain size and therefore a very high specific surface area. The silicate layers reveals a negative surface charge that is balanced by counter-ions of the surrounding solution. The negative charge determines the cation exchange and the swelling. The swelling itself is caused by the uptake of water between the silicate sheets. Swelling of surface layers can cause flaking as for hygric expansion in general.

Osmotic pressure

Osmosis of salts through a solid occurs when a solution is separated from its pure solvent by a semi-permeable membrane. The pure solvent attempts to enter and dilute the solution through the semi-permeable membrane whereby an somotic pressure develops against the walls. Winkler (1973) suggests that adsorbed water or ions held tightly on mineral surfaces (clay) can act as membrane. Suction occurs towards areas of high ionic concentration, but the source for osmotic pressures is difficult to assess, as the various factors, which lead to osmosis, overlap. Therefore, the author does not find the theory convincing.

Chemical weathering

The chemical weathering can be divided into simple solution of the minerals by water or acid as for carbonates and sulfates and weathering by solubilization of silicate rocks.

The solution rate depends on the concentration of the solvent, the solubility of the salt and on solvent motion (transport). The solution of the mineral substance is influenced either by temperature only, as with gypsum or by temperature and the pH of the solvent, as for carbonates. All carbonate minerals are influenced by the amount of CO_2 present in the solvent. Quartz, pyrite and mica flakes are insoluble components of many carbonate rock. As the cementing carbonate is disolved the insoluble grains remains leaving the material weak and crumbled with relief. This can be observed on calcareous sandstone where the material surface becomes loose and sandy. In limestone and limestone-marble weathering is observed along clay fillings in veins.

Vale and Martín (1986) has observed deteriorations of sandstone (79.4% SiO_2, 7.4% CaO) and calcareous stone (18.5% SiO_2, 43.8% CaO) in simulated atmospheres containing SO_2 at various humidities. They found that for sandstone SO_2 did not cause reactions with the compounds of the original material either as a gas or in the form of sulphuric acid. For calcareous stone they found that with SO_2 under saturation conditions gypsum crystals of significant size was formed on numerous discrete areas of the sample surfaces. Under the same conditions, but with cycles of humidity and with intermediate rain, the gypsum crystals disappear completely from the surface, to be replaced by cavities which appear to be the result of the dissolution of the microcrystalline grains of calcium carbonate.

Silicate minerals consists of more or less tight crystal lattices into which the metal cations Ca, Na, K, Mg and others are built in. Leaching (solubilization) can unlock and free the ions. Winkler (1973) describes the process as H^+ ions penetrating the mineral surface and breaking down the silicate structure in three simultaneous steps

1) The parent mineral breaks down with the release of cations and silica, whereby silica in the silicate may either retain its original atomic arrangement or enter the dispersed state.
2) Metal alkalies are removed by solubilization as a result of the breakdown.

3) Reconstitution of the residue may form new minerals from components of the atmosphere which are in a stable or metastable equilibrium with the present environment. The entry of the water molecules takes place into spaces left vacant after leached metal cations (hydrolysis). The process leads to the formation of clays. Kaolinite appears to be the most important clay mineral product of stone weathering when much rain is present with intense leaching and removal of Ca, Mg, Fe, Na, K and some silica under oxidizing conditions.

Konow (1989) has observed solubilization for bricks immersed in different salt solutions for 9 months. Especially 10 wt% NaOH solution was aggressive in average disolving 2-7 wt% SiO_2 and 4 wt% sodium ions. An increase in the content of feldspars was observed but the change in mineral composition was in average small. Even for pure water a slight deterioration was observed.

Formation of crusts on sandstones

Kiessl (1989) describes the formation of crusts on sandstones. Several layers with different properties are formed parallel to the surface of the stone. The outermost layer, the socalled accumulation layer, consitst of dust, dirt, salt efflorescence and biological matter. Below is a layer consisting of former surface, phase exchange products and precipitated salts and behind that a weakened zone containing salts with the calcite binder washed away. Hindmost is the original solid stone. The formation of crust is described in 4 steps by Searls and Thomasen (1991)

1) Sulphate containing water enters the stone, dissolves calcite binder and changes calcite to gypsum.
2) Gypsum is deposited near surface as water evaporates and forms surface crust.
3) The zone behind crust is weakened as calcite binder is washed away. This results in blind exfoliation (loosely attached crust).
4) Surface spalls as gypsum and clays expand through wet/dry cycles.

Kiessl (1989) has measured the profiles of different properties of the sandstone including water vapour conductivity, water uptake coefficient, hygroscopic water uptake, salt content, tensile strength, modulus of elasticity and heat and moisture deformations. For the crust he finds that water vapour conductivity decreases, hygroscopic water uptake and hygroscopic deformations increases, due to the increasing salt content, and tensile strengt decreases. For the remaining properties both increases and decreases are found.

The change in properties is used to explain exfoliation of the crust. Deformations of the surface crust exposed to heat and moisture cycles is different from the underlying solid material resulting in the formation of cracks. Cracks allow more water to enter the stone and this accelerates the process and forms blind exfoliation (bubbles of loose attached crust). Evaporation behind the crust bubble is hindered, the material remains wet and moisture accumulates. This increases the solution of the cementing matrix in the weakened zone and the risk of frost damage.

As long as the crust is entire without cracks it merely protects the underlaying stone from weathering as it is quite tight but as soon as cracks arise the crust only makes things worse because water easily penetrates the surface through the cracks and accumulates in the structure due to hindered evaporation.

A special case of sandstone deterioration is seen on places protected against the climate (rain and sun) of structural elements as cornices and ornamental elements. The weathering side is exposed to rain and sun, salts are washed out and the material are dried out quickly. Salts are washed to the side protected against climate, salts and moisture are accumulated and for this reason deterioration is concentrated here.

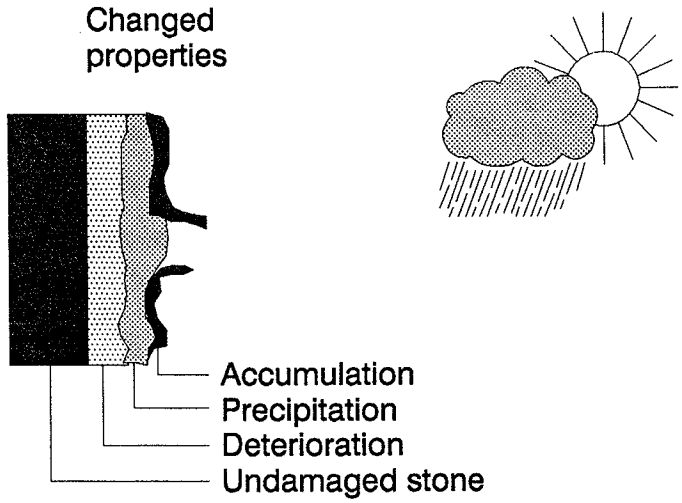

Figure 1.1. *Formation of crust on sandstone by weathering.*

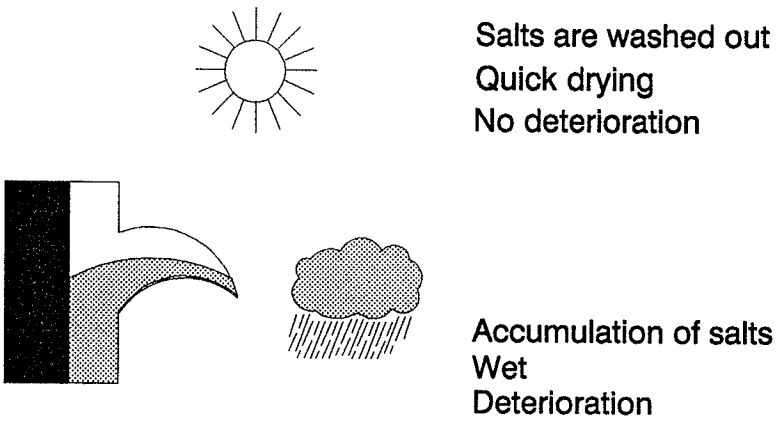

Figure 1.2. *Deterioration on places protected against the climate.*

2. PROPERTIES OF STONE AND SALT

To understand the mechanisms of stone deterioration by salts it is necessary separately to look at the properties of stone and salt, and then combine theese properties in a reasonable way to find the effects of moisture on saline materials. The separate properties are well described in litterature, and in section 2.1 and 2.2 below are given a survey. In section 2.3 a thesis to find the moisture content in a *saline material* in equilibrium at a given relative humidity is proposed. This thesis is the basis for calculations of moisture adsorption, salt and moisture transport and volume changes by adsorption of moisture. The thesis therefore is decisive for calculated results given in this work.

2.1 BUILDING STONE

The description of building stone and brick below is taken from Winkler (1973) and Livingston (1988) and summarizes important properties. The desciption is not complete but gives a broad review as an introduction to the experimental part of the thesis.

Classification

Rocks are classified into three major groups based on their origin

1) **Igneous rocks** are primarily crystallized from a fiery fluid silicate melt, either deep below the earth's surface or at the surface. Texture and fabric of these rocks depend on their environment during crystallization . Granite, gabbro, basalt, porphyry and others belong to this group.

2) **Sedimentary rocks**, or layered rocks, are formed by the concentration of debris of variable size and shape deposited by mechanical means or by precipitation, or by accumulation of organic skeletons and shells. Conglomerate, sandstone, shale, limestone marble, dolomite, travertine and onyx marble are common sedimentary rocks.

3) **Metamorphic rocks** are derived either from igneous or sedimentary rocks recrystallized by the effect of pressure and temperature. Important rocks of this group are gneiss, slate, marble and crystalline quartzite.

Mineral composition, texture, structure and color, are important characteristics of rocks. Rock properties depend on the physical and chemical characteristics of the minerals to a large extent. Texture characterizes the grain sizes, shapes and grain contact. Texture differ greatly among the three major rock groups. Below is classification of sedimentary rocks discussed in more detail because sandstone is used in the experimental work in this thesis and because sedimentary rocks are the most porous amongst rocks, and therefore to a larger extend are exposed to physical deterioration by the action of water and salts.

Sedimentary rocks

Sedimentary rocks are formed either by the accumulation of rock and soil material by streams, waves or wind, or as organic accumulations and chemical precipitates. A flat, layered structure is an important characteristic of sedimentary deposits, known as bedding or stratification. The physical properties of sedimentary rocks depend primarily on mineral composition, texture, structure, and on the cement between the fragments.

Sedimentary rocks are generally classified as

a) clastic sediments, coarse to fine grained: residual rock fragments produced through rock disintegration, result in various sizes and shapes

b) clastic sediments, fine to submicroscopic: residual silt and clay-sized particles form the weathering end product of mostly feldspars and some quartz

c) organic sediments: the remains or products of animals and plants: many limestones, limestone-marbles and dolomites belong to this group of rocks.

d) chemical precipitates: precipitation from ocean waters and brines lead to some limestones, dolostones (dolomites), gypsumrock, saltrock.

Mineral composition

Most minerals in clastic sediments were inherited from primary igneous rocks or from previosly existing sedimentary or methamorphic rocks. The minerals found in sedimentary rocks are quartz, carbonate, feldspars, fero-magnesium silicates and mica. Textures consists of sorting, shape, packing and orientation of grains. The grains can be cemented either in points of contact or in the interstices between the grains. The cementing minerals are siliceous cement, carbonate cement, ferric oxide and ferric hydroxide and clayey cement. Siliceous cement forms rock with high strength, carbonate cement are weaker and ferric oxide and ferric hydroxide are poor. Clayey cement may be sound in dry climate but very poor in humid climate.

Table 2.1. *Solid density, porosity and elasticity of common rocks. Winkler (1973).*

Rock	Solid density [kg/m^3]	Porosity [m^3/m^3]	Elasticity [GPa]
Granite	2600 - 2700	0.005 - 0.015	20 - 60
Basalt	2800 - 2900	0.001 - 0.01	60 - 100
Sandstone	2000 - 2600	0.05 - 0.25	3 - 80
Shale	2000 - 2400	0.10 - 0.30	10 - 35
Limestone	2200 - 2600	0.05 - 0.20	10 - 80
Dolomite	2500 - 2600	0.01 - 0.05	40 - 840
Marble	2600 - 2700	0.005 - 0.02	75 - 85

Brickmaking

Making brick today is a highly industrialized process in contrast to traditional handmoulded brick. Raw materials, shaping techniques and firing cycles differ greatly. In restoring work the knowledge of old brickmaking teckniques is important both if similar bricks with the same appearance are going to replace the old bricks and if the original bricks are going to be preserved. The description below is taken from Livingston (1988), who applies geochemical methods to explain the traditional brickmaking, and Konow (1989).

Making brick by handmoulding depended intirely on manual labor, from quarrying the raw material through forming the brick to firing it. Each individual brick was shaped by hand, stacked for drying and then restacked in the kiln for firing, after which the stack was taken down and sorted according to quality, brick by brick. The process to add significant amounts of water, which then is removed again by drying or in the firing process is known as the soft mud process.

Raw material

The raw material for brickmaking is clay or shale. Clay is a soft but plastic material. Shale is hard and rocklike but when ground and mixed with water it reverts to the consistency of clay. The most important minerals in clay are quartz sand grains, iron oxides and hydroxides and clay minerals. The most important clay minerals consists of kaolinite, smectite and illite. Smectite is expanding when wet in contrast to kaolinite and illite, which is not expandable. The iron minerals are most important as pigments in the clay and in the final brick. The red color is due to iron oxide in the form of hematite.

Table 2.2. *Chemical analysis of brick raw materials. Konow (1989). Livingston (1988). Nielsen and Trudsø (1978).*

Component	Finnish clay	London UK clay	Colonial Williamsburg clay	Danish clay (red bricks)
SiO_2	58.6	61.2	73.8	61.3
Al_2O_3	16.6	12.2	15.1	18.9
MgO	2.8	2.2	0.1	1.2
CaO	2.2	2.2	0.6	1.2
K_2O	3.3	3.0	2.2	1.6
Na_2O	2.7	0.7	0.7	1.6
Fe_2O_3	5.4	8.1	3.4	6.6
TiO_2	0.7	0.8	1.2	-

Moulding

The handmoulding process is limited by the amount of pressure that can be applied to the clay in the mould. A very stiff clay takes a great deal of effort to shape and after removal from the mould may shrink excessively or crack. Clays containing smectites are difficult to dry and are sticky to work and therefore are not used for handmoulded bricks. After moulding the bricks are dried either in a kiln or simply in the sun.

Firing

In the firing process, the objective is to partially melt the constitutents so that they fuse together (sintring), giving the brick its strength. In the traditional brick kiln, the highest practical temperature was in the range 1000 - 1100 °C, usually it was lower. The quartz grains will fuse together and the melt can produce crystals of mullite in the temperatur range 1050 - 1100 °C and crystals of feldspars. The minor constituents Na_2O, CaO and K_2O act as fluxes to lower the melting point of the mixture and react with Al_2O_3 and SiO_2 to form the feldspars. Upon cooling to room temperature, the melt may not completely crystallize but rather remain as a glass.

Each of the phases has a different coefficient of thermal expansion, which varies with temperature. As a result, in such a mixture it is possible to generate tensile stresses in the glass in the temperature range 300 - 600 °C. A rapid rate of cooling through this temperature range may thus result in microcracking in the glass phase which would lead to a less durable brick. The traditionel brickmakers were careful to cool down the killn slowly to avoid this. A calcium rich clay may produce a brick with a very different cooling stress pattern than a potassium rich. When the fired brick is affected by calcium or potassium ions from salts in pore liquids the stress pattern may change giving rise to expansions.

Pore structure

The pore structure of brick is mainly formed in the drying process of the clay. The rest of the latent water is liberated during firing, organic matter is burned and from clay minerals OH^- groups is liberated. While the melt is formed the grains are cemented, porosity decreases and the pores becomes coarser with increasing firing temperature. The brick shrinks about 5% in the drying phase and additionally during firing. Rich clay has a strong shrinkage and normally sand and saw dust is added to make the clay less rich. Due to content of fluxes in the clay, the range of firing temperatures may be very narrow. Small deviations in firing temperature may give large shrinkages during production of the brick.

2.2 PROPERTIES OF SALTS

Salts in brickwork are for a long time known and among others thoroughly described by Suenson (1942) and Arnold (1984). To understand the deterioration mechanisms in porous materials by salts it is necessary first to know some properties of different salts and salt solutions *outside* the porous material. Then in the next section the properties of salts *inside* the porous material are discussed.

Origin of salts

Salts in building materials come from 4 main sources

1) **Raw materials.** Clay used in brick manufacturing contains sulphates, sea sand used for mortar contains chlorides, natural stone can be contaminated with salts from grund-water in the quarry.

2) **Ground water.** Rising groundwater in solid walls carries salts into the construction, especially in cellars and vaults close to the soil.

3) **Use of the building.** Buildings can be used for storage of salts (salt pits). The use of thaw salts in streets and staircases carries salts into the construction.

4) **Air pollution.** The sulphur and nitrogen content of polluted air (acid rain) reacts chemically with components in building materials and form salts. In coastal regions sea salt can be disolved in the mist and be carried into the construction.

$$CaCO_3 \text{ (aragonite)} + H_2SO_4 \text{ (sulphuric acid)} + 2\ H_2O \rightarrow CaSO_4 \cdot 2\ H_2O \text{ (gypsum)} + CO_2 + H_2O$$

$$MgCO_3 \text{ (magnesite)} + H_2SO_4 \text{ (sulphuric acid)} + 7\ H_2O \rightarrow MgSO_4 \cdot 7\ H_2O \text{ (epsomite)} + CO_2 + H_2O$$

Common salts in building materials

In building materials exists a vast number of salts depending on the ions present and the ambiant climate. A review is given by Arnold (1984). Salts in building materials can be divided up into 4 main groups

1) **Sulphates** (raw materials, air pollution)
$MgSO_4 \cdot 7\ H_2O$, $CaSO_4 \cdot 2\ H_2O$ (gypsum), $Na_2SO_4 \cdot 10\ H_2O$

2) **Chlorides** (sea mist, deicing salts)
NaCl, $CaCl_2 \cdot 6\ H_2O$

3) **Nitrates** (ground water, air pollution)
$Mg(NO_3) \cdot 6\ H_2O$, $Ca(NO_3)_2 \cdot 4\ H_2O$, $3Ca(NO_3)_24NO_3 \cdot 10\ H_2O$

4) **Carbonates** (ground water, air pollution)
$Na_2CO_3 \cdot 10\ H_2O$, K_2CO_3, $CaCO_3$

Crystallization

Salts in a solution precipitate out when the concentration exceeds the solubility which takes place if relative humidity of the ambient air is below ϕ_s. The structure of the crystals formed depends on temperature and relative humidity during the drying phase and on how fast relative humidity and temperature changes. Pühringer (1983) states, that salt crystals are formed at the tip of a thin film of salt solution. The crystals are not ideal, solid crystals but forms a fine porous structure which is able to transport salt solution and adsorp water even below the deliquescence point. This explains the ability of salt solutions to climb on vertical glass plates when dried out.

Arnold and Zehnder (1988) describes the crystallization sequence at room temperature and relative humidity around 69 % of sodium nitrate on a porous substrate saturated with a saturated salt solution. They divide the crystallization into 4 phases with decreasing substrate humidity

Phase 1: Large crystals similar to equilibrium form grow immersed in the solution on a wet surface.

Phase 2: Granular crust of isometric crystals grow covered by a thick solution film on a strongly humid surface.

Phase 3: Fibrous crust of columnar crystals grow on a coherent solution film at the air on a moderately humid surface.

Phase 4: Efflorescence of whiskers grow on isolated spots of solution film on a slightly humid surface.

Konow (1989) has made crystallization tests on glass plates with Na_2CO_3, Na_2SO_4 and NaCl crystallized at ϕ=0.45 and ϕ=0.70 and then placed at three different relative humidities. She concludes that the size of the salt crystals decreases with relative humidity. At high relative humidity the crystals clot due to adsorption of moisture. The single crystals are very small, 2-5 μm for crystals dried over $CaCl_2$ and 30 μm for crystals placed at ϕ=0.95. No ideal crystals was observed. The crystals formed near the glas plate was closely packed and the crystals far from the glas plate was a very fine porous efflorescence with a large inner surface.

The crystals formed on the inner surfaces of the pores might be different due to differences in relative humidity in the pore system, but the formation of crystals from a salt film as observed by Zehnder and Arnold (1988) seems reasonable. Thus the crystals formed in a porous material depends on moisture content of the material (substrate humidity in the 4 phases, supply of liquid containing ions) and the ability of vapour transport in the surrounding pore system (relative humdity of the ambient air). In addition crystallization must be dependend on surface forces in narrow spaces between ions and pore surface.

In figure 2.1 is given an example of a halite crystal structure in a whisker found by Pühringer in a closed cellar vault. The crystals are grown as a continuous line of cubic crystals in the direction of the whisker growth. In this direction cylindrical pores are formed which is seen in a polished cross section in figure 2.2.

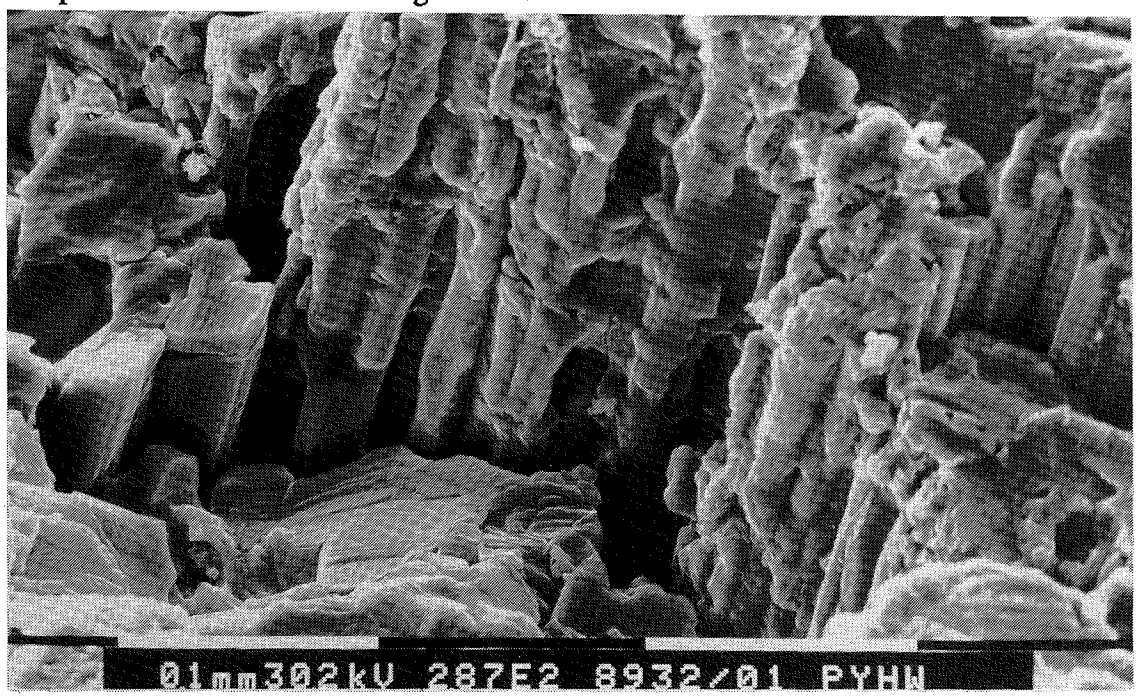

Figure 2.1. *Halite crystal structure in whisker found by Pühringer in a closed celler vault. Crystals are grown as a continuous line of cubic crystals in the direction of the whisker growth.*

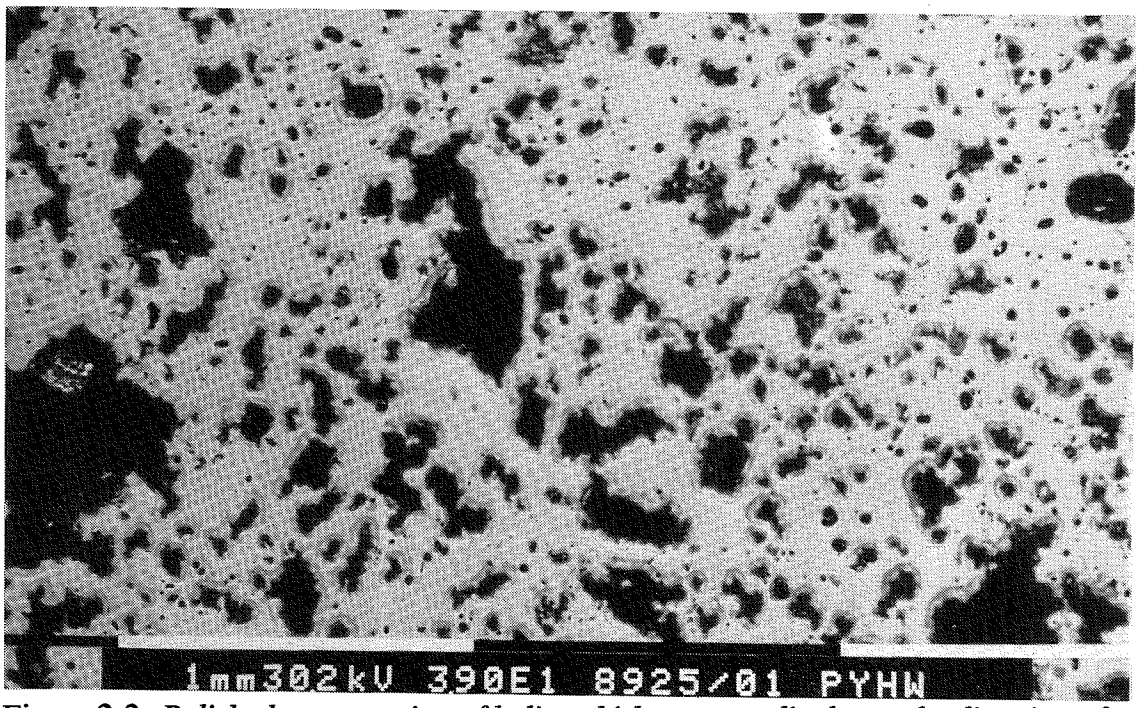

Figure 2.2. *Polished cross section of halite whisker perpendicular to the direction of growth. Cylindrical pores (dark areas) are formed in the direction of growth.*

Solubility and precipitation

Water soluble salts can only be disolved in a certain quantity denoted the solubility. Below this quantity the salt exists as ions in a solution and above the salt starts to crystallize. The solubility depends on salt type and temperature. Solubility covers a wide range from almost infinity (0.24 g/ 100 ml water) for $CaSO_4 \cdot 2\ H_2O$ up to larger quantities (167 g/100 ml water) for $MgCl_2 \cdot 6\ H_2O$. The solubility of NaCl is almost independent of temperature whereas solubility of $Na_2SO_4 \cdot 10\ H_2O$ strongly depends on temperature.

Table 2.3. *Solubility of different water soluble salts in g pr. 100 ml of water. CRC (1984).*

Salt		Cold water [g/100 ml]	Hot water [g/100 ml]
Gypsum	$CaSO_4 \cdot 2\ H_2O$	0.24	0.22
Mirabilite	$Na_2SO_4 \cdot 10\ H_2O$	11	92
Sylvite	KCl	35	57
Halite	NaCl	36	39
Epsomite	$MgSO_4 \cdot 7\ H_2O$	71	91
Bischofite	$MgCl_2 \cdot 6\ H_2O$	167	367
Calcium chloride	$CaCl_2 \cdot 6\ H_2O$	279	536

Hydrates

Some salts take up crystal water and chemically binds it in the crystal lattice if the salt is in contact with liquid water or humid air. The number of absorped crystal water molecyles depends on temperature and relative humidity. The molar volume of the salt increases by the uptake of crystal water. In table 2.4 is given the molar volume of some salts and the hygroscopic range in which the hydrate is stable.

Table 2.4 *Molar volume of salts with crystal water and the relative humidity range in which the salt is stable. CRC (1984).* *) *Robert Waller (1991).*

Salt		Molar volume [cm^3/mole]	Stable ϕ-range at 25 °C*)
Anhydrite	$CaSO_4$	46	0 → 1
Gypsum	$CaSO_4 \cdot 2\ H_2O$	75	0 → 1
Thenardite	Na_2SO_4	53	0 → 0.81
Mirabilite	$Na_2SO_4 \cdot 10\ H_2O$	220	0.81 → 1
Kieserite	$MgSO_4 \cdot H_2O$	57	0.04 → 0.21
Starkeyite	$MgSO_4 \cdot 4\ H_2O$	-	0.21 → 0.37
Hexahydrite	$MgSO_4 \cdot 6\ H_2O$	133	0.41 → 0.51
Epsomite	$MgSO_4 \cdot 7\ H_2O$	147	0.83 → 0.91
Chloromagnesite	$MgCl_2$	41	?
Bischofite	$MgCl_2 \cdot 6\ H_2O$	129	?

Vapour pressure over salt solutions

Relative humidity of vapour in equilibrium with a salt solution on a free surface depends on type of salt and temperature. An ideal solution obeys Raoults' law

(2.1)
$$\phi = \frac{n_1}{n_1 + n_2}$$

where

n_1 = number of moles of water
n_2 = number of moles of salt ions

Only dilluted solutions are approximate ideal. For a non ideal solution Robinson and Stokes (1955) give the expression

$$\ln\phi = -a_i m M_w k_s \tag{2.2}$$

where

a_i = number of ions per salt molecule
m = molality of the solution. Number of moles of solute in 1000 g of solvent.
M_w = molecule weight of water = 0.018 kg/mole
k_s = osmotic coefficient depending on m and temperature

Table 2.5 *Relative humidity over different saturated salt solutions at 20 °C and the corresponding solubility. CRC (1984).*

Salt		ϕ	Concentration [g/100 ml]
Gypsum	$CaSO_4 \cdot 2\ H_2O$	0.98	0.24
Mirabilite	$Na_2SO_4 \cdot 10\ H_2O$	0.93	11
Sylvite	KCl	0.85	35
Halite	NaCl	0.76	36
Epsomite	$MgSO_4 \cdot 7\ H_2O$	0.83	71
Bischofite	$MgCl_2 \cdot 6\ H_2O$	0.33	167
Calcium chloride	$CaCl_2 \cdot 6\ H_2O$	0.29	279

In table 2.5 are given ϕ at 20 °C over different saturated salt solutions and the corresponding solubility. As predicted by Raults law ϕ is close to 1 for salts with low solubility and decreasing for salts with larger solubility. For diluted solutions ϕ can be predicted by (2.2) or (2.3). Another way is to approximate $(1-\phi)$ to be inversely proportional to molality of the salt solution for concentrations between zero and saturation. If molality is transfored to concentration by weight, one obtains the expression

$$\frac{c}{(1-c)} = \frac{c_s}{(1-c_s)} \frac{(1-\phi)}{(1-\phi_s)} \tag{2.3}$$

where

c = concentration by weight of salt solution [kg/kg]
c_s = concentration by weight of saturated salt solution [kg/kg]
ϕ_s = relative humidity over a saturated salt solution

The amount of hygroscopic water bound by the salt can be found from (2.3) using $c=s/(s+u)$

(2.4)
$$u_c = \frac{s(1-c_s)}{c_s}\frac{(1-\phi_s)}{(1-\phi)} - s \qquad \phi > \phi_s$$

where

u_c = amount of water by weight bound hygroscopically by the salt [kg/kg]
s = mass content by weight of salt [kg/kg]

For concentrations above c_s, ϕ equals ϕ_s as salt ions crystallize. Over a solution of KCl and $MgCl_2$ Robinson and Stokes (1955) states that the lowering of relative humidity, $(1-\phi)$, for the mixed salt can be calculated by adding the lowering of relative humidity for the single salts. This rule is speciel and does not take into account the interaction between ions or the formation of combination salts. But it can be used as a rule of thumb to calculate ϕ over other salt mixtures.

Example

A saturated sodium chloride solution contains 36 g NaCl in 100 ml water. Using (2.2) with n_1 = 5.5 moles of water, n_2 = 0.62 moles of salt = 1.23 moles of ions gives ϕ = 0.817. This is 0.06 above the actual ϕ over a saturated NaCl solution indicating that the solution is not ideal. Using (2.3) with k_s = 1.271 (Robinson and Stokes (1955)) gives ϕ = 0.754.

A diluted solution of sodium chloride contains 5 g NaCl in 100 ml water. Using (2.2) with n_2 = 0.17 moles of ions gives 0.970. Using (2.3) with k_s = 0.931 gives ϕ = 0.972 and using (2.4) gives ϕ = 0.966. All values are of the same order of magnitude.

Surface tension, viscosity, density and contact angle

Surface tension, viscosity and density are different for a salt solution than for pure water. These properties are important for the capillary transport of salt solutions in porous materials. In table 2.6 are values given for different salts. Concentration is given for the anhydrous solute and is selected from the maximum surface tension given in CRC (1984). Viscosity and density are calculated from the closest given values using linear interpolation. Generally surface tension, viscosity and density increases with increasing salt content. Values of surface tension and density for other concentrations can be approximated with linear interpolation between the value given in table 2.6 and the value for distilled water. For viscosity a parabolic interpolation (x^2) can be used but values in CRC (1984) should be prefered.

The contact angle Θ is often set to 0° because no better value are known. Holten and Stein (1988) has meassured the contact angle between a liquid and ceramic brick and sand lime brick. The liquid was obtained from a suspension of ground hardened mortar in water (1:2) after standing for 1 h. The contact angle was meassured for an advancing and a receding

waterfront pressed into the material. For ceramic brick was found $\Theta=7.4^{\circ}$ for advancing waterfront and $\Theta=16.1^{\circ}$ for receding waterfront. For sand lime brick was found respectively $\Theta=0.6^{\circ}$ and $\Theta=3.4^{\circ}$. For a salt solution Garrecht et al. (1991) states that the contact angle increases with increasing salt content.

Table 2.6. *Surface tension, viscosity and density for different salt solutions at 20 °C. CRC (1984). Concentrations for anhydrous solute by weight.*

SALT Anhydrous solute	Concentration kg/kg	Surface tension 10^{-3} N/m	Viscosity 10^{-3} kg/sm	Density kg/m^3
Na_2SO_4	0.1244	75.45	1.537	1114.5
KCl	0.2470	78.75	1.046	1167.5
NaCl	0.2592	82.55	1.201	1197.2
$MgSO_4$	0.2453	79.25	6.913	1277.0
Na_2CO_3	0.1372	76.75	2.312	1143.2
$NaNO_3$	0.4706	87.05	2.707	1384.0
$MgCl_2$	0.2544	85.75	4.476	1228.8
H_2O	-	72.75	1.0019	996.7

Diffusion coefficient

If the concentration of a salt solution varies from place to place the ions tend to move from places with high concentration to places with low concentration by diffusion. In table 2.7 is given diffusion coefficients for different salt solutions.

Table 2.7. *Diffusion coefficients for different salt solutions. CRC (1984).*

Salt	Diffusion coefficient 10^{-9} m^2/s Molarity [mole/l]		
	0.001	0.1	1.0
NaCl	1.545	1.483	1.484
KCl	1.917	1.844	1.892
CaCl	1.188	1.110	1.203
Na_2SO_4	1.123	-	-
$MgSO_4$	0.710	-	-

2.3 EQUILIBRIUM FOR SALT IN POROUS MATERIAL

In section 2.1 and 2.2 some properties of stone and salt taken from litterature was presented. The task in this section is then to combine theese properties to obtain a model for the *saline material*. For this purpose we have to consider the equilibrium of salt and moisture in the pores of a porous material.

First let us resume the adsorption of pure water in a porous material as described by Gregg and Sing (1967). At low relative humidities, the water is adsorbed in a mono-layer on all internal surfaces of the pores. As the relative humidity increases, the thickness of this layer (t-layer) increases and micro-pores starts to be filled. At relative humidities above 30-40 %, the water condensates in the capillary pores and a meniscus is formend at the interface between fine and coarse capillary pores. The volume of adsorbed water as function of relative humidity is outlined in figure 2.3. The intervals for the different ways of adsorption are indicated. For a coarse porous material, the volume of capillary condensated water is much larger than the two other contributions.

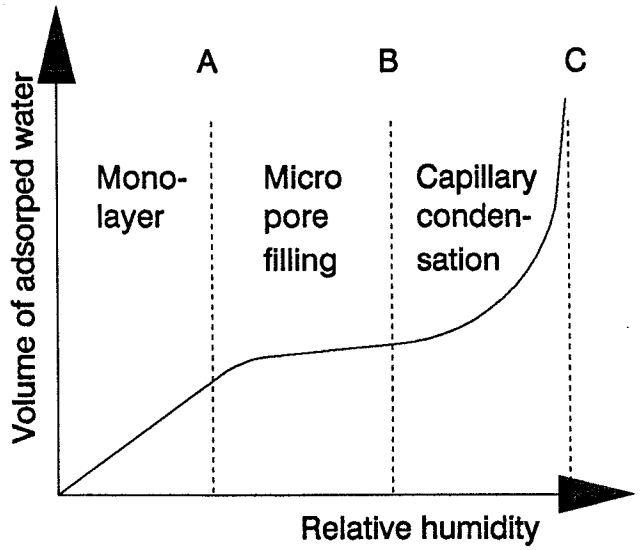

Figure 2.3. *Volume of adsorped water as function of relative humidity. 3 ways of adsorption are indicated; mono-layer below A, micro-pore filling between A and B and capillary condensation between B and C.*

The capillary condensation is described by the Kelvin equation

(2.5) $$\ln\phi = -\frac{2\sigma M\cos\theta}{r_k \rho RT}$$

where

ϕ	=	relative humidity in the pore
σ	=	surface tension of the liquid [N/m]
M	=	molecular mass of the liquid [kg/mole]
Θ	=	contact angle between liquid and pore wall
r_k	=	Kelvin radius of the pore [m]
ρ	=	density of the liquid [kg/m^3]
R	=	Gas constant
T	=	Absolute temperature [$^\circ$K]

The Kelvin equation is not valid at low relative humidities as the concept of meniscus formation in narrow pore spaces makes no sence, because the meniscus would be formed only by a few water molecules.

From the above discussion of adsorption of moisture for salt and for a porous material we have to deduce how moisture is adsorbed for a *saline material*. The situation is outlined in figure 2.4. The relation between relative humidity and the moisture content of a porous material in equilibrium with relative humidity of the ambient air is given by sorption isotherms. The task is thus to find the sorption isotherm for the saline material. To do this we have to decide how the hygroscopic moisture of the material and the hygroscopic moisture of the salt interacts.

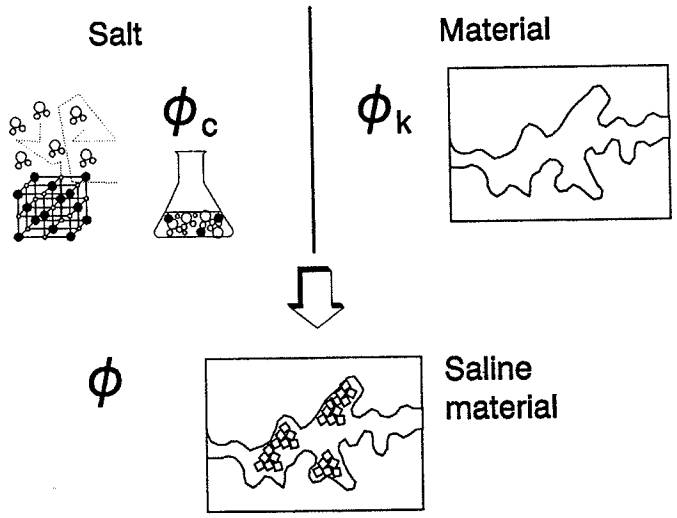

Figure 2.4. *Moisture content at equilibrium for a saline material is obtained from equilibrium for the salt free material and the salt interacting as outlined below.*

A salt solution placed at a given relative humidity will seek towards equilibrium with the ambient air by adsorping or desorping water so that the solution reaches a defenite concentration. This relation is given by (2.4).

The sorption isotherm of a porous material infected with salt will be a mixture of the sorption isotherm for the material and the salt. Assuming that the hygroscopic water of the material does not interact with the hygroscopic water of the salt, the sorption isotherm for the saline material can be found by adding the two sorption isotherms. If relative humidity is below the deliquescence point of the salt the moisture content will exclusively be determined by the porous material, but above there will be a contribution from the salt solution formed in the pores of the material. For non hygroscopic materials like brick the moisture content will principally be determined by the salt.

For hygroscopic materials there will be an interaction between the hygroscopic moisture of the material and the hygroscopic moisture of the salt. At low relative humidities the hygroscopic moisture of the material is strongly attached to the pore walls (mono-layer) and therefore is not able to dissolve the salt. This was found by Litvan (1972) for porous silica glass containing various amounts of NaCl.

Capillary condensated water in the material is not so strongly attached and therefore might be able to dissolve salt and form a saturated salt solution in the pores below the deliquescence point of the salt. Further, small porespaces might exist between salt crystals and the pore-walls as outlined in figure 2.4, and here capillary condensated water, which might be able to dissolve the salt, are trapped. Also, salt-ions might be attached to the pore walls instead of in a salt crystall lattice. The condition for the salt to take up water hygroscopically is also uncertain.

The ability of the hygroscopic water in the material to dissolve the salt and the deliquescence point of the salt is determinded by thermodynamics, but theese calculations are not straight-forward. Instead the following thesis based on the formation of a meniscus is proposed:

THESIS 1:

The relative humidity over a salt solution at a given concentration *in a pore* is reduced compared to both relative humidity over a plane salt solution and relative humidity over a meniscus of pure water.

(2.6) $$\phi=\phi_k \cdot \phi_s$$

Where

ϕ	=	relative humidity over the meniscus with salt solution
ϕ_k	=	partial relative humidity corresponding to the hygroscopicity of the material
ϕ_c	=	partial relative humidity corresponding to the hygroscopicity of the salt

THESIS 2:

At low realtive humidities a saturated salt solution will be formed in the pores due to the hygroscopic water of the material. All hygroscopic water in the material is able to dissolve the salt.

From the two theses the variation of the partial relative humidities with realtive humdity in the saline material is deduced in the following way.

At low relative humidities a saturated salt solution is formed and ϕ_c equals constantly ϕ_s. ϕ_k is found from (2.6). ϕ_c remains constant until all salt are dissolved ($c=c_s$) or until ϕ_k equals 1, which means that the material is no more able to adsorb water hygrocsopically. At this point, the salt starts to act hygroscopically and ϕ_c and ϕ_k increases with relative humidity ending at $\phi_c=1$ and $\phi_k=1$ for $\phi=1$. It is not known how ϕ_c and ϕ_k increases with relative humidity, but as the simplest it is assumed, that the increase in ϕ_c is proportional to the increase in relative humidity. From this the increase in ϕ_k is found from (2.6). The change of ϕ_k and ϕ_c with relative humidity is outlined in figure 2.5. For a given relative humidity of the amibent air (x-axis in figure 2.5) the partial relative humidities ϕ_k and ϕ_c is found by reading the y-axis.

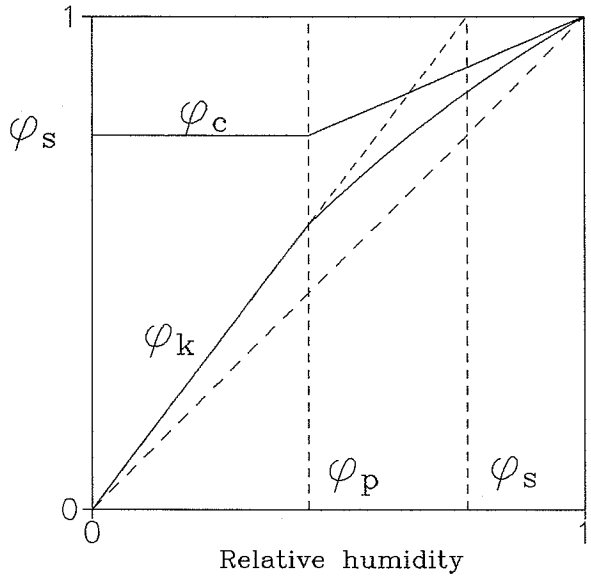

Figure 2.5. *Partial relative humidities ϕ_c and ϕ_k as function of relative humidity ϕ.*

The assumptions above lead to the remarkable result that salts precipitate at a lower relative humidity in the pores of a hygroscopic material than outside the pores.

The relative humidity ϕ_p at which the salt deliqesceses in the material depends on the hygroscopicity of the material (sorption isotherm for the material) and the salt content. At the deliquescence point, the hygroscopic moisture of the material has just disolved all the salt and a saturated salt solution exists in the pores. From the sorption isotherm of the material ϕ_k is determinded. From that and (2.6) the deliquescence point in the material is found. Highly hygroscopic materials and materials with a low salt content has a deliquescence point far below saturation humidity ϕ_s of the free salt solution. Slightly or non hygroscopic materials and materials with a high salt content has a deliquescence point close to the saturation humidity of the free salt solution.

$$u_m(\phi_k)=s\left(\frac{1}{c_s}-1\right)$$

(2.7)

$$\phi_p=\phi_k\phi_s$$

where

ϕ_p = deliquescence point of salt in porous material
ϕ_s = saturation humidity over a free salt solution
u_m = sorption isotherm for material
s = salt content of the material [kg/kg]
c_s = concentration of saturated salt solution [kg/kg]

The equation for the sorption isotherm of the material has to be solved with respect to ϕ_k to find the deliquescence point. This can be done analytically for most fitted equations, otherwise it has to be solved nummerically. As ϕ_k never exceeds 1 it is seen that ϕ_p never exceeds saturation humidity of the salt.

The variation of ϕ_k and ϕ_s with relative humidity is outlined in figure 2.5. The equations corresponding to this and the moisture contents are

Below deliqescence point ($\phi < \phi_p$)

$$\phi_c=\phi_s \qquad \phi_k=\frac{\phi}{\phi_s}$$

(2.8)

$$u=u_m(\phi_k)$$

Above deliqescence point ($\phi > \phi_p$)

$$\phi_c=\frac{\phi(1-\phi_s)+(\phi_s-\phi_p)}{(1-\phi_p)} \qquad \phi_k=\frac{\phi}{\phi_c}$$

(2.9)

$$u=u_c+u_m=\frac{(1-\phi_s)}{(1-\phi_c)}\frac{(1-c_s)}{c_s}s+u_m$$

where

u = moisture content in saline material [kg/kg]

If the hygroscopic wateruptake for the salt was independent of that for the material there would be a sharp rise in sorption isotherm at the deliquescence point of the salt. In practice crystallized salts will form a fine porous network in the pores of the material and hygroscopically take up water below the deliquescence point, and there will be some degree of supersaturation. Adsorption and desorption of moisture for material and salt will be affected by ions content, pure salt content and the properties of the inner surface of the material. This, and the effect outlined above, tends to smoothen out the sorption isotherm at the deliquescence point giving higher moisture content below and lower moisture content above the deliquescence point than would be expected from adding the two sorption isotherms. The smoothening is found by Padfield and Erhardt (1987) but not by Garrect et al (1990).

In chapter 6 are given examples of sorption isotherms for brick and sandstone with different contents of NaCl calculated from the above assumptions.

The theeses above is only valid for capillary condensated water (relative humidities above 30-40 %). The theory is therefore based on a wide extrapolation into the low relative humidity range, in which it might not be valid. But the proposed method may be used as an engineering tool, especially in the high relative humidity range. Though the model might not resemble reality it still may give the right answers.

3. SALT MOVEMENT AND VOLUME CHANGES

In chapter 2 the equilibrium condition for salt and moisture in a porous material was discussed. In this chapter the scope is to discuss how salts are transported to a certain site in a structure and what they do, when they are there (decay mechanisms) under different climate conditions.

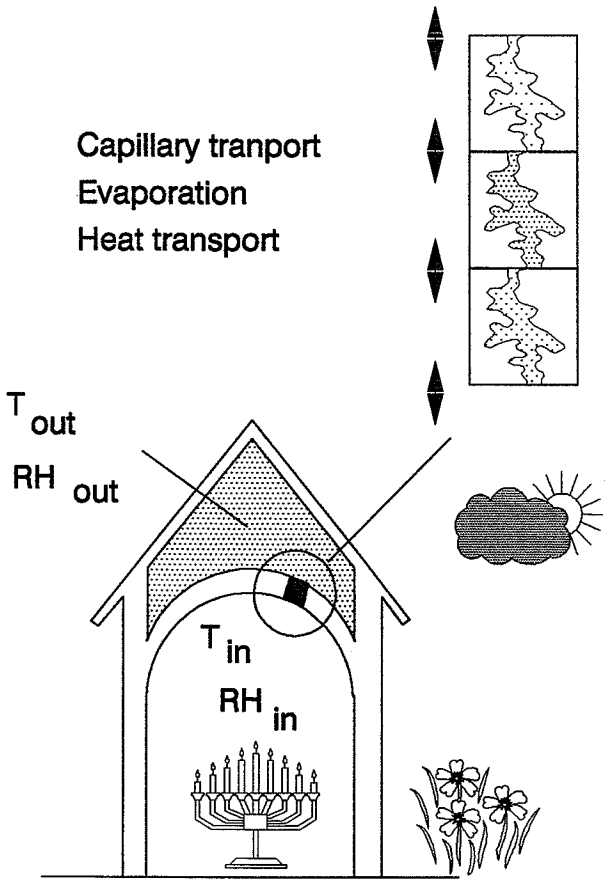

Figure 3.1. *How does salt move to a certain site in a structure, and what happens by climate changes when they are there ?*

In section 3.1 capillary transport of salt solutions in porous materials are discussed and a survey of equations from litterature are given.

Based on the theeses in chaper 2 two models are proposed; in section 3.2 a model to calculate salt and moisture transport in a structure and in section 3.3 a model to calculate volume changes by sorption of moisture. In chapter 5 and 6 theese models are evaluated from experimental results.

3.1 CAPILLARY TRANSPORT OF SALT SOLUTIONS

Capillary rise

Porous materials take up liquid by capillary suction due to the formation of meniscus in the pores. In the contact zone between liquid, material and air the result of the three surface forces determines the contact angle between liquid and material. Assuming cylindrical pores the amount of liquid uptake and the velocity of the capillary liquid uptake are governed by the following forces

(3.1) $$F_K = 2\pi r_k \sigma \cos\theta = K$$

(3.2) $$F_G = r_k^2 \pi \rho g h = Gh$$

(3.3) $$F_V = 8\pi\eta h \frac{dh}{dt} = Vh\frac{dh}{dt}$$

(3.4) $$F_P = r_k^2 \pi p = P$$

where

F_k	=	Capillary force [N]
F_G	=	Gravity force [N]
F_V	=	Viscosity force [N]
F_p	=	External pressure force [N]
r_k	=	capillary radius [m]
σ	=	surface tension [N/m]
Θ	=	contact angle
ρ	=	density of the liquid [kg/m^3]
h	=	capillary rise [m]
η	=	viscosity [kg/m s]

K [N], G [N/m], V [N s/m^2] and P [N] are constants. The equilibrium between capillary force, gravity force and viscosity force gives the velocity of the capillary rise if no external pressure force is acting

(3.5) $$\frac{dh}{dt} = \frac{(K - Gh)}{Vh}$$

The maximum capillary rise is found from (3.5) setting $dh/dt=0$

(3.6) $$H=\frac{K}{G}=\frac{2\sigma\cos\theta}{r_k\rho g}$$

The capillary rise h at time t can be derived from (3.5) using (3.6)

(3.7) $$t=-\frac{V}{G}\left[h+\frac{K}{G}\ln\left(1-\frac{G}{K}h\right)\right]$$

Inserting (3.1-4) and (3.6) gives

(3.8) $$t=-\frac{4\eta H^2}{r_k\sigma\cos\theta}\left[\frac{h}{H}+\ln\left(1-\frac{h}{H}\right)\right]$$

For small values of h/H (3.8) can be further developed as

(3.9) $$t=\frac{2\eta}{r_k\sigma\cos\theta}h^2$$

(3.10) $$h(t)=\sqrt{\frac{r_k\sigma\cos\theta}{2\eta}}\sqrt{t}$$

When a porous material with porosity p takes up liquid by capillary suction through the surface area A_s the mass of liquid pr. area, Q, can be expressed as

(3.11) $$Q=\frac{m(t)}{A_s}=h(t)p\rho=p\rho\sqrt{\frac{r_k\sigma\cos\theta}{2\eta}}\sqrt{t}=W\sqrt{t}$$

(3.12) $$W=p\rho\sqrt{\frac{r_k\sigma\cos\theta}{2\eta}}$$

where

Q = mass of liquid pr. suction surface area [kg/m^2]
p = porosity of material [m^3/m^3]
A_s = suction surface area in contact with liquid [m^2]

The process is dependent on the square root of time. The constant W is the water uptake coefficient. W is dependent on material properties (porosity and poreradius), on liquid properties (surface tension, viscosity, density) and on contact angle. (3.8) and (3.10) are stedy state solutions and are only valid until the rising liquid front has reached the upper rim. From (3.10) an equivalent pore radius can be derived from experimental data

(3.13) $$r_k = \frac{2W^2\eta}{p^2\rho^2\sigma\cos\theta}$$

Instead of using Q it might be more convenient to use the mass content u

(3.14) $$u = \frac{m(t)}{m_d} = \frac{A_s}{m_d} W\sqrt{t}$$

where

m_d = dry mass of the specimen [kg]

From experimental data W can be calculated from the inclination, k_α, in a (u^2-t) graph as

(3.15) $$W = \frac{m_s}{A_s}\sqrt{k_\alpha}$$

During the rise of liquid not all pores of the wetted area are totally filled with liquid. The liquid content of a specimen, just when the rising front of liquid has reached the upper rim, is called liquid capacity u_k. This value therefore is lower than the saturation liquid content u_{ssd}. The ratio between u_k and u_{ssd} defines the degree of capillary liquid saturation S_k.

After filling of the coarse capillary pores the mass content still increases due to filling of the rest of the poresystem. This filling is much slower and is controlled by diffusion of water vapour from capillary pores into air voids, dissolving of air in the liquid and filling of fine pores. Weight increase is therefore mainly exponentially time dependent. This proces also takes place in the first phase during the progress of the rising front and in fact it might only be possible to distinguish the two mechanisms for porous materials with a certain pore size distribution. For brick it is usual to approximate two straight lines in a (Q^2-t) graph and let the intersection determine the time where the rising front reaches the upper rim.

Hoffmann and Niesel propose an imperical function describing the entire liquid uptake

(3.16) $$Q=a(1-e^{-b\sqrt{t}})$$

The formula is statistically confirmed by evaluation of around 230 testruns but it reveals no further physical understanding of the process besides including the exponentially time dependence of the air void filling.

Capillary transport

In general capillary transport of a liquid in porous material can be described by Hagen Poiseuille' law

(3.17) $$q=\frac{\rho r_k^2}{8\eta}\frac{\partial P}{\partial h}$$

Capillary rise is a speciel case of (3.17). (3.11) can be derived from (3.17) setting

(3.18) $$\Delta P=-\frac{2\sigma\cos\theta}{r_k}$$

Evaporation

Besides the characteristics already mentioned, the capillary rise of a liquid containing water soluble salts is different from capillary rise of pure water in the sence that salts may precipitate during capillary rise and change liquid properties and properties of the pore system. Precipitation takes place if water evaporates inside the pore system (due air voids and cracks) or from the surface of the material.

The capillary rise of liquid in a wall is limited by evaporation. If the rate of evaporation from a site equals the capillary transport to that site there will be no increase in capillary rise. But if water soluble salts are present, there will still be an increase in mass content due to precipitation of the salts. Depending on type of salt and climate at the site, a layer of precipitated salt will be build up either at the surface or inside the material. Lewin (1981) uses this to calculate the thickness of the decaying layer of a stone surface. The amount of salt precipitated out can be used as a tracer for the rate of evaporation at the site.

Evaporation takes place, if there is a gradient in water vapour pressure between the ambient air and the material. For practical reasons relative humidity multiplied by the saturation water

vapour pressure is used instead of water vapour pressure. One dimensional flow of water to the surface, where the water evaporates, can as stated by Knöfel et al (1987) be divided into two periods

Period 1: the water content u close to the surface is greater than a certain critical moisture content u_{kr}. The following relation holds

(3.19) $$q_e = p_s \beta (\phi_o - \phi_a)$$

where

q_e	=	amount of evaporated water [kg/m²s]
ß	=	convective moisture transfer coefficient [kg/m²Pas]
p_s	=	saturation water vapour pressure [Pa]
ϕ_o	=	relative humidity at the surface
ϕ_a	=	relative humidity of the ambient air

Weight loss is linear related to time. Evaporation depends only on environmental conditions and is independent of the physical structure of the material. Drying of a material with salt solution is slower than for pure water due to the lower vapour pressure over the salt solution as described in section 2.2. In this period salts precipitate out close to or at the surface and this might change the evaporation rate.

Period 2: Water content is lower than u_{kr}. The following relation holds

(3.20) $$q_e = p_s \frac{\delta}{d} (\phi_1 - \phi_2)$$

where

δ	=	coefficient of water vapour conductivity of the material [kg/msPa]
d	=	thickness of the layer which water vapour passes through [m]
ϕ_1	=	relative humidity at one side of the layer
ϕ_2	=	relative humidity at the other side of the layer

Weight loss is exponentially time dependent. u_{kr} and the time of drying is dependent on the relative humidity and the wind velocity at a given temperature. Again drying is slower for a material with salt solution than with pure water due to lower vapour pressure over a salt solution. The coefficient of water vapour conductivity of the material might be influenced by precipitated salts in the pore system.

During capillary suction evaporation from the surface decreases mass content in the specimen. The water uptake coefficient therefore is smaller if it is calculated from experimental data

from specimens with evaporation. Assuming that evaporation is constant with time from the surface area, which is capillary saturated with the rising liquid, the ratio between water uptake coefficient W and water uptake coefficient W_e for specimens with evaporation can be calculated as

(3.21)
$$\frac{W_e}{W}=1-\frac{q_e b}{p\rho A_s}t_k$$

where

W_e = Water uptake coefficient calculated from specimens with evaporation [kg/m^2 s$^{1/2}$]
q_e = rate of evaporation [kg/m^2 s]
b = circumference of the rising front at the surface [m]
t_k = time interval of capillary suction used for calculation of water uptake coefficient [s]

q_e can be calculated from (3.19) or measured by drying of specimens after capillary suction. When the liquid content in a porous material has reached the liquid capacity all further liquid uptake is controlled by evaporation from the surface of the specimen and internal evaporation and condensation into corse pores and cracks. By capillary suction of pure water specimen weight will only increase due to internal condensation but for salt solutions precipitation of salts will give an increase in weight as well. By capillary suction of a salt solution with concentration c the amount of precipitated salts can be used as a tracer to calculate the corresponding amount of solution necessary to give this salt content. From that, the rate of evaporation during capillary suction can be calculated.

(3.22)
$$q_e=\frac{\left(\frac{s}{c}+1\right)m_d-m_k}{A_e t_k}$$

where

q_e = amount of evaporated water [kg/m^2 s]
m_d = dry mass of specimen [kg]
m_k = mass of specimen after capillary suction [kg]
s = salt content in specimen after suction [kg/kg]
c = salt content by weight in liquid for capillary suction [kg/kg]
A_e = area of evaporation surface [m^2]
t_k = time during which capillary suction has taken place [s]

Salt content in the specimen at the end of the capillary suction can be found by drying the specimen at 105 °C after suction. If the salt content at a given time is not known it can be calculated from (3.22) using (3.19) with an estimated value of ß. This assumes that moisture content is above the critical moisture content. For specimens without salt (3.15) is not valid and q_e can only be calculated from (3.19) or (3.20). q_e can be found from weight loss curves of specimens drying in laboratory climate.

Salt transport

Water soluble salts can only be transported as ions dissolved in water. Ions can be transported in two ways

1) The ions follow the water in a capillary flow. Equations for the stedy state transport are set up above.

2) The ions are transported due to differences in concentration (diffusion). The steady state equation corresponding to Hagen Poiseulles law are

(3.23) $$j=D_c\frac{(c_2-c_1)}{d}$$

where

j	=	flux of salt ions [kg/m^{2}s]
D_c	=	salt diffusion coefficient [m^2/s]
c_1	=	salt concentration at one end of the layer [kg/m^3]
c_2	=	salt concentration at the other end of the layer [kg/m^3]
d	=	distance over which concentration difference acts [m]

Theese two ways of transport require the pores to be filled with liquid. From the way salts are able to climb vertical glass cups it is obvious that salt can be transported in another way as stated by Pühringer (1983). When salt precipitates a fine porous structure rather than solid crystals are formed on the inner surface of the porous material. In this porous salt structure salt solutions can be transported as a thin salt film although the pore of the porous material itself are not filled with water. On the tip of the salt film salts can precipitate out and form new porous salt structures. In principle the transport can be described by equations corresponding to those above, but the pore structure of the precipitated salts changes with climate during transport which makes things a lot more complicated. Instead, for use in calculations, capillary transport can be assumed, even at low moisture contents.

Non steady state transport

For non steady state transport the following equations can be set up

Moisture transport

(3.24) $$\frac{\partial u}{\partial t}=\frac{\partial}{\partial x}(D_w\frac{\partial u}{\partial x})$$

Salt transport

(3.25) $$\frac{\partial c}{\partial t}=-\frac{1}{\rho}\frac{\partial(qc_b)}{\partial x}+\frac{\partial}{\partial x}(D_c\frac{\partial c}{\partial x})$$

where

u	=	moisture content [kg/kg]
D_w	=	moisture transport coefficient [m^2/s]
c	=	salt content [kg/kg]
D_c	=	salt diffusion coefficient [m^2/s]
q	=	flux of moisture [kg/m^2s]
c_b	=	salt concentration in moisture flux [kg/m_3]

For each type of salt an equation like (3.25) is needed. The first term in (3.25) corresponds to salt transported by capillary flow of the salt solution, the second term to the transport by diffusion. Usually (3.24) and (3.25) are solved using steady state approximations in small time intervals.

3.2 MODEL FOR MOISTURE AND SALT TRANSPORT

In this section a model to calculate moisture and salt transport in a construction is proposed. The model is based on the equilibrium theeses in chapter 2 and is outlined in figure 3.2.

The model consists of equally sized boxes of material vertically stacked. Each box is characterized by the moisture and salt content and the temperature. If salt concentration exceeds solubility, the salt precipitates out and is assumed to be fixed to the element. In this way concentration of salt solution is assumed never to exceed saturation. Moisture and salt are transported by capillary transport inside the material as described by (3.26-27). Transport of salt by diffusion is neglected. Moisture is transported as vapour as described by (3.20). Heat is transported as described by (3.28). All potentials (suction and vapour pressure) are assumed to act at the centre of the element.

Boundary conditions are that the material is isolated from the ambiant air at the vertical surfaces. At the horizontal surfaces moisture and salts can be taken up by capillary suction and vapour is transported by convection as described by (3.19). Suction pressure at the boundary is calculated from (3.26) assuming the degree of saturation to be 0.995. Heat is transported by convection only through the horizontal surfaces.

A one dimensional model for moisture and salt transport can be obtained from stedy state approximations of (3.24) and (3.25). In this model it is important to distinguish clearly between moisture adsorbed due to hygroscopicity of the material, and moisture adsorbed due to hygroscopicity of the salt, as relations between hydraulic pressure, vapour pressure and salt concentration in the pore liquid depends on the partial relative humidities corresponding to salt and material, as stated in section 2.2.

It is assumed, that the moisture and salt content are known from the start. As potential for capillary transport of moisture and salt the hydraulic potential as defined by the La Place equation is used. The potential is multiplied by the logarithm to the degree of moisture saturation. In this way dry areas have a larger potential than wet areas and therefore moisture

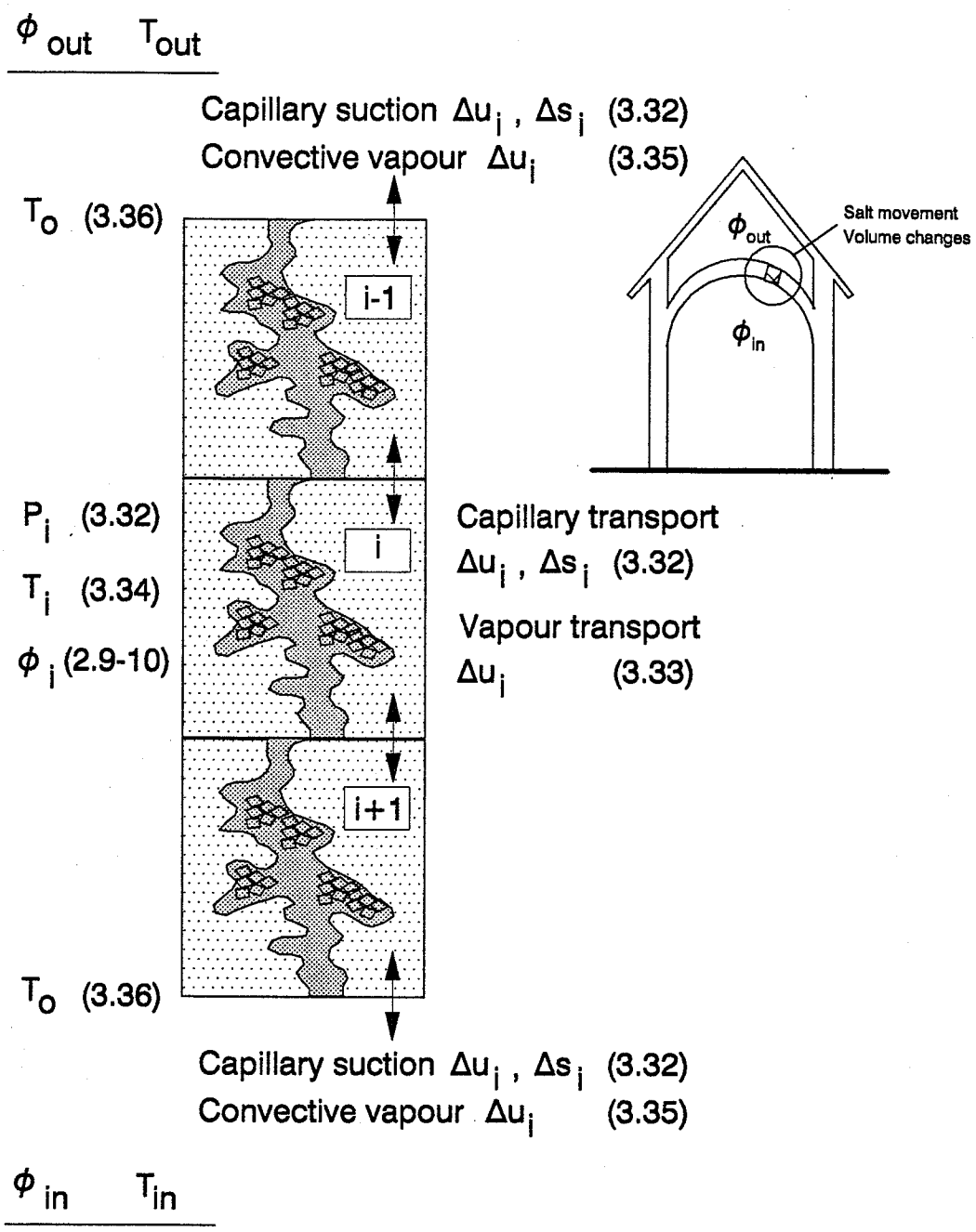

Figure 3.2. *Model to calculate moisture and salt transport in a structure consisting of equally sized boxes of material vertically stacked.*

is transported towards dry areas corresponding to moisture movement in a partly saturated material. When the material is dried from the surface, salts are transported by capillary suction to the surface where they precipitate.

(3.26)
$$P_h = \frac{2\sigma\cos\theta}{r_k} \ln\left(\frac{u}{u_{ssd}}\right)$$

For a given moisture content hydraulic pressure numerically increases with increasing salt concentration due to an increase in surface tension, which means that the liquid is transported towards areas with high salt concentrations. The numerically largest potential is found for an almost dry material with a saturated salt solution.

The capillary liquid flux is calculated from Hagen Poiseulles law (3.17) to take into account the effect of change in density and viscosity of the salt solution. The transport coefficient is multiplied by an exponential factor including the dependency of transport coefficient on moisture content. The transport coefficient is increasing with moisture content starting at no moisture transport for a dry material. In practice, the material never completely dries out, the hygroscopic adsorped water ensure that moisture transport allways is possible. To obtain a numerical more stable solution the conversion below is used

(3.27)
$$q = K_k \frac{\partial P_{suc}}{\partial x} = K_k P_{suc} \frac{\partial \ln P_{suc}}{\partial x}$$

$$K_k = (e^{u/u_{ssd}} - 1)\frac{\rho r_k^2}{8\eta}$$

where $P_{suc} = - P_h$ is the suction pressure. The moisture and salt transport is calculated from the transport of salt solution. Vapour transport is calculated from (3.19) and (3.20). Temperature is calculated from stedy state approximations of

(3.28)
$$\frac{\partial T}{\partial t} = \alpha \frac{\partial^2 T}{\partial x^2} \qquad \alpha = \frac{\lambda}{\rho_d C_p}$$

where

T	=	temperature of material [°C]
λ	=	thermal conductivity [J/s m K]
ρ_d	=	dry density of material [kg/m^3]
C_p	=	specific heat capacity [J/kg^3 K]

λ, ρ_d and C_p is for simplicity assumed independent of moisture and salt content. Surface tension, density and viscosity for sodium chloride solution below solubility (0.26 kg/kg) are fitted from measured data in CRC (1984)

$$\sigma = 0.07286 + 0.02568c + 0.04477c^2 \tag{3.29}$$

$$\rho = 996.7 + 753.3c \tag{3.30}$$

$$\eta = 10^{-3}(1.019 + 0.5819c + 11.24c^2) \tag{3.31}$$

where

c	=	concentration of salt solution [kg/kg]
σ	=	surface tension [N/m]
ρ	=	density of salt solution [kg/m^3]
η	=	viscosity of salt solution [kg/s m]

For simplicity σ, ρ and η is assumed independent of temperature although this is not the case, especially for viscosity, but in most situations temperature is only varied in a narrow range and for salt solutions it is hard to get data for variations with temperature.

Moisture and salt are transported from the element with the lowest suction pressure (element i) to the element with the highest suction pressure (element $i+1$). Therefore the transport coefficient for the element with the lowest suction pressure is used. By selecting the element with the lowest suction pressure and using the transport coefficient for this element salt transport is calculated from the salt concentration in the element from which the transport actually takes place. Moisture and salt transport in the time interval Δt from element i to element $i+1$ is calculated from (3.27) as

$$\begin{aligned}
\Delta u_i &= -\Delta u_{i+1} = (1-c_i)K_i \frac{(P_i + P_{i+1})}{2} \ln\left(\frac{P_i}{P_{i+1}}\right) \\
\Delta s_i &= -\Delta s_{i+1} = c_i K_i \frac{(P_i + P_{i+1})}{2} \ln\left(\frac{P_i}{P_{i+1}}\right) \\
K_i &= (e^{u/u_{ssd}} - 1)\frac{\rho_l r_k^2}{8\eta}\frac{p}{\rho_d h^2}\Delta t \\
P_i &= \frac{2\sigma_i \cos\theta_i}{r_k} \ln\left(\frac{u_i}{u_{ssd}}\right)
\end{aligned} \tag{3.32}$$

where

Δu_i = change in moisture content [kg/kg]
Δs_i = change in salt content [kg/kg]
Δt = time interval [s]
p = porosity of material [m^3/m^3]
ρ_d = material density of element [kg/m^3]
h = height of element [m]
K_i = transport coefficient for element i [Pa^{-1}]
P_i = Suction pressure for element i [Pa]

The vapour transport in the time interval Δt from the element with the lowest relative humidity (element i) to the element with the highest relative humidity (element $i+1$) is calculated from (3.20) as

(3.33)
$$\Delta u_i = -\Delta u_{i+1} = \frac{P_s p \Delta t}{\rho_d h^2} \delta(\phi_{i+1} - \phi_i)$$

where

P_s = saturation water vapour pressure at the given temperature [Pa]
δ = coefficient of water vapour conductivity of the material [kg/m s Pa]
ϕ_i = relative humidity of element

The temperature change in the time interval Δt in element i is calculated from steady state approximation of (3.28) as

$$T_i^* = RT_{i+1} + RTi - 1 + (1-2R)T_i$$

(3.34)
$$R = \frac{\lambda \Delta t}{\rho_d C_p h^2}$$

where

T_i^* = new temperature in element i [°C]
h = height of the element [m]

Evaporation in the time interval Δt from the surface element i to the ambient air is calculated from (3.19) as

(3.35)
$$\Delta u_i = \frac{P_s p \Delta t}{\rho_d h^2} \beta h(\phi_a - \phi_i)$$

where

ß = convective moisture transfer coefficient [kg/m² Pa s]

ϕ_a = relative humidity of the ambient air [Pa]

The temperature of the surface is calculated as

(3.36)
$$T_o = \frac{\left(\beta_T T_a + \frac{2\lambda T_i}{h}\right)}{\left(\frac{2\lambda}{h} + \beta_T\right)}$$

where

T_o = temperature of the surface [°C]

T_a = temperature of the ambient air [°C]

$ß_T$ = convective heat transport coefficient [J/s K]

The moisture and salt transport and the change in temperature in the time interval Δt is calculated for all elements. All calculations starts from old values of moisture content, salt content and temperature. From theese values surface tension, density, viscosity, suction pressure, transport coefficient and sorption isotherm are calculated. For all elements the change in moisture content, salt content and temperature in the time interval Δt are calculated as described above. New values of moisture content, salt content, salt concentration and temperature are calculated. If the ratio between salt and moisture content exceeds saturation, salt concentration is set to saturation and the rest of the salt is assumed to be precipitated and fixed to the elemtent. All data except relative humidity is assumed independent of temperature.

Relative humidity in an element is calculated from the moisture content and the sorption isotherm of the saline material. The sorption isotherm is found as described in section 2.2. Equations fitted from experimental data for sorption isotherms of different materials are given by Hansen (1986). From the sorption isotherm for the material and new salt and moisture content the corresponding new relative humidity for the element can be calculated from 2.8-10. Sorption isotherm (relative humidity in the material) is assumed to be constant with temperature. An increase in temperature thus causes an increase in vapour pressure due to the increase in saturation vapour pressure.

3.3 SHRINKAGE AND SWELLING OF SALINE MATERIALS

In this section a model to calculate shrinkage of saline materials is proposed. The model is based on the formation of meniscus in the material and the action of surface tensions on the pore walls causing the material to shrink and swell.

When a porous material adsorb or desorb water, the material swell or shrink. Three important theories to explain this mechanism exist, as discussed by Powers (1965). At low relative humidities the adsorption of water on inner surfaces decreases the surface free energy, which causes the material to shrink (Gibbs-Bangham shrikage). At high relative humidities the tension in the pore water due to capillary forces causes compressive forces in the material, which causes volume changes in the material (capillary shrinkage). The mechanical equilibrium between two adsorped water films of different thickness results in a difference in the pressures on the films. In Micro pores the adsorption of water films thicker than a certain thickness is hindered and a pressure (disjoining pressure) is build up in the pore liquid causing the material to swell. As the quantitative calculations of disjoining pressure is very uncertain it will not be discussed furter in this work.

Gibbs-Bangham shrinkage

The Gibbs-Bangham stress-induced shrinkage is discussed by Hansen (1987) for cement paste. The linear expansion of materials with high inner surface area was empirically predicted by Bangham as

$$\varepsilon = \lambda \Delta F \tag{3.37}$$

where

ε	=	linear expansion of the material [m/m]
λ	=	a constant [m/N]
ΔF	=	calculated decrease in surface free energy [N/m]

The decrease in surface free energy can be calculated by the Gibbs adsorption equation

$$\Delta F = \frac{RT}{V} \int_{\phi_1}^{\phi_2} \frac{V_l}{S} d(\ln\phi) \tag{3.38}$$

where

ΔF	=	change in surface free energy [N/m]
R	=	the gas constant [N m/mol K]
T	=	absolute temperature [$^{\circ}$K]
V	=	molar volume of adsorbed moisture [m^3/mol]
V_l	=	specific volume of adsorbed moisture [m^3/kg]
S	=	specific surface area of the solid [m^2/kg]
ϕ	=	relative humidity

From the sorption isotherm and the thickness of the adsorbed moisture (t-layer) the voloume of adsorbed moisture as function of t can be obtained (V-t curve) as suggested by Gregg and Sing (1967). The shape of the V-t curve indicates how moisture is adsorbed in the pores, and the inclination at origo corresponds to the specific surface area of the solid. From the V-t curve analysis the volume of adsorbed liquid can be separated from the capillary water, and from (3.38) the change in surface free energy can be calculated in different relative humidity segments.

The constant λ in (3.37) is related to the elastic modulus of the solid. For a porous material consisting of thin slices of solid material λ can be calculated as

$$\lambda = \frac{2(1-\nu)\rho_s}{3(1-2\nu)E_s} S \tag{3.39}$$

where

ν_s	=	poisson's ratio of the solid
E_s	=	E-modulus of the solid [Pa]
ρ_s	=	density of the solid [kg/m^3]
S	=	specific surface area of the solid [m^2/kg]

Capillary shrinkage

According to Fagerlund (1975) the pressure of the pore water can be expressed by the La Place or the Kelvin law

$$P_h = -\frac{2\sigma\cos\theta}{r_k} = \frac{\rho_l RT}{M}\ln\phi \tag{3.40}$$

where

P_h	=	hydraulic pressure in the pores [Pa]
σ	=	surface tension between liquid and air [N/m]
θ	=	contact angle between liquid and material
r_k	=	Kelvin pore radius [m]
R	=	the gas constant [N m/mol K]
T	=	absolute temperature [$^\circ$K]
ρ_l	=	density of liquid [kg/m^3]
M	=	molar weight of liquid [kg/mole]
ϕ	=	relative humidity

All pores with radii smaller than r_k are assumed to be filled with liquid and all pores larger than r_k are airfilled. The hydraulic pressure in all pores filled with liquid is given by (3.40). The tension in the pore liquid causes compression in the material and for this reason the material contracts compared to complete saturated material. According to Fagerlund (1975)

the mechanism is only active as long as pore liquid stresses are less than the tensile strength of the liquid. For relative humidity below this point, the material expands and at $\phi=0$ the material recovers its original size.

In order to calculate the volume change a geometrical model must be used. Hansen (1967) suggests a model consisting of a hollow sphere with the hole correspondent to all water filled pores. As drying proceeds, the volume of the hole decreases, and the elastic properties of the shell changes as it become more porous. According to Fagerlund (1975) the length change can be calculated as

(3.41)
$$\varepsilon = -\frac{3}{2}\frac{(1-\nu_s)}{(1-2\nu)E_s}\frac{\rho_t RT}{M}\frac{p_w}{(1-p_w)}\frac{(1+p)}{(1-p)}\ln\phi$$

where

p	=	porosity of the material [m^3/m^3]
p_w	=	water filled porosity [m^3/m^3]
E_s	=	E-modulus of the solid material [Pa]
ν_s	=	poisson's ratio of the solid material
ν	=	poisson's ratio of the porous material

The water filled porosity at a given relative humidity can be found from the sorption isotherm of the material.

Shrinkage of saline materials

In order to calculate the shrinkage of saline materials it is important to distinguish between moisture taken up due to hygroscopicity of the material and moisture taken up due to hygroscopicity of the salt. The first causes shrinkage due to capillary forces in the pores and the uptake is controlled by the size of the pores as described by the Kelvin equation. The moisture taken up due to hygroscopicity of the salt is not controlled by the size of the pores, moisture would be taken up even in a non-hygroscopic material, and the moisture therefore will not necessarily cause capillary shrinkage except if it is situated in a fine pore.

Consideration to the interaction between salt and material is taken by using the partial relative humidity ϕ_k corresponding to the Kelvin equation in (3.41) instead of relative humidity. The variation of the partial relative humidities with relative humidity is assumed to be as outlined in figure 2.5.

The effect of this is that the deliquescence point ϕ_p is lowered. Below the deliquescence point swelling increases compared to a salt free material due to an increase in ϕ_k. Further density and surface tension is changed a little which changes the rate of shrinkage. Above the deliquescence point the rate of increase in ϕ_k decreases due to the increase in ϕ_c, and therefore the swelling mechanism by adsorption decreases compared to salt free material. The physical reason for this is that moisture is adsorped not only by the pores but also by the salt, and only adsorption by the pores gives a change in capillary tensions leading to swelling.

4. MICROSTRUCTURAL INVESTIGATIONS

4.1 INTRODUCTION

Two bricks placed next to each other in a structure is often observed to deteriorate quite differently. As climate conditions have been exactly similar, the difference must be related to pore structure. Strength, stiffness, thermal and hygric movements, sorption, capillary suction and transport of moisture and salts are all dependent on pore structure.

Numerous attempts are made to connect pore structure and material properties. Fagerlund (1972) discusses the connection between porosity and mechanical properties. Quiblier (1984) gives a bibliographic survey on the relationships between structure of porous media on the microscopic level and their overall properties. Berryman and Blair (1986) discusses the use of ditigal image analysis to estimate fluid permeability of porous material. Scrivener and Pratt (1987) discusses the characterization and quantificaiton of cement and concrete microstructures from analysis of backscattered electron images of polished surfaces. Hansen (1987) relates drying shrinkage in portland cement paste and pore stucture measurements using nitrogen sorption and mercury intrusion porosimetry.

The pore structure is usually described from a model. An implicit model introduces into experimental results the expression of fundamental physical laws such as capillarity laws. The models have a lack of realism when compared to the actual porous network, but they are only build to approximate an experimentally observed behavior and must therefore be judged only on their abillity to reach their specific objective. The models introduced in chapter 3 are examples of implicit models.

Explicit models are built to simulate the actual behavior of porous media and consists of elements with certain shapes and properties connected into a network. The models start from the geometry of the pore structure and leads to material properties.

The techniques used to achieve such models can be divided into indirect methods or "black-box" methods and direct observations of the porous medium itself. By indirect methods the material is exposed to a certain physical action, and the response is measured regarding the material as a black box with a certain unknown porestructure. Indirect methods are connected with implicit models, and examples are mercury intrusion porosimetry, nitrogen sorption, low temperature calorimetry and nuclear magnetic resonance.

Visualization of the porous network is mainly achieved by injecting various substances capable of producing an optical contrast with the matrix, thus allowing further observation in thin or polished sections. In these observations of two-dimensional sections quantitative stereology and mathematical morphology can be used for further characterization of the geometry of pores.

It is the scope of these investigations to find a methology to describe pore structure of building stone. Experiments will include analysis of polished sections in scanning electron microscopy (SEM) using digital image processing. These results will be compared to results from mercury intrusion porosimetry (MIP).

4.2 PREPARATION OF MATERIALS

Preparation of the material is a very important but also difficult part of pore structure analysis. Only by careful preparation details of the pore structure can be seen. It is important to know which temperature, moisture and mechanical conditions the material has been exposed to, as pore structure can change with theese influences. Strong drying may cause cracks, temperatures above 50 °C may cause phase changes like drying of crystal water from gypsum. If water soluble salts are going to be observed water can not be used in preparation of the material. Often differences in pore structure, due to climate influences between the choosen material and a similar unexposed material, are of interest. This is the case by investigations of the weathering of building materials.

Fragments

To get an overview of the composition and macro porestructure of the building stone it is often convenient to look at fragments in light microscope at low magnification. This will give usefull information about homogenity and corse cracks. It is a very stright forward examination as preparation is very simple. Fragments can be examined in more detail in scanning electron microscope (SEM) at low magnification. The high spatial resolution in SEM is very usefull for this purpose.

Polished sections

Quantitative analysis requires a plane cross section of the material, because measurements of pore structure in three dimensions is very complicated. Stereological analysis of several plane sections can give some information about the three dimensional pore structure. Polished sections is made by vacuum impregnating the material with epoxy resin mixed with fluorescense or colored dye. Lapping and polishing with SiC-powder and diamonds on cast iron or ceramic discs gives a surface with sufficient contrast to be examined in microscope with reflecting light or SEM.

Thin sections

Thin sections of the material is impregnated with epoxy and grinded to a thickness of 20μm. Hereafter they can be analysed in optical microscope with transmitted light.

4.3 ANALYSIS

Pore structure is analyzed by water saturation, scanning electron microscope (SEM) and, mercury intrusion porosimetry (MIP). Below, further details are only given for water saturation and SEM.

Water saturation (total porosity and density)

Total porosity and dry density is measured by water saturation of specimens. Saturation can be achieved either by pressure, vacuum or boiling. Only open porosity, i.e. pores with connection to the surface, can be filled. The minimum pore space, which can be filled, is determinded by the pressure used, and may be derived from (3.18). By vacuum the atmospheric pressure only can fill pores larger than 1.4 μm. By pressure enclosed air may hinder saturation. After filling by vacuum or pressure the specimens therefore is left immersed in the water for at least one day to ensure filling of narrow pores and pores with entrapped air. For coarse porous materials like brick saturation is easily achieved by all three methods. Experiments with brick gave a total open porosity of 0.32 m^3/m^3 with standard deviation (4 specimens) 0.018 m^3/m^3 for pressure saturation (15 MPa), 0.009 m^3/m^3 for vacuum saturation and 0.021 m^3/m^3 for boiling in 4 hours.

Bulk density is determinded by pyknometric measurements on grinded material. From this total porosity is determinded as

(4.1)
$$p_{tot} = 1 - \frac{\rho_d}{\rho_{ssd}}$$

where

p	=	total porosity [m^3/m^3]
ρ_{dry}	=	dry density of material [kg/m^3]
ρ_{ssd}	=	bulk density of material [kg/m^3]

If all porosity is assumed to be open porosity, bulk density can be determinded from water saturation and (4.1).

Scanning Electron Microscopy (SEM)

In the SEM two types of electrons, which are emitted from the specimen, may be detected and used to form images. The most common type of imaging makes use of secondary electrons which result from the enelastic scattering of the incomming electrons. These have much lower energies than the incident electrons and so only escape from a thin layer at the surface of the specimen are collected by a detector. The intensity of secondary electrons depends on the local inclination of the specimen surface, so a topographic image is produced. Combined with a high spatial resolution secondary electrons are very suitable to produce pictures of fragments.

Backscattered electrons have energies similar to the incident electrons and so are emitted and detected from greater depths than the secondary electrons. Therefore the maximum attainable resolution with backscattered electrons is slightly poorer than with secondary electrons. The intensity with which electrons are backscattered depends principally on the local atomic number of the specimen, but it is also affected by topography. The intensity increases monotonically with mean atomic number. Pores filled with resin appear dark and matrix material with silicates appear bright giving good contrast between pores and matrix.

Digital Image Processing

Digital image processing is concerned with the computer processing of pictures or, more generally, pictures that have been converted into a numeric form. This conversion or digitalization may be produced from analogous electric signals from a videocamera by a scanner (frame grabber). In general, the purpose of digital image processing is to enhance or improve the image in some way, or to extract information from it. Typical operations are as stated by Niblack (1986) to

- Remove the blur from an image
- Smooth out the graininess, speckle, or noise in an image
- Improve the contrast or other visual properties of an image prior to displaying it
- Segment an image into regions such as object and background and quantify objects
- Magnify, minify, or rotate an image

Enhancement

Enhancement or digital convolution is performed by using a filter mask array of size n x n pixels for all pixels in the picture. The new pixel value at the center of the filter is given by the sum of the old pixel values around the center pixel, each multiplied by the corresponding term of the filter mask array. In this way the gray level of a pixel becomes dependent on the gray level of the surrounding pixels. The size and shape of the filter and the weights may be varied over the picture.

The simplest form of filtering is an average filter, where the new pixel value is the average of the surrounding pixel values, designed to reduce the noise in an image. It is easy to smooth out an image, but it should be done without blurring out the interesting features. If several copies of the picture are available reducing the noise may also be obtained by averaging pixel by pixel. Other filters are designed to give the gradient of pixel values (Laplacian filters) or to enhance edges in the picture. Filtering can also be used to choose the minimum, maximum or typical pixel value inside the filter mask.

Diversely lightning can be corrected by a calibration using a large average filter (99 x 99 pixels). Shapes can be smoothed out by a small (local) average filter (3 x 3 pixels). Contrast can be improved by shifting gray level values, so that they are distributed over the entire range of gray levels, or by gain/offset adjusting of the analogous signal from the video camera.

Segmentation

Image segmentation is the process of dividing an image into meaningful regions. The simplest case is to have only two regions, an object region and a background region for instance pore regions in a material matrix. The picture is segmented only on the basis of pixel gray level values.

The simplest and most common way is to select a certain fixed threshold value, i.e. all pixels with gray level values below the threshold are pore regions, and all pixels with gray level values above the threshold are background. The threshold can be choosen manually by the user from markings on the original picture and a histogram of gray levels in the picture. This demands a knowledge and judgement from the user of which areas are pores and which are background. In this way the segmentation might become very subjective and might be hard to reproduce.

Winslow and Shi (1988) propose a method to automatic segmentation based on one threshold using fuzzy probability. Assuming dark pores on a light background they use a socalled membership function $\mu_O(x_i)$ defining the degree of membership for pixel x_i to the subset "pores" as function of the gray level i. From this, a single threshold between pores and background can be calculated.

Gray level distribution of pore regions and background generally overlap and the user must select among thresholds none of which gives all the pore regions without including extra noise or background. One alternative is to use multiple thresholds or thresholds that vary across an image.

Niblack (1986) propose a procedure with two thresholds t_1 and t_2 segmenting the picture into three regions; pores below t_1, uncertain regions between t_1 and t_2 and background above t_2. The uncertain regions are then assigned to either object or background depending on the assignment of the majority of their neighbors. This method must be iterated to resolve large areas of pixels with values between t_1 and t_2.

If the graylevel of the background varies over the image the thresholds can be found from the local pixel value mean and standard deviation.

If the area fraction of pores are known, and the graylevel histogram is assumed to be a normal distribution, the threshold can be found from the global (for the entire image) pixel value mean and standard deviation by chossing a certain fractile.

Quantifying pores

After segmentation there might be noise (small dots of pores or background selected due to uncertain thresholding) left in the segmented image. To isolate pores and remove defects filters as described above can be used. Especially small average filters, minimum and maximum filters and type number filters are efficient. Another way is to use shrink/expand methods. By shrinking an object the edge of for instance one pixel width is removed from the object. By expanding one pixel is added to the edge.

A convex defect of a pore may be removed by shrinking the pore and then expanding. As this operation tends to separate or open pore regions the operation is denoted "opening". A concave defect may be removed by expanding and then shrinking the pore. As this operation tends to assemble or close isolated areas the operation is denoted "closing".

After this cleaning out the pore regions selected should correspond to the pores seen on the original graylevel image. The one thing left now is to characterize the selected areas on the binary image. In doing this one should remember that the binary image is only a cross section of a three-dimensional structure and so, a detailed description of the two-dimensional structure might not make any sence. Only by serial section reconstruction it is possible to obtain meassures of for instance connectivity but for very fine porous materials an enormous number of sections would be needed.

The total area fraction is easily measured by most image processing systems. The area fraction of pores in a two-dimensional section is a direct estimate of the volume fraction. Scrivener and Pratt (1987) states, that only for spheres and other regular shapes exact relationships between three-dimensional distributions and measurements in two-dimensions exist. Such relations are given by Gundersen (1988) and for concrete testing by Chan (1987). When a single phase region connected in three dimensions appears as separated regions on a section, as it is the case with most porous materials, the concept of pore size distribution in terms of equivalent sphere diameters is relatively meaningless. In this case two characterization strategies can be used; pore opening distributions (Serra (1982)) and two-point correlation functions (Beryman and Blair (1986)).

The opening and closing techniques mentioned above can be used to determine a distribution of pore structure sizes seen on a binary image of a two-dimensional section. The opening may be performed by a geometrical element (template) of a certain size and shape, so that the edge of the pore region is shrinked and expanded with the width of the template. The effect of opening is that pore regions with dimension less than the template disappear. If increasing template sizes are used and the area fraction that disappears are measured, a distribution of pore structure dimensions can be obtained.

4.4 EXPERIMENTAL WORK

Materials

The materials used are brick, sandstone and mortar. Red brick and calcareous sandstone as described in chapter 5, silicious sandstone from Obernkirchen, pit lime mortar (K100/750, sand grain size 0-2.2 mm) and slaked lime mortar (K100/750, sand grain size 0-2.2 mm).

Equipment

The image analysis system used in this work consists of a personal computer with a PC Vision Plus frame grabber card capable to digitize the image into an array of 512 x 512 pixels with 255 gray levels. Images are scanned by a ccd-video camera through an optical lens or through two different light microscopes.

The pores that can be detected depends on pixel size which again depends on the magnification. The resolution of individual pores increase with magnification but the number of fields needed to give reasonable estimates of porosity and poresizes increases drastically with magnification. In table 4.1 is given an overview of the possible pixel sizes for the actual system. The SEM-images used are 13 x 18 cm high resolution paper copies. The video camera can be mounted on a stand, so it is possible to zoom with an optical lens with fixed focal distance.

Table 4.1. *Measured pixel size obtained by different image forming equipment for digital image analysis. Field size 512 x 512 pixels, aspect ratio 0.68.*

Equipment	magnification	Pixel size (μm)	Field size (mm)
Optical lens	min.	220 x 150	112 x 76.8
(zoom)	max.	16.7 x 11.3	8.55 x 5.79
Microscope I	min.	16.8 x 11.6	8.65 x 5.94
(zoom)	max.	3.39 x 2.31	1.74 x 1.18
Microscope II	M1	1.51 x 1.03	0.77 x 0.53
(fixed)	M2	0.76 x 0.52	0.39 x 0.27

Experimental procedures

The materials in this work were analysed from 13 x 18 cm high resolution paper copies of SEM-backscatter images of polished sections. There were used 4 different images for brick and 2 different images for the other materials. Each image was analyzed in 2 fields, each covering half of the image. The field was digitized into a 512 x 512 array of pixels in 255

gray levels and transformed into a 640 x 480 array of pixels, because images were analyzed on a different computer. The size of one field on the SEM-image was 115.0 by 78.5 mm. The actual field size is found from division by magnification of the SEM-image. Each image was sampled 6 times to minimize noise. A narrow border of the field was removed to exclude boundary effects, so that the working field analyzed was approximately 620 x 460 pixels.

Before segmentation a 3x3 average filter was used to smoothen the image. Segmentation was done with i fixed threshold chosen by judgement of the user from gray level histogram and markings on gray level image. For all images there was two sharp peaks corresponding to pores and matrix. Pore pixels were selected in the gray level range 0-70 and matrix pixels in the range 71-255 for all images.

Total area fraction of pores and opening distribution was determinded as described above. The element used for dilation was an approximated circle in a 9x9 matrix corresponding to a 1-pixel, 2-pixel and a 4-pixel opening size. The 4-pixel element was used 1 to 5 times corresponding to respectively 4-pixel, 8-pixel, 12-pixel 16-pixel and 20-pixel opening size. Below is for each material given the original graylevel image, segmented image for one field, the corresponding 8-pixel opened image and opening distribution.

Total porosity and density determinded from water saturation are given for each material.

Table 4.2 *Measured area fraction of pores from image analysis compared to porosity measured by water saturation.*

Material	Magni-fication	Number of fields	Area fraction		Water saturation	
			Avg.	Std.	p	ρ_d
Brick	350	8	0.28	0.03	0.29	1870
Calc. sandst.	113	4	0.22	0.01	0.21	2120
Silic. sandst.	113	4	0.18	0.05	0.16	2226
Pit lime mortar	40	4	0.20	0.03	0.29	1890
Slaked lime mortar	40	4	0.22	0.05	0.27	1930

Red brick

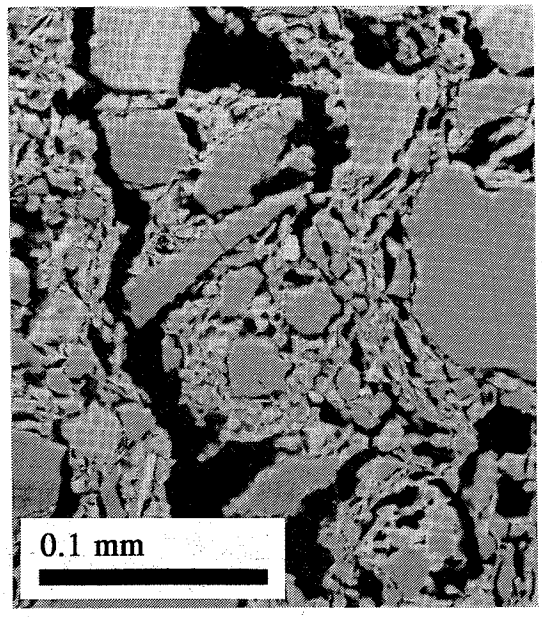

Figure 4.1. *Original graylevel image of red brick.*

Figure 4.2. *Segmented image of red brick. Area fraction of pores 0.266.*

Figure 4.3. *Opened image of red brick. Area fraction of pores 0.138.*

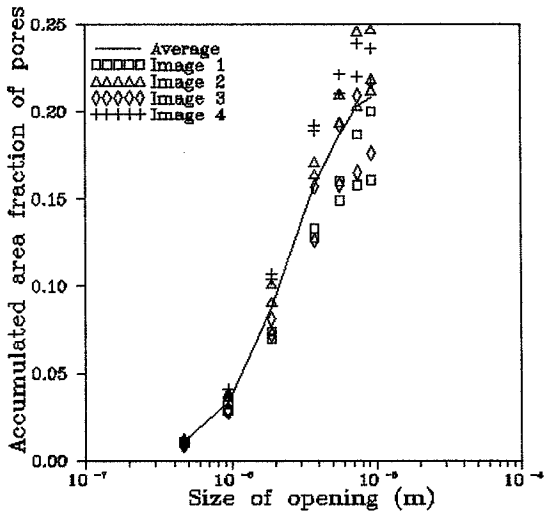

Figure 4.4. *Opening distribution for red brick. Average total area fraction of pores 0.28.*

Calcareous sandstone

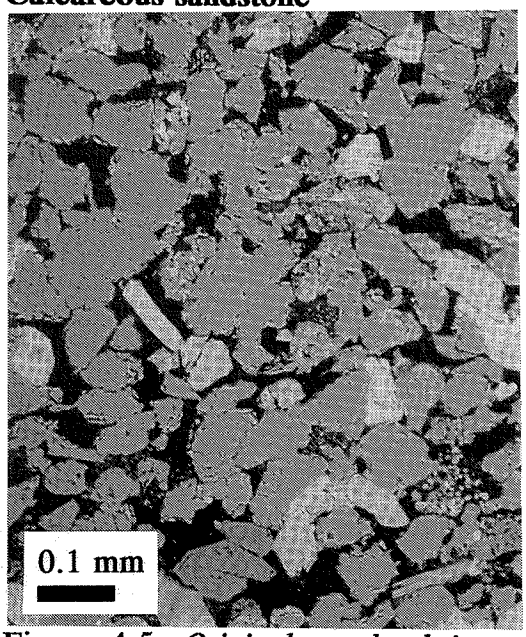

Figure 4.5. *Original graylevel image of calcareous sandstone.*

Figure 4.6. *Segmented image of calcareous sandstone. Area fraction of pores 0.215.*

Figure 4.7. *Opened image of calcareous sandstone. Area fraction of pores 0.064.*

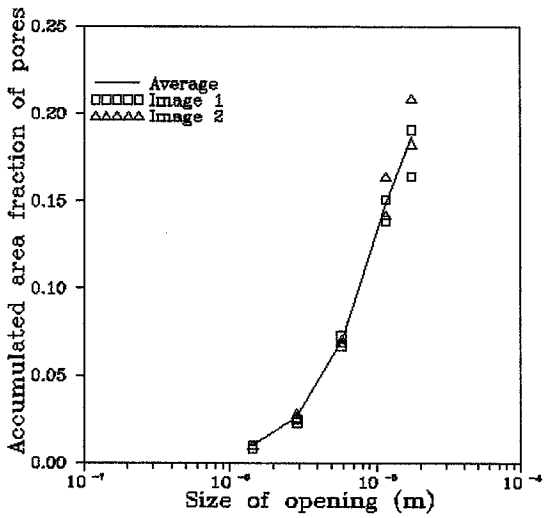

Figure 4.8. *Opening distribution for calcareous sandstone. Average total area fraction of pores 0.22.*

Silicious sandstone

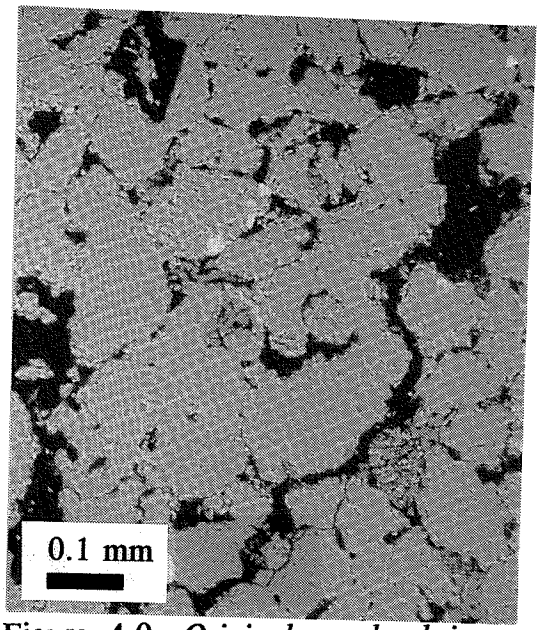

Figure 4.9. *Original graylevel image of silicious sandstone.*

Figure 4.10. *Segmented image of silicious sandstone. Area fraction of pores 0.175.*

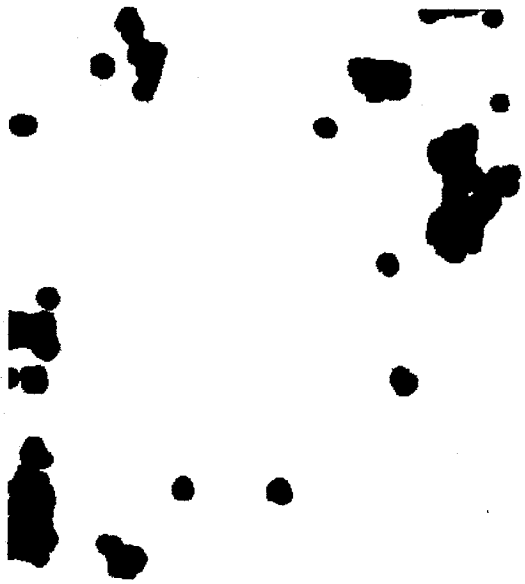

Figure 4.11. *Opened image of silicious sandstone. Area fraction of pores 0.084.*

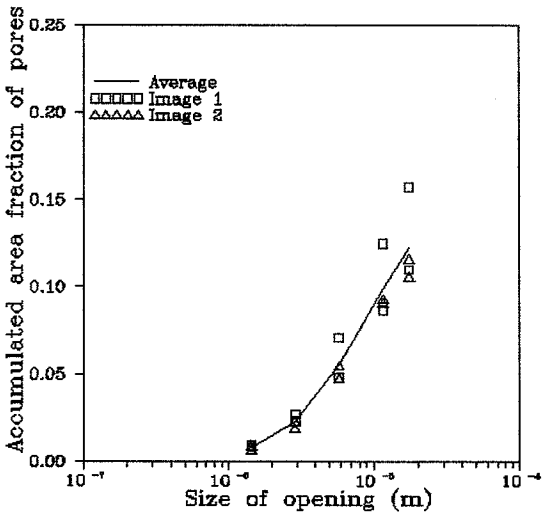

Figure 4.12. *Opening distribution for silicious sandstone. Average total area fraction of pores 0.18.*

Pit lime mortar

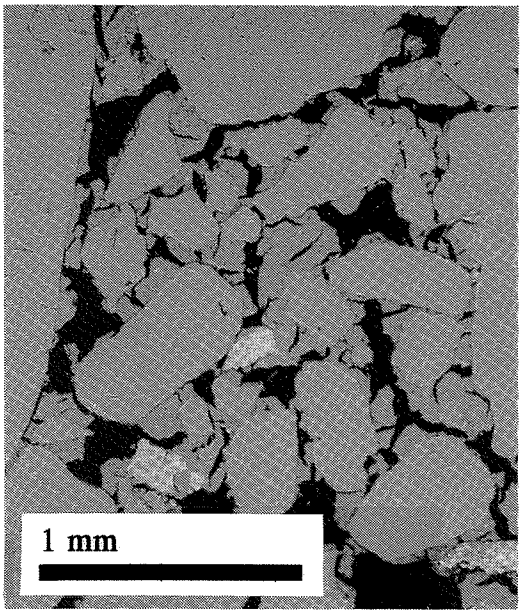

Figure 4.13. *Original graylevel image of pit lime mortar.*

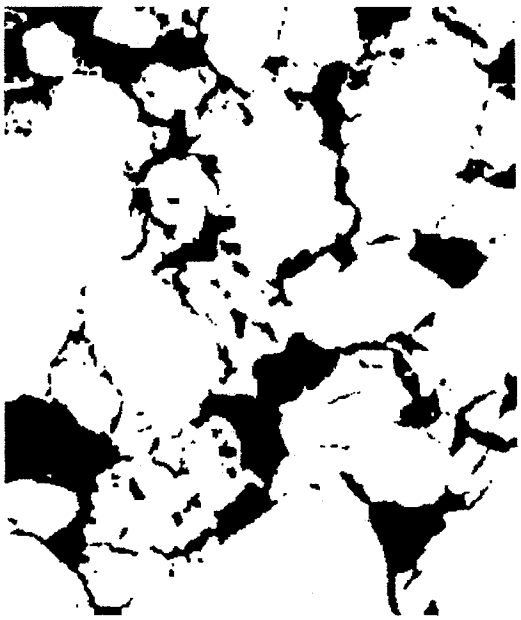

Figure 4.14. *Segmented image of pit lime mortar. Area fraction of pores 0.203.*

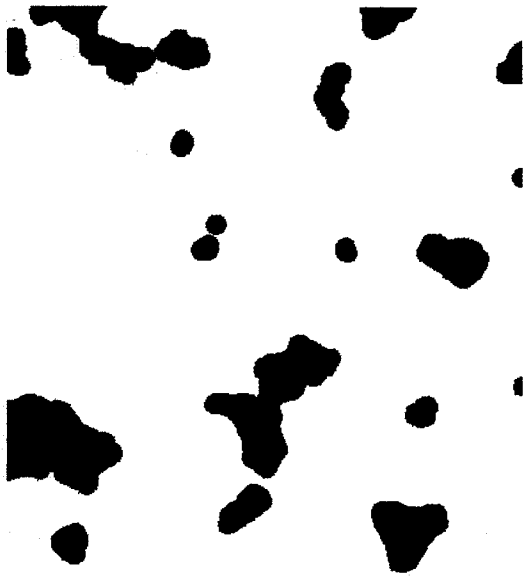

Figure 4.15. *Opened image of pit lime mortar. Area fraction of pores 0.125.*

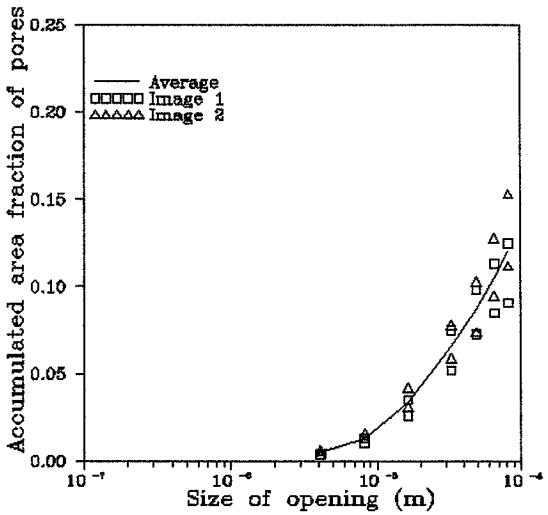

Figure 4.16. *Opening distribution for pit lime mortar. Average total area fraction of pores 0.20.*

Slaked lime mortar

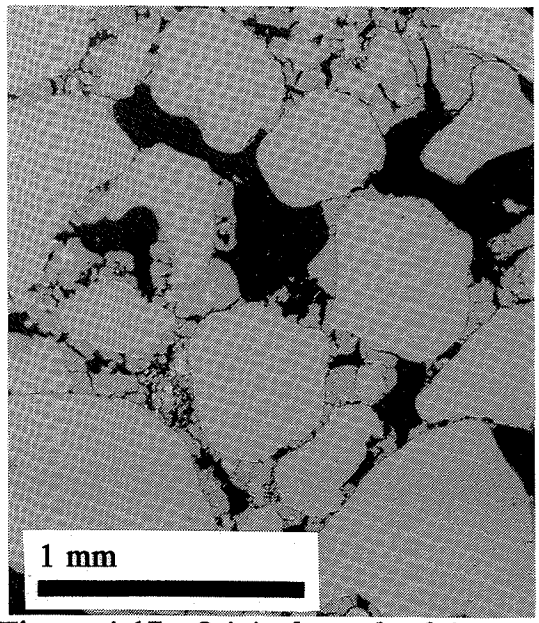

Figure 4.17. *Original graylevel image of slaked lime mortar.*

Figure 4.18. *Segmented image of slaked lime mortar. Area fraction of pores 0.210.*

Figure 4.19. *Opened image of slaked lime mortar. Area fraction of pores 0.158.*

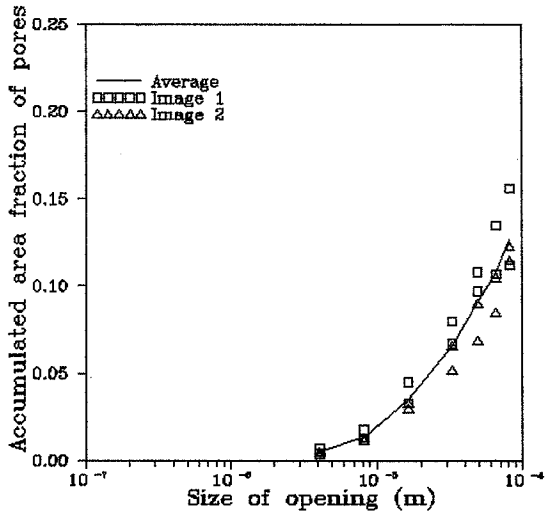

Figure 4.20. *Opening distribution for slaked lime mortar. Average total area fraction of pores 0.22.*

Mercury intrusion porosimetry (MIP)

Red brick, medieval brick from Odden church and pit lime mortar K100/1200 was analyzed in MIP. Sample size was 2-5 g. Results are given in figure 4.21 as accumulated fraction of pores at a given pore size and compared with results from digital image analysis.

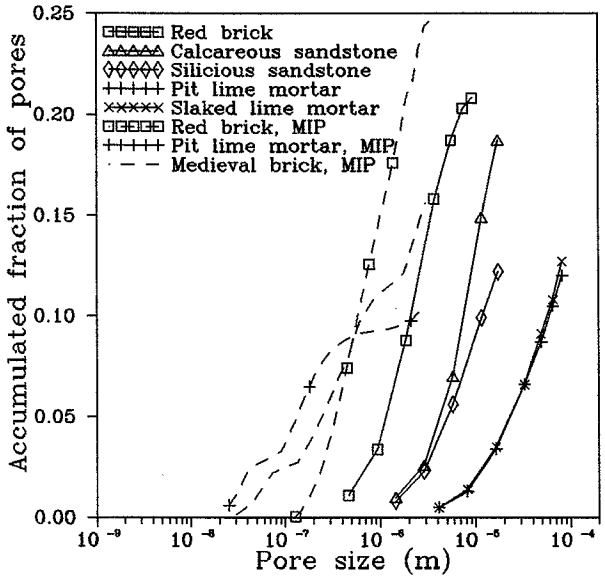

Figure 4.21. *Pore size distribution determinded by MIP and digital image analysis for brick, sandstone and mortar.*

4.5 DISCUSSION

The brick seen in figure 4.1 is composed of quartz grains (sand) seen as large bright particles in a matrix of an amorphous glass phase. Pores are seen as dark areas. Coarse pores and cracks are seen in a matrix of sand grains and glass phase and finer pores are observed in the glas phase. As the magnification of the SEM-image is rather high, the very coarse pores are not seen.

The calcareous sandstone seen in figure 4.5 is composed of quartz grains (sand) and feldspars (bright particles) in a matrix of calsite and quartz. Coarse pores are seen between sand grains and finer pores exist in the calcite cementation, but theese are not seen at this magnification. The packing of the sand grains is rather loose.

The silicious sandstone seen in figure 4.9 is similar to that of calcareous sandstone, but the packing is closer and only few feldspars is observed. The cementation consists only of quartz.

The lime mortar as seen on figure 4.13 and 4.17 is composed of quartz grains (sand) in a matrix of calcite cementation. The pores between sand grains are rather coarse and is

dependent on grain size. The packing is very loose. Fine pores exist in the calcite cementation, but theese are not seen at this magnification.

The total area fraction of pores in the image equals porosity determinded by water saturation for brick and sandstone, but is less than porosity for lime mortar. Total area fraction of pores depends on magnification. At low magnification the area fraction includes only coarse pores and at high magnification only fine pores. The total area fraction of pores equals porosity determinded by water saturation, if the main part of pores is seen in the image at the magnification selected. This must be the case for brick and sandstone but not for lime mortar. In lime mortar the fine pores in the calcite cementation and the very coarse pores are not seen.

The variation on area fraction of pores between fields is increasing with opening size due to accumulation of variations. For brick the variation is quite large approximately 10% for the largest opening size. For the other materials the maximum variation is approximately 5%. This variation is only due to inhomogenity of the material and the way images are selected. Repeated analysis of the same images and with the same equipment as described would give the same opening distribution.

In this work the standard deviation on total area fraction is not unreasonable large with only 4 fields. This is probably because only coarse pores are regarded and therefore the fields are relatively large. By increasing magnification and corresponding decreasing field size, the standard deviation would increases due to increasing inhomogenity between fields and therefore, a larger number of fields would be necessary to give a good estimate of the area fraction.

The area fraction of pores for maximum opening size is smaller than the total area fraction which means, that the maximum opening size should have been larger. This was not carried out as time for analysis on the computer used drastically increased with opening size.

For each material the total area fraction of pores are seen in the figure at the right of the original graylevel image, and the area fraction after a 8-pixel opening are seen in the figure below at the left. From theese the effect of opening is clearly seen. Opening removes fine pores and leaves the area fraction of coarse pores in the image.

In the same way, the area fraction of pores in the other pore size ranges are determined. For each material the accumulated area fraction of pores is determinded for 1, 2, 4, 8, 12, 16 and 20-pixel opening size. The pixel size is found from the field size and the number of pixels in the field as given above. For brick 8 fields was used and for the other materials 4 fields to determine an average opening distribution. The opening distribution for each field is given together with the average distribution.

As stated above, the range of pore sizes determinded is dependent on image magnification. Therefore, the pores determinded for brick are finer than for sandstone, which again are finer than for lime mortar. But this is not *caused* by image magnification, rather image magnification was selected to show the typical pore sizes existing in the material. The

minimum pore size which can be detected in SEM-backscatter images, is approximately 0.1 μm, which is regarded as coarse pores compared to pores in cement paste and lime cementation. The ranging of pore sizes in the materials above thus concerns coarse pores. In lime mortar and calcareous sandstone fine pores exist in the calcite cementation, and theese are finer than pores in brick. In brick probably no finer pores than detected in the SEM-image exists, but there may be very coarse pores and cracks which is not seen in the SEM-image at the selected magnification.

There is no difference in pore sizes between the two lime mortars. For the two sandstones, the difference in packing of sand grains is clearly seen, because the calcareous sandstone with loose packing has a larger area fraction of pores in the entire range.

Enhancement and segmentation in this work is quite simple. As enhancement only repeated sampling and an average filtering are used. Segmentation is done simply by one fixed threshold. This is possible because the contrast in the SEM-backscatter images are so high. When it is possible to obtain high contrast in the original graylevel images, this should be prefered to advanced image processing, as it is much more safe and less time consuming.

The images used in this work are selected so that they are "interesting", they include a reasonable mixture of pores and matrix. This way to select images is of course very subjective and dependent on the user judgement. The only objective way to select images is by statistical chance, but this would cause a lot of "wasted" images in which mainly pores or matrix were seen. The worst case would be to have 30 images only with pores and 70 images only with matrix giving the correct area fraction of pores, but no other information. This would be a rather expensive way to find total porosity. Of course, in practice things are not that bad, but a lot of effort could be saved by making a reasonable selection of images beeing aware that the method is subjective. This work indicates that although the way images are selected is subjective, it still gives a lot of information on pore structure.

Pore sizes determinded by MIP generally are smaller than by digital image processing. There are two reasons for this

1) pore sizes detectable by MIP are smaller than by digital image processing
2) pore sizes detected by MIP are decreased by the "ink bottle effect".

For red brick both the total volume fraction of pores detected by MIP and by digital image processing are of the same order of magnitude as total water filled porosity. There is an overlap in pore sizes between the two methods in the range 0.5 - 4.3 μm, in which MIP gives porosity 0.17 m^3/m^3 and digital image processing 0.16 m^3/m^3, which is not significantly different. In the pore size range 0.13 - 0.5 μm MIP gives porosity 0.08 m^3/m^3 and in the pore size range 4.3 - 9.4 μm digital image processing gives porosity 0.12 m^3/m^3. Assuming that the two methods are simply measuring pore sizes in two overlapping ranges, and therefore pore size distributions are additive, results in a total porosity of 0.37 m^3/m^3, which is larger than total water filled porosity. This indicates, that the pore sizes measured are not directly comparable. The main reason for this is attributed to "the ink bottle effect" in MIP, which results in a shifting against smaller pore sizes compared to digital image processing.

For pit lime mortar pore size ranges detected by the two methods do not overlap. Total porosity detected by MIP in the pore size range 0.03 - 3.2 μm is 0.10 m^3/m^3 and by digital image processing, in the pore size range 4.1 - 82 μm, 0.12 m^3/m^3. The total 0.22 m^3/m^3 is less than the total water filled porosity 0.29 m^3/m^3 which might be attributed to porosity out of the detected pore size ranges. It seems, that "the ink bottle effect" is of minor importance for pit lime mortar. Pit lime mortar has, as stated above, two distinct pore size ranges; fine pores in the calcite cementation and coarse pores in between sand grains. The "ink bottle effect" might be of minor importance because the fine pores do not block the access to the coarse pores, which is observed in figure 4.13. The coarse pores are not detectable in MIP because detection demand very low pressure, and because they are crushed in the relatively small sample used for MIP. The fine pores are not betectable in digital image processing because they are finer than the resolution in SEM backscatter images. The fine pores are seen in polished sections as a light blue colouring of the calcite cementation by the dark blue dye used in the resin for imbending.

Comparing volume fraction of pores detected by MIP for modern, red brick and medieval brick it is seen, that medieval brick has finer pores than modern brick. Theese finer pores are in the same pore size range as the fine pores detected in pit lime mortar and therefore, they are not detectable in digital image processing, as stated above. Total porosity detected by MIP is 0.16 m^3/m^3 which is only half the total water filled porosity. It seems that MIP are not able to detect the very coarse pores and cracks that exist in medieval brick.

Although not complete comparable, MIP and digital image processing seems to complement each other, especially for materials with two distinct pore size ranges. MIP is suitable to detect fine pores and digital image processing to detect coarse pores. For materials with a continuous pore size distribution one should be aware that the "ink bottle effect" might influence the results from MIP. Though fine pores are not detectable in digital image processing, the method is advantageous compared to MIP in the sence that the geometrical composition of the material and the geometrical distribution of pores are seen in two dimensions in polished sections and in SEM-backscatter images. On the other hand, it might be difficult to use the information quantitatively, and for this purpose MIP is advantageous.

5. EXPERIMENTS ON TRANSPORT AND EXTRACTION OF SALTS

In this chapter experimental results to demonstrate the effect of salts on porous materials are presented. This include sorption isotherms (equilibrium), capillary suction (salt movement) and salt extraction. Salt extraction are carried out on a large-scale in medieval brick church vaults and in laboratory (electro-chemical extraction). Observations from accelerated and natural weathering of small brick walls are presented. Finally the model to calculate salt and moisture transport presented in section 3.2 is used to simulate transport in a church vault and the result is compared to observations from Odden church.

5.1 CHARACTERIZATION OF MATERIALS

Introduction

Two different materials are used in most of the experiments in this work to show how salts affects material properties. These materials are brick and calcareous sandstone. The effect of salt ions and crystallized salt on material properties depend on both pore structure and mineralogical composition of the material. Below is for that reason given a charaterization of these two materials.

Brick

The brick was a red, modern brick burned at low temperature (980 $^{\circ}$C) size 215 by 103 by 65 mm (British Standard). Dry density was 1870 kg/m^3, bulk density 2650 kg/m^3 and porosity 0.29 m^3/m^3. From thin section analysis and X-ray diffraction the brick was found to consist of quartz, feldspar (plagioclase), hematite (red colour) and an amorphous glass phase.

Calcareous sandstone

The sandstone was an exposed swedish calcareous sandstone (Gothlandish sandstone) taken from Lerchenborg castle. Dry density was 2120 kg/m^3, bulk density 2670 kg/m^3 and porosity 0.21 m^3/m^3. Gothlandish sandstone is a fine granular, homogeneous gray blue stone with calcite and rich in mica. From thin section analysis and X-ray diffraction the sandstone was found to consist of quartz, calcite, feldspars (microcline, anorthite) and clay-minerals (illite, kaolinite). By EDAX-analysis of the elements, the sandstone was determinded to consist of 9 wt% calcite ($CaCO_3$), 15% feldspar (microcline ($KAlSi_3O_8$)) and 76 wt% quartz (SiO_2). Calcite is found both as grains and as cementation. A large part of the cementation is quartz grains grown into an interlocking lattice.

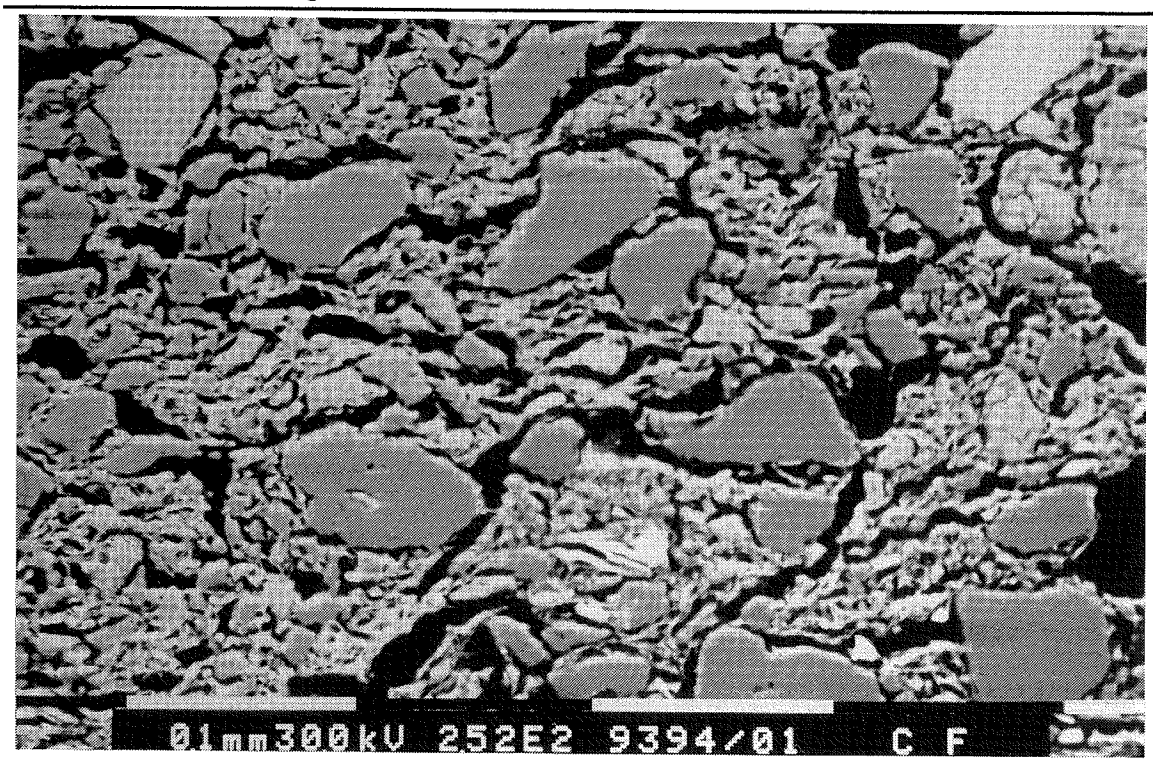

Figure 5.1. *Pore structure in red brick seen in SEM-backscatter image of polished section.*

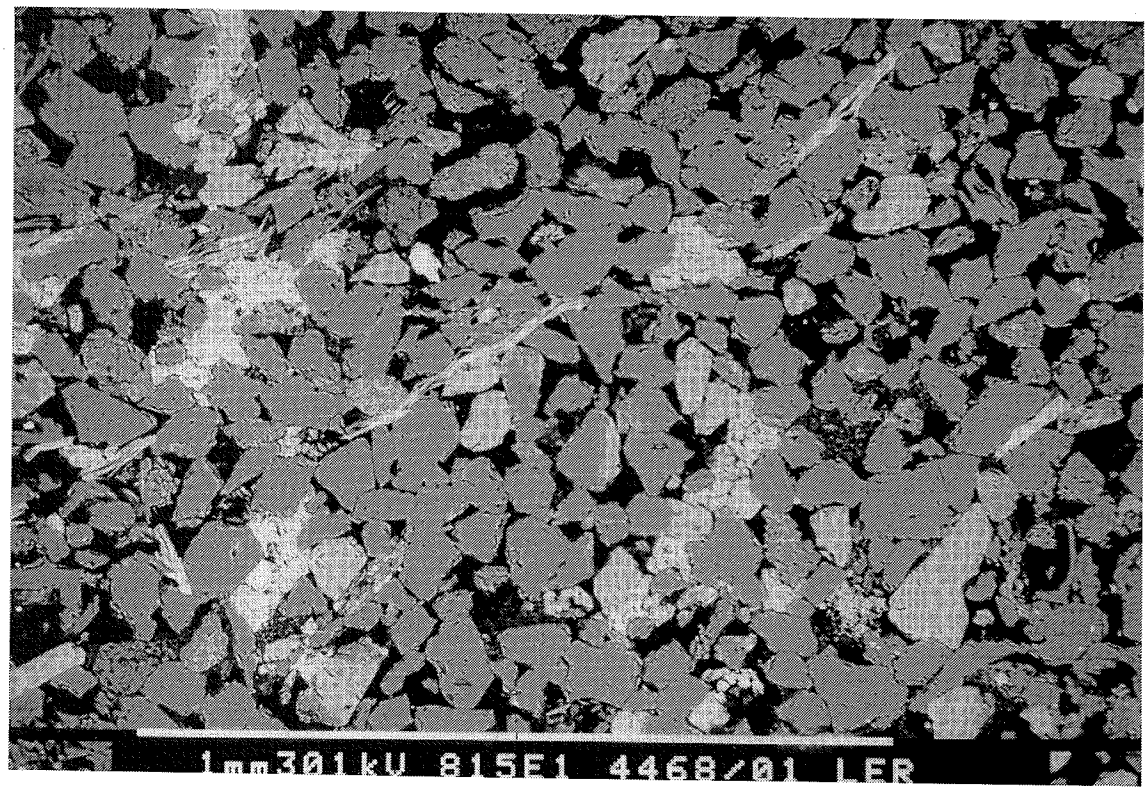

Figure 5.2. *Pore structure in calcareous sandstone seen in SEM-backscatter image of polished section.*

5.2 SORPTION ISOTHERMS

Introduction

Materials containing salts act hygroscopically even though they are not hygroscopic themselves. This is due to the hygroscopic properties of the salt as described in section 2.2. As an approach, the sorption isotherm of a slightly hygroscopic material with salts is calculated by simply adding sorption isotherms for the material and sorption isotherms for the salts. The purpose of these experiments was to test this approach and to see how long time it takes to reach equilibrium for a salt solution.

Experimental procedures

14 samples of approximately 75 g cut from brick and calcareous sandstone described in section 5.1 was immersed in 7 different salt solutions for 4 hours and dried at 105 °C until mass equilibrium. The dried samples were crushed into grains of size 1-5 mm and left in desiccators at 20 °C above saturated salt solutions at 33 %, 85 %, 92 % and 96 % relative humidity. Hygroscopic water uptake was determined by weighing after 13, 55 and 91 days. Samples of the 7 salt solutions was left at the same relative humidity, and hygroscopic water uptake determined in the same way. Salt content of solutions and samples after capillary suction is given in table 5.1. All results are average of two samples.

Table 5.1. *Salt solutions for capillary suction and salt content of samples for sorption isotherms.*

Nr.	Salt in 1000 g water	Salt content (wgt%)	
		Brick	Sandstone
1	Distilled water	-	-
2	40 g NaCl	0.38	0.25
3	120 g $MgSO_4 \cdot 7\ H_2O$	0.52	0.32
4	20 g Na_2SO_4	0.19	0.13
Two salts			
5	a: 40 g NaCl b: 120 g $MgSO_4$	0.35 0.52	0.24 0.36
6	a: 40 g NaCl b: 20 g Na_2SO_4	0.37 0.19	0.26 0.13
7	a: 20 g Na_2SO_4 b: 120 g $MgSO_4 \cdot 7\ H_2O$	0.18 0.54	0.12 0.36

Results

All measured data are illustrated in figure 5.3-8. Data for 33 % relative humidity is neglected. Moisture contents after 93 days are used. To compare, the theoretical approach found by adding moisture content for the salt free material, and moisture hygroscopically bound by the salt, is calculated for the three relative humidities and for saturation humidities of the salts.

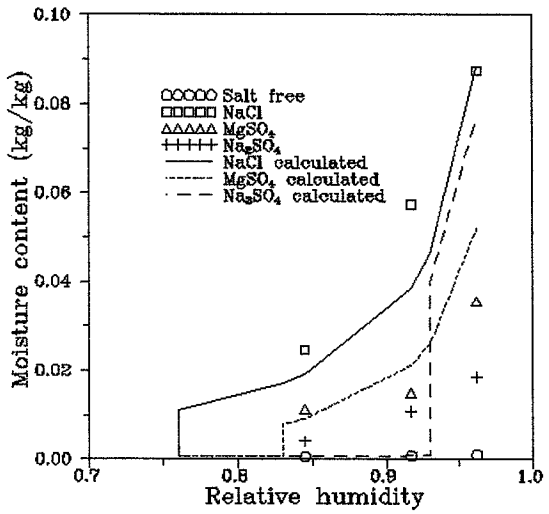

Figure 5.3. *Sorption isotherm at 20 °C for brick with one salt.*

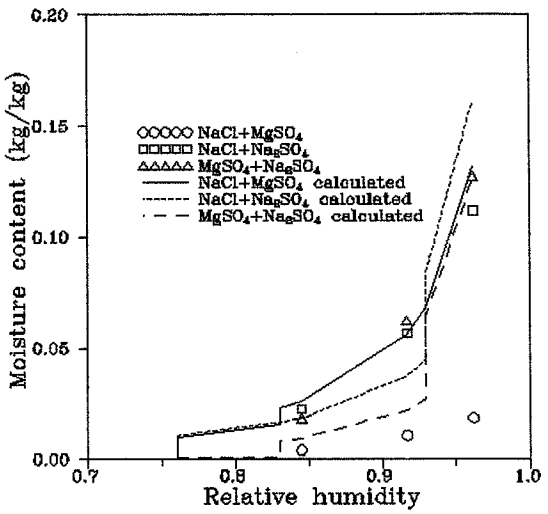

Figure 5.4. *Sorption isotherm at 20 °C for brick with two salts.*

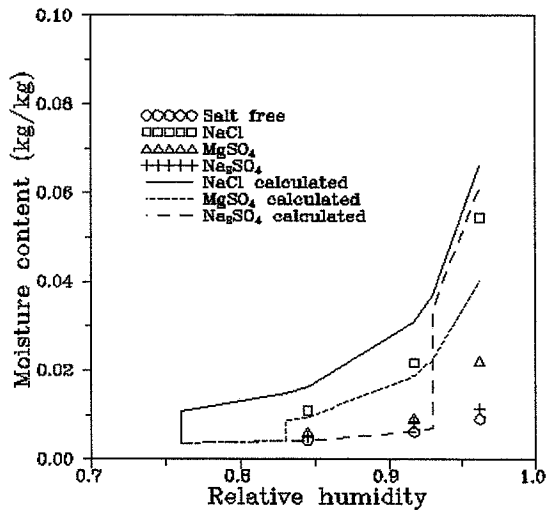

Figure 5.5. *Sorption isotherm at 20 °C for calcareous sandstone with one salt.*

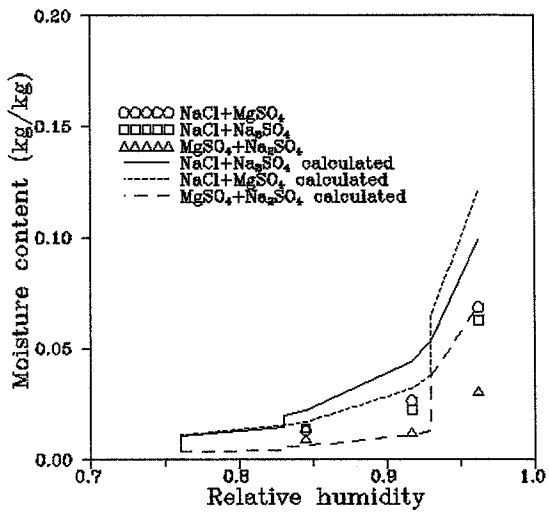

Figure 5.6. *Sorption isotherm at 20 °C for calcareous sandstone with two salts.*

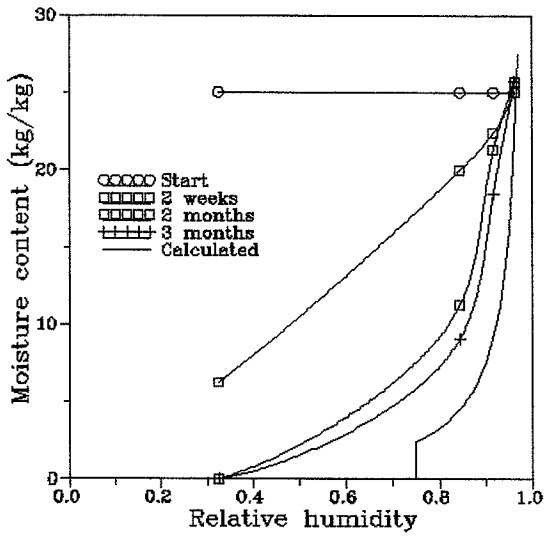

Figure 5.7. *Course of desorption at 20 °C for a NaCl-solution starting at 3.8 wt% concentration.*

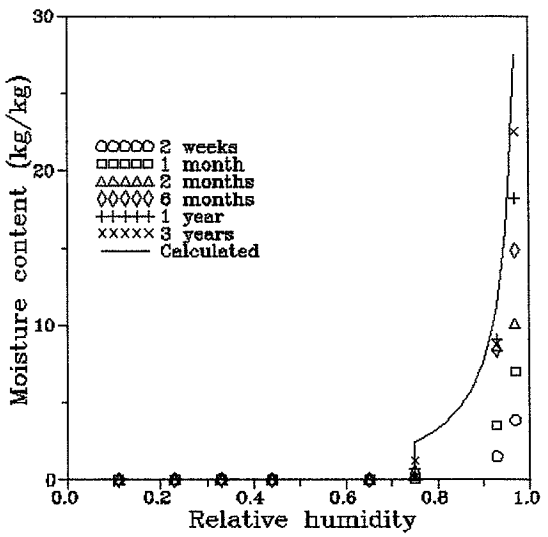

Figure 5.8. *Course of adsorption at 20 °C for NaCl starting as dry salt. Experiments by AN/br, Building Materials Laboratory.*

Discussion

Data for 33 % relative humidity is neglected as moisture content was very low, and there was no significant difference between salt free material and saline material. Data for moisture content after 13 and 55 days is neglected as there was no significant difference between moisture contents and therefore, the course of sorption could not be determinded.

The measured adsorption of material with sodium chloride is nearly as calculated, for brick it is a little above and for sandstone it is a little below. The measured adsorption for material with magnesium sulphate is less than calculated for both brick and sandstone, most for sandstone and at high relative humidities. For material with sodium sulphate adsorption is larger than calculated below the deliquescence point and much less above.

The measured adsorption of brick with mixed sodium chloride and magnesium sulphate is much less than calculated. It almost seems, that a new combination salt with different adsorption is formed. With the present ions it is possible to form magnesium chloride, and sodium sulphate as well. Adsorption of sandstone with sodium chloride and magnesium sulphate is also less than calculated.

Adsorption of brick with mixed sodium chloride and sodium sulphate is larger than calculated below the deliquescence point and less above. For sandstone adsorption is always less than calculated.

Adsorption of brick with sodium and magnesium sulphate is larger than calculated below the deliquescence point and and as calculated above. For sandstone adsorption is as calculated below the deliquescence point and much less above.

It seems that adsorption below the deliquescence point is larger than calculated. This migt be caused by the interaction between moisture from the material and moisture from the salt as stated in section 2.2. Interaction also means, that moisture content above the deliquescence point should be larger than calculated by adding sorption isotherms. This is not observed.

On the contrary for all measured data it seems that adsorption at high relative humidities is less than calculated. This might be because equilibrium is not reached within 3 months or, because there is a lack in moisture capacity of the salt solution in the desicator. In this case relative humidity decreases and a new equilibrium is reached depending on the amounts of salts in the desiccator.

From the course of desorption of a sodium chloride solution it is seen, that even after 3 months the solution has not reached the calculated equilibrium. To reach equilibrium at high relative humidities by adsorption for dry salt takes up to 3 years. Therefore, to reach equilibrium in a porous material at high relative humidities by adsorption might take very long time, as the proces is controlled by diffusion of vapour into the porous material. At lower relative humidities equilibrium is reached quicker as smaller quantities of moisture has to be transported into the material.

5.3 CAPILLARY SUCTION OF SALT SOLUTIONS

Introduction

Capillary suction of salt solutions is different from capillary suction of pure water due to differences in surface tension, liquid density and viscosity of the salt solution as described in section 2.1. Evaporation of water from the surface during capillary suction will cause precipitation of salts inside or at the surface of the material, as it is seen on solid walls with rising groundwater. Crusts on the surface influence evaporation and precipitation of salts. The purpose of these experiments was to determine the water uptake coefficient, water capacity and evaporation rate for different solutions in brick and sandstone, and to see how much salt content would increase during two days suction.

Experimental procedures

24 specimens of average size 57 by 57 by 104 mm were made out of brick described in section 5.1 and conditioned at 20 °C, 50 % relative humidity. Specimens were immersed a few mm in 6 different liquids to absorb liquid by capillary suction from one end (size 57 by 57 mm). The other surfaces of the specimens were *not* covered to prevent evaporation. Mass content was determined by weighing after 1, 2, 4, 8.. minutes until 2 days. After this

specimens was left to dry at 20 °C, 50 % relative humidity for 5 days and mass content was determined by weighing with the same intervals as for capillary suction. Finally specimens were dried at 105 °C to determine the increase in mass content due to precipitations. The 6 different liquids used and some properties are given in table 5.2.

12 specimens of average size 45 by 36 by 120 mm were made out of calcareous sandstone described in section 5.1 and conditioned at 20 °C, 50 % relative humidity. 6 specimens had a crust on one side (size 45 by 120 mm) from exposure at Lerchenborg castle of the original structural element. From the others the crust was cut off. Specimens were immersed a few mm in 2 different liquids; distilled water and a NaCl-solution (2) as described in table 5.2. Specimens were absorbing the liquid by capillary suction from one end (size 45 by 55 mm) parallel to the crust. The other surfaces were left uncovered for free evaporation. Mass content was determinded in the same way as for brick specimens.

Table 5.2. *Liquids for capillary suction and some properties (CRC 1984).*

Nr.	Liquid	σ 10^{-3} (N/m)	ρ (kg/m^3)	η 10^{-3} (kg/s m)
1	Distilled water	72.75	997	1.002
2	295 g NaCl 1000 g water	80.95	1138	1.7
3	144 g Na_2SO_4 1000 g water	75.45	1066	1.2
4	8 g detergent 1000 g water	< 72	979	Unknown
5	4 g detergent 148 g NaCl 1000 g water	< 72	1066	Unknown
6	96 vol% ethanole	22.75	807	1.2

Results

Mass content of the specimens as function of time is given in figure 5.9-10. From this liquid uptake coefficient, liquid capacity and evaporation after suction is calculated for all specimens and given in table 5.3.

From capillary suction of distilled water the equivalent poreradius for brick and sandstone is calculated from (3.13). With this value the water uptake coefficient W is calculated from (3.12) for salt solutions and ethanole. Evaporation during suction is calculated from (3.22) and the salt salt content after suction. Evaporation surface is calculated as total surface area of specimen excluding suction surface area. Time during which capillary suction took place was 2 days.

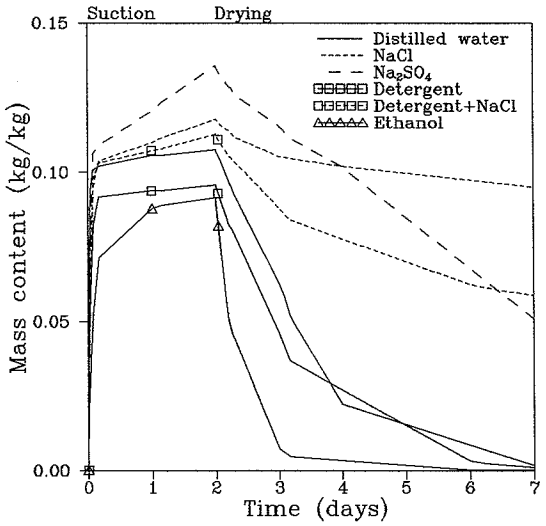

Figure 5.9. *Capillary suction and drying of brick with different liquids.*

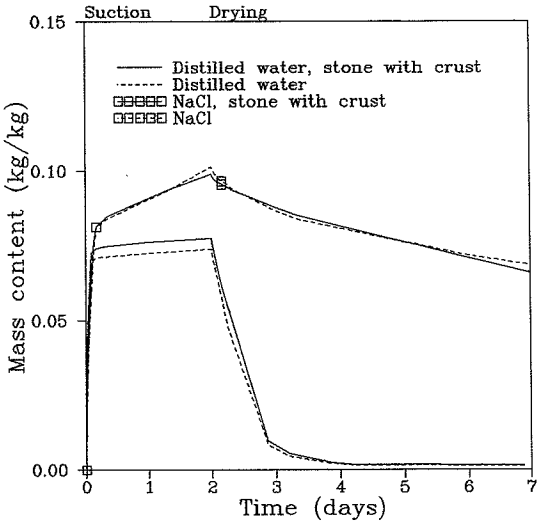

Figure 5.10. *Capillary suction and drying of calcareous sandstone.*

Table 5.3. *Moisture transport data for brick and calcareous sandstone with different liquids given in table 5.2.*

	Liquid uptake cofficient, W [kg/m² s½]		Liquid capacity, u_k [kg/kg]	Evaporation after suction 10^{-5} [kg/m² s]	
	Avg.	Std.	Avg.	Avg.	Std.
BRICK (average of 4 specimens)					
Water	0.30	0.02	0.101	1.21	0.05
NaCl	0.23	0.01	0.095	0.55	0.05
Na_2SO_4	0.27	0.03	0.106	0.53	0.02
Detergent	0.20	0.02	0.092	1.33	0.07
Deterg. + NaCl	0.23	0.03	0.103	0.68	0.02
Ethanole	0.12	0.003	0.089	5.4	0.2
CALCAREOUS SANDSTONE (average of 3 specimens)					
Water, clean	0.21	0.01	0.071	2.35	0.05
Water, crust	0.25	0.003	0.074	1.84	0.03
NaCl, clean	0.18	0.02	0.081	0.6	0.2
NaCl, crust	0.21	0.003	0.081	0.4	0.1

Table 5.4. *Calculated moisture transport data for brick and calcareous sandstone for different liquids given in table 5.2.*

	W, calculated (3.12) [kg/m² s^{½}]	Evaporation during suction (3.15) 10^{-5} [kg/m² s]	Salt content after suction [kg/kg]
BRICK	r = $2.9 \cdot 10^{-8}$ m (3.13)		
NaCl	0.27	2.9	0.076
NaCl+detergent	-	0.9	0.023
Na_2SO_4	0.30	2.2	0.037
Ethanole	0.12	-	-
CALCAREOUS SANDSTONE	clean: r = $2.8 \cdot 10^{-8}$ m (3.13) crust: r = $3.9 \cdot 10^{-8}$ m		
NaCl	0.20	0.64	0.036
NaCl, crust	0.23	0.49	0.032

Discussion

The liquid uptake coefficient is calculated for specimens with evaporation and therefore is smaller than the actual liquid uptake coefficient. The decrease can be estimated for capillary suction of water from (3.21). Assuming that evaporation rate is $1.2 \cdot 10^{-5}$ kg/m² s (measured evaporation rate after suction of water), the perimeter for a brick specimen 22.8 cm, porosity 0.29 m³/m³, suction surface 32 cm² and the time interval for calculation of water uptake coefficient 1 hour gives a decrease in water uptake coefficient of 1%. This is of the same order of magnitude as standard deviation and is therefore neglected in the calculations below.

The liquid uptake coefficient for sodium chloride is significantly less than for water, only about 75 % of the water uptake coefficient. The calculated liquid uptake coefficient is larger then the measured, about 90% of the water uptake coefficient. In this calculation the contact angle is assumed to be $\Theta=0^\circ$. As stated in section 2.2 the contact angle increases with salt content. The calculated liquid uptake coefficient equals the measured for $\Theta=43^\circ$. This value is not unlikely for a nearly saturated salt solution.

Detergent in the sodium chloride solution does not seem to have any effect on the liquid uptake coefficient, even though surface tension decreases. This might be due to a simultaneous decrease in contact angle or an increase in viscosity.

For sodium sulphate, the liquid uptake coefficient is not significantly less than the water uptake coefficient compared to standard deviations. The calculated value equals the water

uptake coefficient, but as before contact angle is assumed to increase with salt content, and for $\Theta=36^{\circ}$ the calculated liquid uptake coefficient equals the measured.

For ethanole, the liquid uptake coefficient is much less than the water uptake coefficient. As the calculated liquid uptake coefficient equals the measured, this must be due to decrease in surface tension. The error calculated from (3.21) on the measured liquid uptake coefficient from evaporation is about 7%.

For brick there is no significant difference in liquid capacity between different liquids.

As the water content immediately after capillary suction is controlled by convective moisture transfer, evaporation after suction can be calculated from (3.19). The convective moisture transport coefficient is calculated from the rate of evaporation for brick with water. The Kelvin equation and equivalent pore radius gives 96 % rh in the pores at the surface of the material. Assuming that relative humidity of the ambient air is 50 % at 20 °C one obtains $\beta=1.1 \cdot 10^{-8}$ kg/m^2 Pa s.

For a saturated sodium chloride solution in brick at the given equivalent pore radius relative humidity in the pores is 72 %. With the assumptions above calculated evaporation rate is then $0.57 \cdot 10^{-5}$ kg/m^2 s which agrees quite well with the measured evaporation rate. For a saturated sodium sulphate solution in brick relative humidity is 89 % which gives a calculated evaporation rate of $1.0 \cdot 10^{-5}$ kg/m^2 s. This is twice the measured value. This might be caused by efflorescence on the surface, which decreases evaporation rate. This is not observed for sodium chloride, because efflorescence is much less due to the lower deliquescence point of sodium chloride.

Detergent solution has a larger evaporation rate due to the low surface tension. If relative humidity is assumed to be 99 % the calculated evaporation rate is $1.26 \cdot 10^{-5}$ kg/m^2 s, which is less than the measured value. The surface tension corresponding to 99 % rh calculated from the Kelvin equation is $19 \cdot 10^{-3}$ N/m which is not unlikely.

Sodium chloride solution with detergent has a larger evaporation rate than without. The calculated evaporation rate equals the measured at relative humidity 0.76 which, according to the Kelvin equation, corresponds to surface tension $\sigma=47 \cdot 10^{-3}$ N/m. This is in the range between surface tension for detergent solution and surface tension for a saturated sodium chloride solution.

Calculated evaporation during suction for brick with sodium chloride or sodium sulphate is more than 5 times the evaporation after suction and more than twice the evaporation for brick with pure water after suction. This might be caused by an increase in surface during suction due to precipitated salts on the material surface. As more and more salt precipitate pores are blocked and evaporation decreases.

By capillary suction of sodium chloride solution with detergent, the salt content after suction is less than one third of the salt content obtained by capillary suction of sodium chloride solution without detergent. Initial capillary suction is not different, and therefore the different

salt content must be caused by different evaporation during suction, as calculated in table 5.4. Detergent might influence precipitation of the salt and decrease the surface of precipitated salts on the material surface.

Calcareous sandstone has a smaller water uptake coefficient than brick. The water uptake coefficient for sandstone with crust on one side is larger than without crust corresponding to a larger equivalent pore radius for sandstone with crust. This might be due to decay of the surface causing larger pores.

The calculated characteristic pore size is about 100 times smaller than measured geometric pore size in chapter 4. The characteristic pore size is not a geometric meassure, it includes the resistance to moisture transport due to pore shape and connectivity, and therefore the two pore sizes are not directly comparable.

Calculated liquid uptake coefficients for sandstone with sodium chloride is larger than measured assuming contact angle $\Theta=0^{\circ}$ but equals measured value for $\Theta=35^{\circ}$. This is a little less than for brick, which is not unlikely.

Evaporation after suction for sandstone with water is larger than for brick. The crust decreases significantly evaporation at about 20%. Sandstone with crust thus has larger rate of liquid uptake parallel to the crust surface (rising groundwater) and less rate of evaporation than sandstone without crust.

Evaporation after suction for sandstone with sodium chloride solution is of the same order of magnitude as for brick. Convective moisture transport coefficient, calculated from the rate of evaporation for sandstone with water, is $1.7 \cdot 10^{-8}$ kg/m^2 Pa s for sandstone with crust and $2.2 \cdot 10^{-8}$ kg/m^2 Pa s for sandstone without. Assuming the same relative humidities as for brick this gives a calculated evaporation rate after suction for sandstone with NaCl and crust at 0.9 kg/m^2 s and 1.1 kg/m^2 s for sandstone with NaCl and without crust. This is about twice as much as measured evaporation rates. This might be due to an observed strong efflorescence on the surface.

Efflorescence on sandstone specimens is seen in figure 5.11. From left to right are A) specimen without crust with water, B) specimen without crust with NaCl-solution, C) specimen with crust with water and D) specimen with crust with NaCl-solution. Damage was only observed for specimen with crust and NaCl-solution. By drying of specimen the crust was split up in thin layers and a distinct bubble was formed on the surface. Initially the bubble was growing and later a crack was formed on top of the bubble horizontally across the specimen.

The behaviour is similar to that observed for stone and mortar layers on buildings as described in section 1.2. By drying the crust initially shrinks less than the underlying stone giving the bubble due to bad adherence between crust and stone. Later on the crust shrinks more, and a crack is formed across the top of the bubble.

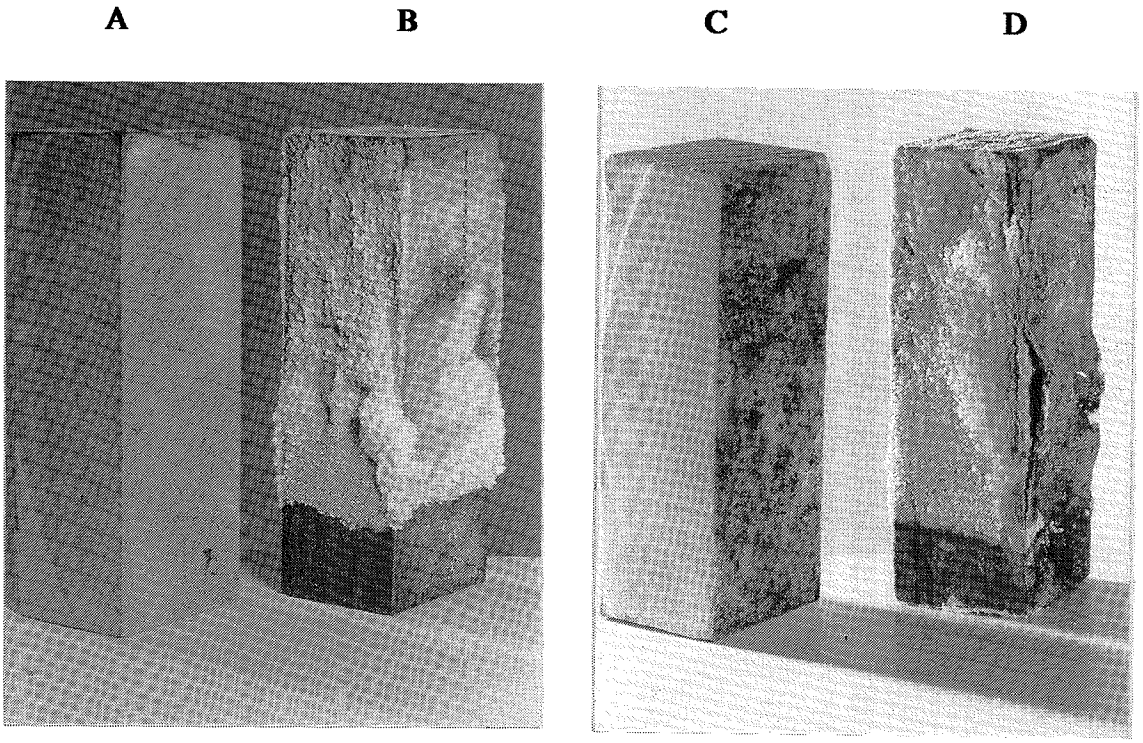

Figure 5.11. *NaCl-efflorescence on sandstone with crust compared to sandstone without crust. Crust is peeling by drying on specimen with salt.*

5.4 EXTRACTION OF SALTS IN CHURCH VAULTS

Introduction

Dust and powderfall has been observed in medieval churches in the western part of Jutland in Denmark, mainly in coastal regions. The problem seems to be the same in other parts of Denmark and in foreign countries, and the cause is clearly the contents of water soluble salts in the vault. By restoring of churches and uncovering of wall paintings it is common to plaster the top side of the vault to protect the medieval bricks against deterioration. Scientists in Denmark and foreign countries agree that the only effective way to stop deterioration is to extract the salts. The Towers of London is an example of an attempt reported by Bowley (1975) to extract salts by plastering with clay on the surface of the wall. Other materials used for salt extraction are paper pulp and lime mortar. The plastering of the church vaults was expected to extract salts, but theese plasterings was left for a long time, and there was no measurements of to what extent the mortar really extracted salts.

The method used for extraction of salts are the socalled "sacrificial material method". The principle is to move the soluted salts by capillary suction from the material that has to be protected to a sacrificial material where the salts will precipitate. The sacrificial material containing the salts can then be removed. The principle is illustrated in figure 5.12.

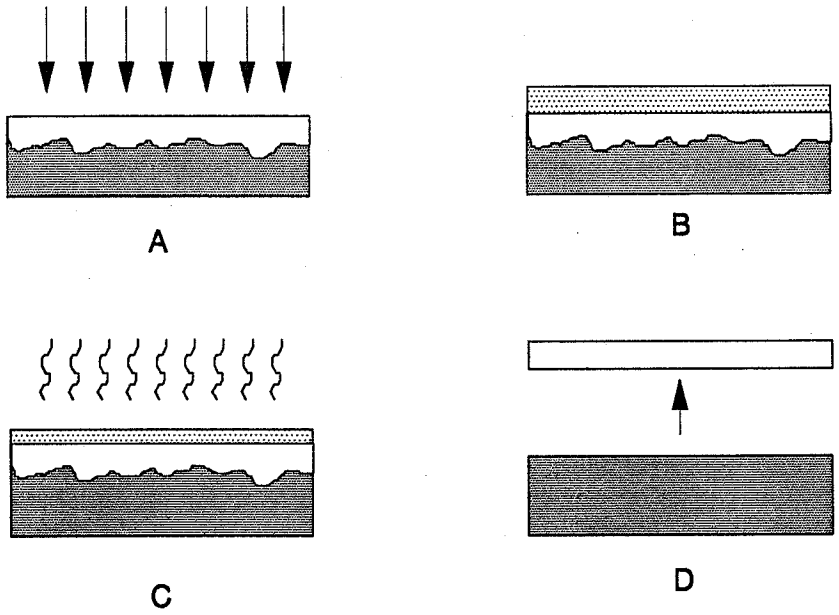

Figure 5.12. *Extraciton of salts by sacrificial layer method. A) Wetting of material. B) Plastering with sacrificial layer. C) Evaporation and extraction. D) Removal of sacrificial layer.*

Investigations in Alslev church in western Jutland - a case story

Alslev church is situated in the southwestern part of jutland. The church has a relatively narrow tower with a small vault inside. Above the nave are two and in the chancel one vault with eight ribs. About 20 years ago a heating fan system was established with warm air blown from the tower room over the underneath of the western vault in the nave. Powder fall has not been reported in this period, but by stages repairs with tar and emulsion paint was carried out. In 1979 the spalling was so servere that a complete restoration was needed. In this connection wall paintings was discovered on the vaults of the nave and chancel. The wall paintings was uncovered and restored. The heavy powder fall continued, and investigations established that the vaults contained salts which, in connection with periodic changes in climate, caused the plaster to fall. In figure 5.13 are given the amount of dust fall as a function of mean relative humidity. It indicates that dust fall is at its maximum when mean relative humidity is around 0.75, the deliquescence point of sodium chloride.

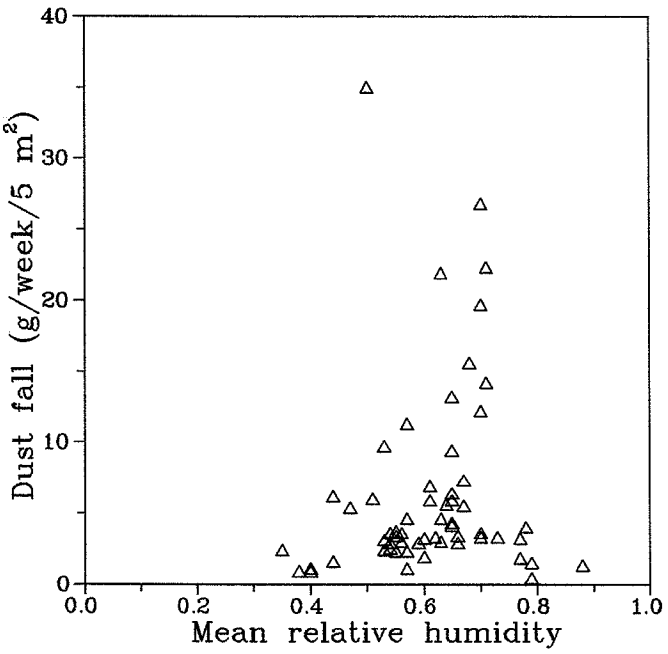

Figure 5.13. *The quantity of dust fall as a function of the weekly mean relative humidity in Alslev church. Larsen and Nielsen (1990).*

In the summer 1988 the heating system was changed to a convective heating system. The vaults were cleaned with water and whitewashed underneath. The wall paintings was restored in the eastern vault in the nave and the vault in the chancel, whereas they were not restored in the western vault.

In december 1988 the western vault in the nave was cleaned underneath with a steel brush and treated with limewater, and one fourth of the top side was plastered with lime mortar. The church loft over the western vault was at the same time isolated with plastic foil from the rest of the loft, and the climate was controlled to 15 °C, 50-60 % relative humidity by a heater and dehumidifier.

The most servere damages are through the entire period observed on the western vault in the nave, smaller damages are observed on the other vaults. The roof over the western vault has been leaky for 6-7 years. Today this is repaired, but considerable amounts of moisture and salts must have been carried to the vault. Combined with the fan heater this may have given the servere damages of particularly the western vault.

In the heating season the temperature in the church was kept at 8 °C when not in use, at services raised to 20 °C which made the relative humidity to drop from 70-80 % rh to 50-60 % rh. With the old heating fan, the heating started on saturday to make the church warm till sunday morning. With the new heating system, the heating starts only 4 hours before the service, and the entire heating period is at most 5-6 hours.

The dust fall is most intense after heating but is also observed in between heatings. The dust fall in between heatings may be material that are loosened during heating and then fall by air flow and minor climate changes. The dust fall was stopped in a period of 1-2 months after the change of the heating system and the cleaning with water. Samples from the lower side of the brick in the vault showed a considerable decrease in chloride content, but as samples from the upper side of the vault was not analyzed, one cannot exclude the possibility that chlorides was concentrated in the upper side of the vault. About two months later dust fall was again observed, though in smaller amounts. This reduction might be caused by the lower chloride content or by the change in heating system.

After cleaning the vault, plastering one fourth of the top side and start of climate control on the loft in december 1988 the dust fall stopped. Two months later, the climate control was stopped, and the dust fall started again to the same extent as before. Climate control started again a month later but now there was no effect. What was the reason for this ? As three different attempts was carried out at the same time, trying to stop the dust fall, it is very difficult to tell. The control of the climate may have kept the salts in the upper side of the vault during the first period of climate control, between the two periods the salts may have moved to the lower side, and then in the second period it was not possible to draw the salt back. It is also possible that climate control had no effect and that the cleaning alone stopped the dust fall. A similar improvement of the same duration was observed after cleaning the vault with water the previous summer.

The plastering on the top side of the vault combined with climate control did not stop the dust fall. Water will necessarily be carried to the vault by plastering from the top side and this will move the salts towards the lower side of the vault. If evaporation is heavy here, the salts may precipitate, and it will not be possible to extract them. Samples taken in mortar and brick from the top side showed that chloride content was much larger in the brick just below the mortar layer than in the mortar. The drying and heating of the loft may have been too heavy which, has dried out the mortar and made the salts precipitate below the mortar layer.

The case story from Alslev shows how important it is to take one step at a time to find out what is actually happening. It is most common to make at least two or three attempts at the same time to improve the situation, but in this way one does not know which of the three did work or rather, as it often is, did not work. Interactions between methods some times results in a bad result even though, applied alone, one of the methods would have worked. Investigations in Odden church therefore was an attempt to look at one single method (extraction of salts with sacrificial layer) and watch salt movements closely.

Investigations in Odden church on Zealand

The purpose of the investigations in Odden church was to find to what extent lime mortar on the top side of the church vault was able to extract salts from the vault.

Odden church is build in the last part of the 13. century. In the 15. century the vaults in the nave was build and in the 18. century the church tower and the vault there. Odden church is situated high up close to the coast both in the south and north direction on a rather wind-swept spot. The church is periodic heated. Severe damage has been observed in the medieval bricks on the top side of the vault. Underneath the vault no damages are observed, and no dust fall are reported.

The top side of the vault in the church tower was plastered with a 3-5 cm layer of pit lime mortar 1:3 (K100/750) with sand grain size 0-3 mm on one fourth of the vault (test field), another fourth remained uncovered as a reference field. The investigation started in march 1989 and was completed a year later. Bored dust samples were taken from the top of the vault in the mortar and in three depths in two undamaged and three damaged bricks in the test field, and two undamaged and two damaged bricks in the reference field. Dephts of borings were 0-1 cm, 1-3 cm and 3-7 cm which was only half way through the vault, which had a total thickness of 13 cm. Samples were taken before plastering and after 52, 175 and 344 days, and the chloride content was determined. A few samples were analysed for contents of different ions.

From the chloride content of the samples, the total chloride contents of the vault are calculated assuming 1/3 damaged and 2/3 undamaged bricks. The result are given in table 5.6. The chloride contents relative to contents before plastering are given in table 5.7. Climate above the church vault for the entire period and below the vault for a part of the period are given in table 5.8.

Tabel 5.5. *Contents by weight of different ions and water soluble substance (WSS) for samples taken on top of vault of the church nave.*

Ion	SO_4^{2-}	Cl^-	Mg^{2+}	Ca^{2+}	K^+	Na^+	Σ	WSS
Wt %	0.30	0.53	0.07	0.31	0.11	0.38	1.68	1.94

Table 5.6. *Total chloride concentration [kg/m³] in the upper 7 cm of a 13 cm thick vault with 1/3 damaged and 2/3 undamaged bricks. Dry density of bricks is 1850 kg/m³. Nielsen (1991).* *) *Average value for 9 churches in Denmark. Dry density of bricks is 1710 kg/m³. Larsen (1988).*

Field	Time (days)	Mortar 3.5 cm	Brick			
			0-1 cm	1-3 cm	3-7 cm	Σ
Test field	March (0)		5.8	6.0	5.4	5.6
	May (52)	1.5	1.7	1.8	2.2	2.0
	Sept. (175)	4.2	4.4	4.9	4.6	4.6
	March (344)	2.7	2.7	3.7	4.1	3.8
Reference field	March (0)		4.1	4.1	4.1	4.1
	May (52)		3.8	3.8	3.5	3.6
	Sept. (175)		5.2	4.8	4.9	4.9
	March (344)		4.2	4.2	4.1	4.1
Other churches *)	June 1987		12.3	8.1	6.3	7.7

Table 5.7. *Chloride contents relative to chloride contents before plastering in the upper 7 cm of a 13 cm thick vault with 1/3 damaged and 2/3 undamaged bricks. Mortar layer is 3.5 cm thick. NOTICE: Chloride contents in test field and reference field are not equal before plastering. Nielsen (1991).*

Time (days)	Test field			Reference field
	Mortar	Brick	Total	
March (0)		1.00	1.00	1.00
May (52)	0.13	0.35	0.48	0.86
Sept. (175)	0.27	0.83	1.10	1.17
March (344)	0.12	0.60	0.72	1.00

Table 5.8. *Climate in Odden church in the three periods between inspections. Minimum value, maximum value, average and standard deviation. Nielsen (1991).*

	Min.	Max.	Avg.	Std.
17.04-19.05.1989				Loft
Temperature (°C)	6	14	9.4	2.0
Relative humidity	0.57	0.85	0.709	0.067
19.05-19.09 1989				Loft
Temperature (°C)	11	23	15.9	2.4
Relative humidity	0.45	0.85	0.645	0.071
20.08-19.09 1989				Church room
Temperature (°C)	15	20	16.1	1.2
Relative humidity	0.85	0.98	0.930	0.030
19.09 1989 - 07.03.1990				Loft
Temperature (°C)	0	14	5.6	4.2
Relative humidity	0.50	0.99	0.764	0.095
19.09.1989 - 16.11.1989				Church room
Temperature (°C)	8	19	11.8	2.0
Relative humidity	0.76	0.99	0.945	0.045

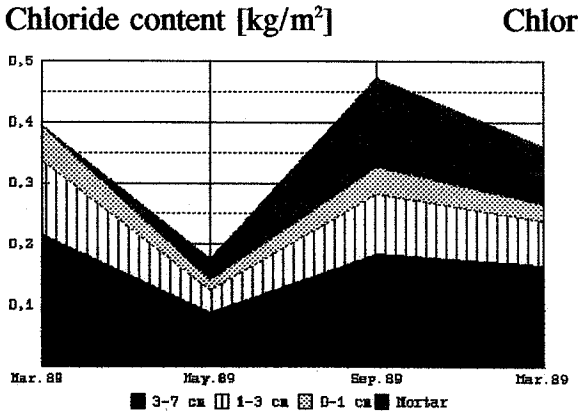

Figure 5.14. *Chloride content in testfield in Odden church.*

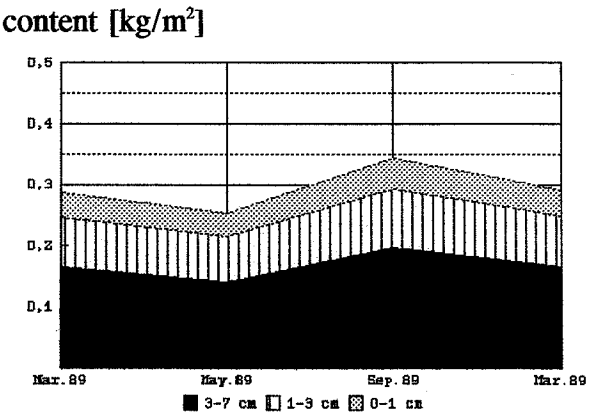

Figure 5.15. *Chloride content in reference field in Odden church.*

Discussion of results from Odden church

The evaluation of the sacrificial layer effect is based on measurements of chloride content in brick and mortar. The reason for this is that testing for chloride is simple, compared to other ions, and by previous investigations by Larsen (1988) a high chloride content was observed in the vaults in Odden church. The evaluation below is based on average values of chloride content from borings in 9 bricks. It is assumed that the vault has 1/3 damaged bricks and 2/3 undamaged bricks, and that the mortar layer has an average thickness of 3.5 cm. The evaluation gives an estimate of the sacrificial layer effect for other salts with a similar solubility, whereas the results can not directly be used for salts with low solubility.

The chloride content in the investigated vault in Odden church is generally low. For 9 churches in Denmark the average chloride content in a damaged brick was 0.9 wt% and in an undamaged brick 0.2 wt%. Before plastering the chloride content in a damaged brick in Odden church was 0.5 wt% and in an undamaged 0.1 wt%. The coefficient of variation on chloride content is 10% for a damaged brick and 100% for an undamaged brick. The chloride content in a damaged brick is significantly higher than in a undamaged brick. The average chloride content in the test field is a bit higher than in the reference field.

After plastering the chloride content in the test field strongly decreases in the upper 7 cm (table 5.7, figure 5.14). 52 days after plastering only 35% of the original chloride content is left in the brick, 13% is taken up by the mortar and 52% has been washed to the lower part of the vault and partly to the tower wall. In the reference field 86% of the original chloride content is left. The chloride content in the lower 6 cm of the vault is not known as the Danish National Museum did not want the borings to go through the vault.

In the summer period, from May to September, the chloride content in the upper 7 cm of the test field increases to 110% of the original content and to 117% in the reference field. Independent of the mortar layer the chlorides move towards the top side of the vault, though the amount of chlorides transported is almost twice as high in the test field than in the reference field. The mortar layer extracts additionally 14% of the original chloride content, a total of 27%. The content in the bricks is 83% in September.

In the winter period, from September to March, the chloride content in the upper 7 cm of the test field decreases to 72% and in the reference field to 100%. The chlorides move towards the lower side of the vault in the winter period. The chloride content in the mortar decreases from 27% to 12%.

Generally it is difficult to evaluate the climate close to the vault (micro climate) from measurements with a thermal hygrograph at some distance from the vault, because it takes not into consideration the convective moisture and heat transfer resistance, but the measurements can be used in a rough estimate of the climate effect on chloride movements. The climate above the vault is mainly determined by the outdoor climate. Unfortunately climate measurements below the vault are missing for most of the period. Though not satisfactory, climate measurements from other churches must be used for the estimate instead.

In the winter period relative humidity is above the deliquescence point of sodium chloride on both sides of the vault when the church is not heated. The vault hygroscopically takes up water from both sides. When the church is heated relative humidity drops below the vault. As relative humidity in the pores is independent of temperature due to sodium chloride the heating of the outer few mm of the vault will start evaporation from the lower surface causing the chlorides to move downwards by capillary suction of salt solution. This is consistent with the observations above.

In the summer period relative humidity is above the deliquescence point of sodium chloride below the vault and below the deliquescence point above the vault. The vault thus hygroscopically takes up moisture from the church room and moisture evaporates at the church loft causing the chlorides to move upwards. This is consistent with the observations above. The heating of the loft by the sun will cause an effect similar to the heating of the church room, but resulting in an upward chloride movement instead.

In both winter and summer period short climate changes will affect the chloride movement in a similar way. Theese short changes particularly affects the outer few mm of the vault where precipitation of salts, hygric and thermal movements break down the surface.

By the sacrificial layer method the chlorides are extracted by capillary suction from bricks in the vault to the sacrificial layer. This is only possible, if the sacrificial material is more fine porous than the brick. It is advantageous to have capillary transport as long as possible into the sacrificial layer to be sure that salts do not precipitate in the brick. Downwards against the brick the pore structure of the sacrificial layer should be coarser and coarser, but the sacrificial material should always be more fine porous than the brick. Evaporation from the surface of the sacrificial material should be as heavy as possible to give large capillary transport without drying the sacrificial material before the brick is dried out.

Investigations in Skt. Pauls church in Copenhagen

Skt. Pauls church is situated in the centre of Copenhagen. The church was build in 1872-1877 inspired by north italian Romanesque style in red bricks on a plinth of granite. In front of the south end is build a 47 m high tower with a conic 12 m high brick spire. The spire consists of a solid 1 1/2 stone wall of bricks laid in a speciel pattern with a semicircular end sticking out to the exterior, and the courses staggered a few centimeters horizontally with 5 courses of glaced and 7 courses of unglaced bricks. In this way small shelves exposed to rain are formed on the top of the bricks.

The church has been repaired several times the tower as early as in 1896. In 1989 it was observed that the spire was deteriorated on the inner side, with dented flakes of high porous brick sitting on the surface (exfoliation). A sample showed a content of water soluble salts, mainly gypsum, of 7 wt%. In 1990 the Building Materials Laboratory made a registration of the state of the church spire. Samples were taken from the inner side in two damaged and two undamaged bricks. Dry density of the brick was 1837 kg/m^3, bulk density 2733 kg/m^3 and porosity 0.33 m^3/m^3. The average content of gypsum ($CaSO_4 \cdot 2\ H_2O$) was 3.5 wt% in a

damaged and 1.4 wt% in an undamaged brick. The gypsum content in the exfoliated flakes was up to 50 wt%. Pictures taken in scanning electron microscope with backscatter electrons from polished sections of an undamaged brick revealed a zone with gypsum 1-2 mm below the surface. In the zone 1-2 mm wide crakcs can be observed which means that the layer is about to exfoliate (figure 5.16).

In an attempt to extract gypsum two fields of approximate size 1.5 by 1.5 m was plastered with a 1-3 cm thick layer of lime mortar. 7 months later 12 samples were taken from the lime mortar fields. The average gypsum content was 0.14 wt%, fairly higher over a damaged brick than over an undamaged. The degree of extraction (ratio between extracted gypsum and total gypsum content in the bricks) was only 0.01.

Discussion of results from Skt. Pauls church

As the solubility of gypsum is very low (0.24 g pr. 100 ml of water) very large quantyties of water are needed to deliquesce gypsum and transport it through capillary suction into the mortar layer. The spire wall contains at least 3 kg/m^2 of gypsum, which needs 1250 liter of water to be dissolved. In practice more water is needed, if not a saturated solution are formed. Precipitation in Denmark is around 60 cm a year giving 600 liters of water pr. square meter. On a almost vertical surface like the spire precipitation is much less. The content of gypsum in the mortar was in average 30 g/m^2 build up in 7 months corresponding to a flow of 21 l/m^2 a year. As the summer 1990 in Denmark was fairly dry a flow of 50 l/m^2 could be expected. Washing out with rainwater will then take at least 50 years, and in this period new gypsum will be formed.

Extraction of precipitated gypsum with mortar is therefore inefficient on a short time scale. As gypsum is concentrated on the surface the most efficient way to remove gypsum seems to be a mechanical cleaning with steel brushes or sandblasting of the deteriorated surface (1-5 mm). The static safety of a cleaning should be assessed by an expert. One should be aware that seemingly undamaged bricks could be damaged, as was found for the sample in figure 5.16. Gypsum is seen as precipitaions in a band behind the crust zone, which is about to be exspalled. Caused by leaky joints, gypsum is formed on the inner side of the brick from incomming, sulphurous rainwater and calcite in the mortar.

Plastering of the inner side of the spire will not efficiently extract precipitated gypsum but will protect the brick against future precipitations caused by sulphurous rainwater. Precipitations will take place in the mortar, which will deteriorate. Further, the mortar will stabilize the brick surface. Before plastering a thorough cleaning of the surface is needed to obtain good adherence of the mortar.

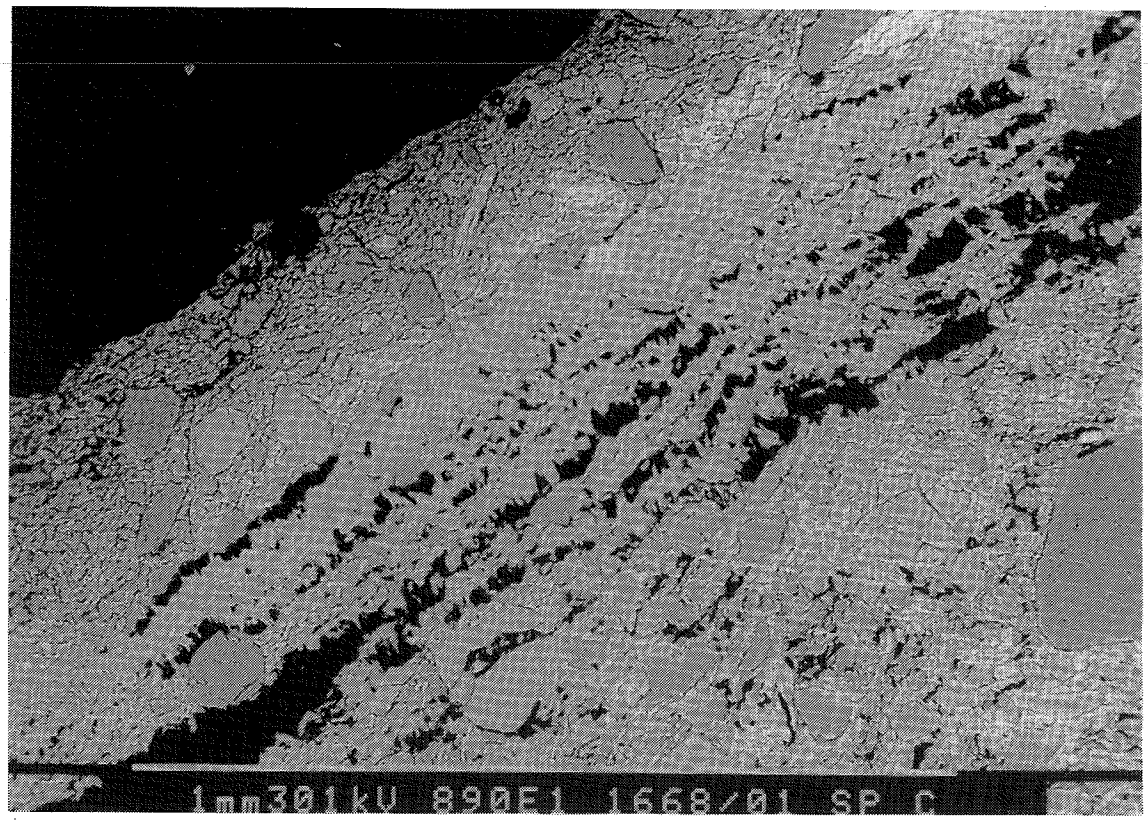

Figure 5.16. *Seemingly undamaged brick from Skt. Pauls church in Copenhagen with precipitations of gypsum in a band behind crust. Bright areas are gypsum.*

5.5 Electro-chemical extraction of salts

Introduction

Electro-chemical extraction of salts and drying of brickwork is described by Friese (1984) and Wittmann and Boekwijt (1982). Water in a porous material will be slightly dissociated as cathions H^+ and anions OH^-. The anions is adsorbed in a boundary zone between solid and liquid, while the cathions can move freely in the liquid. If the porous material is put into an electric field the cathions will start to move towards the cathode and drag the surrounding water with them resulting in drying of the material.

Solutions of water soluble salts in porous materials will be completely dissociated for concentrations below the solubility. Sodium chloride will be dissociated as cahtions Na^+ and anions Cl^-. In an electric field Na^+ will move towards the cathode and Cl^- towards the anode. As the number of Na^+ and Cl^- ions are the same the electric current will be equal in both directions and theoretically there will be no transport of water before all salts are removed.

The following reaction will take place at the anode

$$2\ Cl^- \rightarrow Cl_2 + 2e^-$$
$$4\ OH^- \rightarrow 2\ H_2O + O_2 + 2e^-$$

If iron are used as anode material
$$Fe \rightarrow Fe^{+++} + 3e^-$$

At the cathode the following reaction will take place

$$2\ H^+ + 2e^- \rightarrow H_2$$
$$2\ Na^+ + CO_2 + H_2O \rightarrow Na_2CO_3 + 2\ H^+$$

Experimental procedures

27 bricks BS-red of approximate size 215 by 103 by 65 mm was immersed in three different solutions of sodium chloride for 20 hours. The salt solutions and the resulting salt content found by weighing of the saturated bricks are given in table 5.9. Three bricks were put into a plastic box on brass rail supports immersed a few mm in distilled water. Stainless steel plates connected to a D.C. power supply were placed at the top and at the bottom of the bricks. The plastic box was tightly covered. The arrangement is shown in figure 5.17. The bottom steel plate immersed in water was acting as anode attracting chloride ions, and the top steel plate as chatode.

Table 5.9. *Salt solutions for saturation of bricks and resulting salt contents in brick after 20 hours immersion.*

Nr.	Solution	Salt concentration in brick [kg/kg]	
		Average	Std.
1	300 g NaCl + 1000 g water	0.027	0.002
2	150 g NaCl + 1000 g water	0.014	0.0008
3	Distilled water	-	-

The plastic boxes were arranged in three columns, each with three plastic boxes containing bricks with three different salt concentrations (figure 5.18). The steel plates in two columns were connected in parallel to seperate D.C. power supplies, the third was left without voltage.

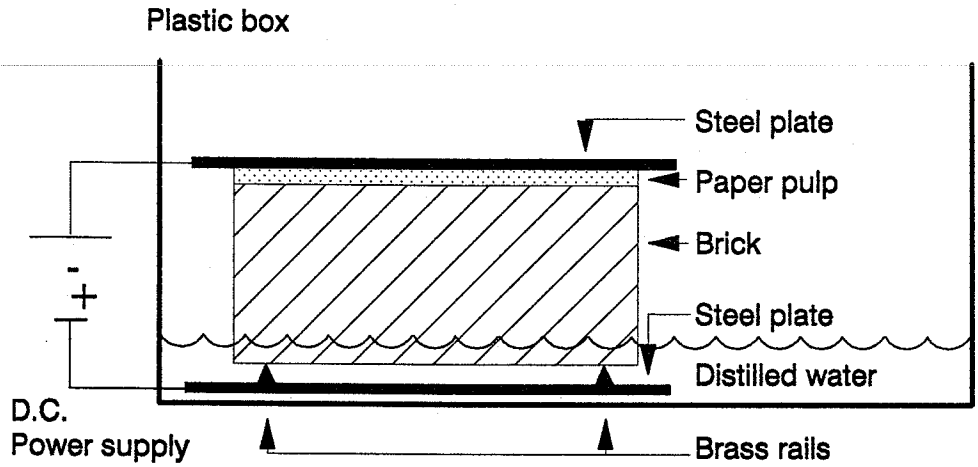

Figure 5.17. *Arrangement for electro-chemical salt extraction of brick.*

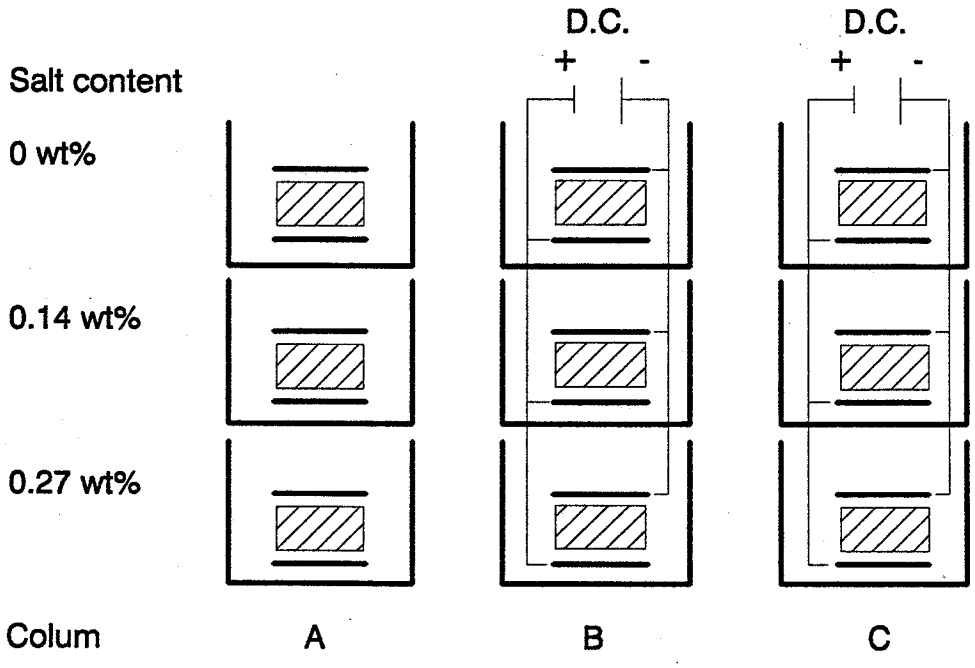

Figure 5.18. *Arrangement of plastic boxes in colums for electro-chemical salt extraction.*

Voltage and current were measured with intervals as a function of time for each plastic box. The chloride concentration in the water in the plastic boxes was analysed by potentiometric titration after 23, 70, 142, 239 and 310 hours from a sample of 25 ml for each box. From the total weight of water in each box the amount of extracted NaCl was calculated. The degree of extraction is calculated as the ratio between the amount of extracted salt and the original salt content in the brick.

Results

Table 5.10. *Degree of extraction of NaCl from brick with electro-chemical extraction.*

Column	Average salt content in brick [kg/kg]	Degree of extraction [kg/kg] Extraction time [hours]				
		23	70	142	239	310
A	0.027	0.14	0.26	0.33	0.37	0.40
	0.014	0.12	0.21	0.27	0.30	0.34
B	0.027	0.45	0.55	0.73	0.77	-
	0.014	0.52	0.59	0.77	0.80	-
C	0.027	0.29	-	0.41	-	0.70
	0.014	0.41	-	0.45	-	0.62

The voltage of the D.C power supplies was varied in the range 0-15 V to fit the maximum current limit, but the effort failed as one power supply broke in the beginning and left column C without voltage most of the time. The current varried with the voltage, and the resistance of the specimens increased with time due to changes in salt content. The integrated effect of voltage and current are calculated as accumulated supplied electric energy pr. gram of salt in the specimens as function of time. The relative charge is calculated as the ratio between supplied electric charge and the charge of the total chloride content in the specimen. If all electric current was caused by transport of chloride ions, the degree of extraction should equal the relative charge. Degree of extraction as a function of relative charge are given in figure 5.21.

Salts are extracted from specimens immersed in distilled water without voltage (coloumn A). Diffusion coefficient for specimen A1 and A2 is calculated from the theory of linear diffusion (3.25) assuming constant salt concentration in extraction water. Salt concentration in extraction water is calculated as half the salt concentration of the entire system in equilibrium. For specimen A1 this is 35 kg/m^3 and for specimen A2 18 kg/m^3. Salt concentration in specimen is calculated from salt content assuming full saturation of specimen. Calculated diffusion coefficient is given in table 5.11.

Table 5.11. *Calculated diffusion coefficient for sodium chloride in brick at two different salt contents.*

Specimen	Salt content [kg/kg]	D_s 10^{-9} m^2/s	
		Average	Std.
A1	0.027	2.8	0.7
A2	0.014	1.9	0.3

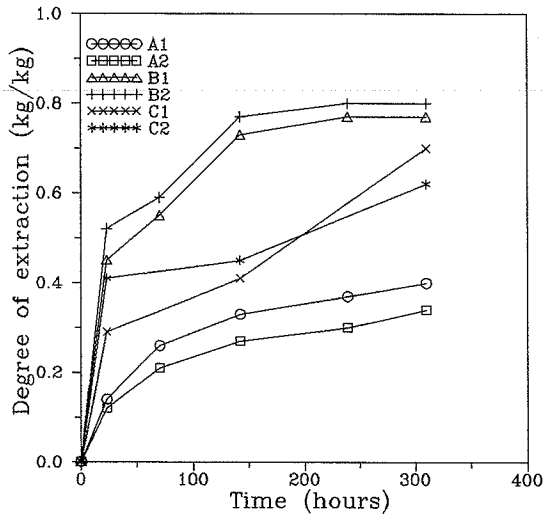

Figure 5.19. *Degree of extraction of NaCl as a function of time for brick.*

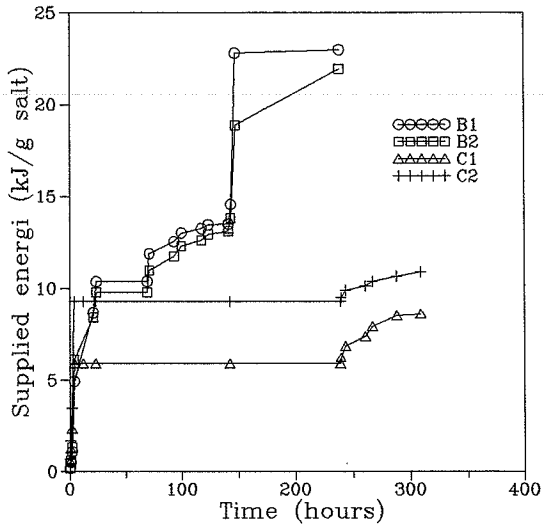

Figure 5.20. *Supplied electric energy pr. gram NaCl as a function of time for brick.*

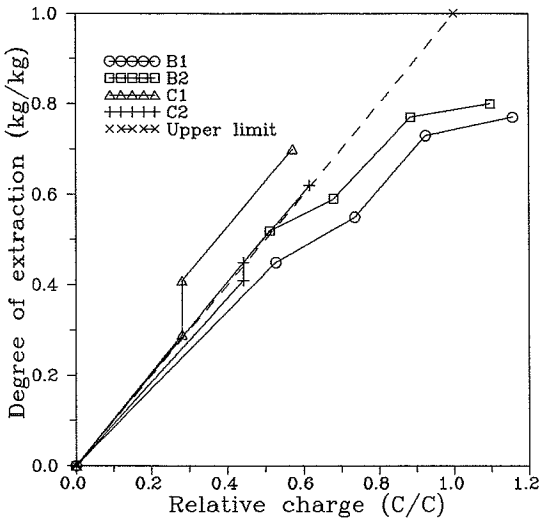

Figure 5.21. *Degree of extraction of NaCl as a function of relative charge (ratio between supplied electric charge and charge of the total salt content in the brick).*

Discussion

Sodium chloride is extracted from brick even without voltage. As brick was saturated with salt solution by capillary suction for 20 hours and specimens were kept in closed plastic boxes at 100% relative humidity, no capillary flow could have taken place. The only way salts could have been extracted was by diffusion as described in section 3.1. The calculated diffusion coefficients is of the same order of magnitude as given in CRC (1984) in table 2.4. Diffusion coefficient is not significantly larger for the high salt content. Extraction decreases with time not only due to change in salt content of the specimen, but also due to changes in salt concentration of the extraction water. This effect is not taken into consideration by calculation of diffusion coefficient, and it might change diffusion coefficient slightly.

Only by diffusion up to 35% of the original salt content is extracted within 12 days. This value is average for six full size bricks. By supplieing electric energy, the degree of extraction is increased with a factor of two up to 78% within 12 days. Rate of extraction is clearly influenced by supply of electric energy. When the power supply is cut off, the extraction continue corresponding to extraction by diffusion. When the power supply is reconnected, the rate of extraction increases as seen for specimen C1 and C2. An increase in supplied energy at the end of the extraction period for specimen B1 and B2 does not result in any increase in degree of extraction. It seems that about 20% of the originally salt content can not be extracted.

The extraction seems to be quite efficient. From figure 5.21 it is seen that nearly all supplied electric energy is used for extraction, as the relative supplied electric charge equals the degree of extraction. In this calculation, though, the diffusive extraction is not incalculated, and therefore the degree of extraction due to supplied electric energy is lower. This must be the case as the degree of extraction for specimen C1 exceeds relative charge. Towards the end of the extraction period, the efficiency of the electric extraction clearly decreases as degree of extraction is less than supplied relative charge.

During extraction specimen and water was warmed up and unidentified reaction products was formed on the surface of the brick and in the water, some of them due to the brass supporting rails. Though electric extraction seems efficient it can not be recomended without further experiments, as it is not clear how theese reaction products influence deterioration of the brick. It could be, that one problem was solved, but another was created.

5.6 WEATHERING OF BRICK WALLS

Introduction

Mortar in brickwork build during periods with frost often contains chlorides from freezing point depressing agents. These agents spread into the bricks and may cause decay of mortar and brick. Freezing point depressing agents are not allowed in Denmark according to DS 414, but the ban is relatively new. Butterworth (1964) gives a thorough review of results from outdoor exposure tests and laboratory tests since about 1926 for brickwork including freezing tests, soluble salts analysis, efflorescence tests and water absorption. Bowler and Fisher (1989) discuss the risk of sulphation of low-strength mortars from bricks containing different levels of various salts.

The purpose of theese experiments is to observe if brickwork with low-strength mortar containing freezing point depressing agents is deteriorated in an accelerated weatering test compared to outdoor weathering.

Experimental procedures

Four different mortars were made from pit lime, standard portland flyash cement, sand grain size 0-4 mm and freezing point depressing agent (Cero Frost) consisting of calcium chloride.

1) Lime mortar K100/1200 (K)
2) Lime mortar K100/1200 with Cero Frost (Ks)
3) Lime cement mortar KC 50/50/750 (KC)
4) Lime cement mortar KC 50/50/750 with Cero Frost (KCs)

6 mortar bars size 20 by 20 by 120 mm was made with each mortar and stored at 20 °C, 100 % relative humidity for 7 days and then at 20 °C, 65 % relative humidity for 4 months.

With each mortar 2 brickwork walls were build in steel frames, one for outdoor exposure and one for accelerated weathering. The walls was 2 bricks wide, 8 courses high and 1/2 brick deep made from red maschinemolded bricks size 226 by 108 by 53 mm. Compression strength was 18 MPa. The joints in the brickwork were scrabed out till 15 mm and filled with the same mortar. The walls was stored at 20 °C, 65 % relative humidity for 4 months.

The brickwork was isolated with 50 mm polystyrene plates and wraped up in plastic foil on all sides except the front to be exposed. 4 walls, one with each mortar, was used for accelerated weathering test as described in DS 1127 (1985) in the climate cycle below

1) Light and heating (sun)
2) Wetting (rain)
3) Freezing (-20 ± 5 °C) (frost)
4) Laboratory climate (thaw)

The exposure took place in the given order. Each position lasted one hour giving 6 cycles a day. Samples in brick and mortar were taken after 0, 65 and 300 cycles to determine chloride content. Samples were taken as powder with 10 mm drill from the exposed front of the brickwork in positions given below

Brick	T1: Upper left side, 0-10 cm
	T2: Middle, 0-3, 3-7 and 7-10 cm
	T3: Middle right side, 0-10 cm
Mortar	M1: Middle horizontal joint
	M2: Middel vertical joint

Samples were taken in different bricks after each of the given number of cycles. After drilling holes were closed with a rubber plug. Chloride was extracted from powder in 10 ml extraction liquid (acid) and chloride content in the solution was measured with a chloride sensitive electrode (Rapid Chloride Test (RCT)). All measurement are average of two tests.

4 similar walls were used for outdoor exposure at a western houseend for 17 months (december 1988 - april 1990). Samples in brick and mortar were taken before and after exposure similar to accelerated weathering. Density and porosity was measured for mortar bars and bricks by water saturation. Capillary suction tests were carried out for mortar bars and bricks in different directions.

Results

Materials data for mortar and brick are given in table 5.12. Temperature in accelerated weathering test was measured at the surface of the exposed front and at the back of the brickwork just before 300 cycles. Chloride content in brick is given for three depths and as average for all samples. Chloride content in mortar is given as average for the two samples.

Table 5.12. *Materials data for mortar and brick used for brickwork. H=horizontal, V=vertical.*

		Mortars				Brick
		K	Ks	KC	KCs	
Density [kg/m^3]	Fresh	1975	1950	2025	2010	-
	Dry	1865	1890	1960	1980	1750
	Solid	2640	2585	2635	2585	2640
Air cont. [m^3/m^3]		0.03	0.07	0.04	0.06	-
Porosity [m^3/m^3]		0.29	0.27	0.26	0.23	0.34
Water capacity [kg/kg]		0.106	0.110	0.105	0.104	0.135
Water uptake coefficient [kg/m^2 s$^{1/2}$]		0.35	0.38	0.15	0.11	H: 0.30 V: 0.27

Table 5.13. *Temperature measured at the surface of the brickwork after exposure to climate in accelerated weathering test.*

Nr.	After exposure to	Temperature [°C]	
		Front	Back
1	Sun	28.1	22.0
2	Rain	24.6	24.5
3	Frost	13.4	21.7
4	Thaw	18.9	18.6

Table 5.14. *Chloride content [wt%] during production of mortar specimens in mix-water and in mortar bars after mixing and after hardening.*

	Ks	KCs
Mix-water	9.3	9.3
Fresh mortar bar	1.73	1.57
Dry mortar bar	0.71	0.83

Table 5.15. *Chloride content [wt%] in brickwork measured in brick and mortar during accelerated weathering test.*

Accelerated weathering		0 cycles		65 cycles		300 cycles	
		Ks	KCs	Ks	KCs	Ks	KCs
Brick	0-3 cm	0.43	0.28	0.00	0.07	0.00	0.01
	3-7 cm	0.21	0.19	0.05	0.14	0.02	0.00
	7-10 cm	0.29	0.18	0.22	0.22	0.03	0.02
	Average	0.30	0.24	0.11	0.21	0.02	0.03
Mortar		0.46	0.65	0.53	0.21	0.05	0.10

Table 5.16. *Chloride content [wt%] in brickwork measured in brick and mortar during natural weathering test.*

Natural weathering		Before exposure		After exposure	
		K	KC	K	KC
Brick	0-3 cm	0.34	0.17	0.21	0.29
	3-7 cm	0.17	0.10	0.21	0.29
	7-10 cm	0.17	0.08	0.26	0.30
	Average	0.26	0.12	0.26	0.29
Mortar		0.58	0.45	0.35	0.51

From table 5.15-16 is calculated the absolute chloride content for one brick and the mortar belonging to it (vertical and horizontal 12 mm joint) during the exposure period. In table 5.17-18 this is compared to the chloride content in the fresh mortar.

Table 5.17. *Absolute chloride content by natural weathering in brick and mortar joints belonging to brick compared to absolute chloride content in fresh mortar.*

		Before exposure		After exposure	
	Fresh mortar	Brick	Mortar	Brick	Mortar
Ks	1	0.48	0.33	0.48	0.20
KCs	1	0.24	0.28	0.57	0.32

Tabel 5.18. *Absolute chloride content by accelerated weathering in brick and mortar joints belonging to brick compared to absolute chloride content in fresh mortar.*

		0 cycles		65 cycles		300 cycles	
	Fresh mortar	Brick	Mortar	Brick	Mortar	Brick	Mortar
Ks	1	0.56	0.25	0.20	0.30	0.04	0.02
KCs	1	0.47	0.41	0.42	0.13	0.06	0.06

At the end of the outdoor exposure (april 1990) the appearance of each of the 8 brickwork wall was characterized as below. For all brickwork walls no deterioration of the brick was observed.

Accelrated weathering

K	Joints were deteriorated 2 cm on the upper half of the brickwork. Less/none deterioration of joints below. Minor efflorescence on brick.
Ks	Rugged surface of joints (slight deterioration). Mortar and brick is humid. Slight efflorescence on brick.
KC	No deterioration of mortar. Mortar yellow/green (alga growth, ochre). Minor/no efflorescence on brick.
KCs	Rough surface of joints (minor deterioration). Mortar yellow/green (alga growth, ochre). No efflorescence on brick.

Natural weathering

K	No deterioration of brick or joints. Minor efflorescence.
Ks	Rugged surface of joints (slight deterioration). Mortar and brick is humid. Slight efflorescence on brick.
KC	No deterioration of mortar. No efflorescence.
KCs	Rough surface of joints (minor deterioration). Slight efflorrescence on brick.

Discussion

Total porosity and water uptake coefficient is larger for lime mortar than for lime-cement mortar. By adding Cero Frost total porosity decreases and for lime mortar water uptake coefficient increases (coarser pores) whereas for lime-cement mortar water uptake coefficient decreases (finer pores).

Chloride content in the mix-water is the same for lime mortar and lime-cement mortar, but as the amount of water needed for mixing is less for lime-cement mortar, chloride content in fresh lime-cement mortar is less than in lime mortar. For dry mortar bars and mortar in brickwork there is no relations between mortar type and chloride content. The uptake of chloride-containing mix-water in bricks by bricklaying is dependend on local conditions and varies with site. In average it seems that brick take up half the chloride content of the fresh mortar, one third is left in the mortar and the rest is lost by bricklaying or fixed in the mortar.

By accelerated weathering the chloride content clearly decreases and at 300 cycles almost all chloride is washed out. During accelerated weathering brickwork was wet and by exposure to rain chlorides were washed to the backside of the brickwork and out of it. This is clearly

seen from brick chloride profiles. Before exposure chloride content is highest at the front side of the brickwork, but after 65 cycles the back side has the highest chloride content.

By natural weathering the chloride content does not change significantly. Before exposure chloride content in brick in brickwork with lime-cement mortar is low compared to the corresponding brickwork used for accelerated weathering. This must be due to local conditions as chloride content measured after exposure is larger than before exposure. By both natural and accelerated weathering no deterioration of brick due to chloride content was observed. Chlorides might deteriorate the bricks by long term outdoor exposure, as chlorides are left in the brickwork, but on short term problems with brick is limited to efflorescence and discolouring of the surface.

Joints were deteriorated during weathering. The most servere damage was observed on lime mortar without chlorides in accelerated weathering. Deterioration was only seen on the upper half of the brickwork, and a similar damage was not observed in the lime mortar with chlorides or on lime mortar from outdoor exposure. The damage might be caused by dissolution of the lime cementing and thermal and hygric movements by repeated wetting and drying. Lime mortar without chlorides is exposed to stronger drying in accelerated weathering, and therefore paradoxically deteriorate stronger than lime mortar with chlorides, as chlorides keeps mortar wet and decrease the rate of drying. Lime mortar without chlorides is not deteriorated by natural weathering as drying rate here seems to have been slower.

Except for pure lime mortar, the deterioration of mortar in accelerated weathering was similar to that in natural weathering. No damage was observed for mortar without chlorides, minor deterioration was observed for lime-cement mortar with chlorides and slight deterioration was observed for lime mortar with chlorides. Deterioration was seen as a rough or rugged surface. Most important was, that brickwork with chlorides looked (and was) wet. This tends to give a discoloured surface of the brickwork. The difference in deterioration between lime mortar and lime-cement mortar is caused by the difference in strength.

The accelerated weathering was supposed to include freeze thaw cycles, but from table 5.13 it is seen that tempereture never is below zero, because freezing period (one hour) is too short. On the other hand, the winter period during outdoor exposure was mild with almost no frost.

Accelerated weathering is not similar to natural weathering as chlorides is washed out and lime mortar is strongly deteriorated in accelerated weathering and not in natural weathering. From theese experiments it can not be established if not, on long term, chlorides would be washed out by natural weathering, but it seems, that the intensity of wetting and drying by natural weathering is not strong enough for this, and therefore, with respect to chloride transport, the accelerated weaterring is not similar to natural weathering.

On the other hand, as chlorides was washed out by accelrated weathering, it indicates, that washing with water might be an efficient way to extract chlorides from brickwork.

5.7 CALCULATIONS OF MOISTURE AND SALT TRANSPORT

The one dimensional model for moisture and salt transport outlined in section 3.2 is implemented in a comercial worksheet, Symphony from Lotus. The model consists of 10 equally sized boxes vertically stacked. Moisture and salt content are calculated in 6 situations

1) Capillary suction at 20 °C, 50% relative humidity of distilled water and NaCl-solution for brick specimen corresponding to experiments in section 5.3 (verification of capillary transport in model).

2) Capillary suction at 20°C, 50% relative humidity of distilled water from the upper side of a church vault with 0.4 wt% sodium chloride evenly distributied as measured in section 5.3 (plastering of vault with sacrificial layer).

3) Drying of church vault with sacrificial layer after capillary suction at 95 % relative humidity, 20°C below, and 50% relative humidity, 20°C above the vault (extraction of chlorides with sacrificial layer).

4) Drying of church vault with an even distribution of sodium chloride without initial capillary suction at 95 % relative humidity, 20°C below, and 50% relative humidity, 20°C above the vault (chloride movement without extraction).

5) Heating to 20°C in 2 days below church vault in equilibrium at 10 °C, 95% relative humidity with even sodium chloride distribution followed by cooling at 10 °C below vault in 5 days (heating of church room in winter).

6) Heating to 40°C in 12 hours above church vault in equilibrium at 20°C, 70% relative humidity with even sodium chloride distribution followed by cooling at 20°C above vault in 12 hours (heating of church loft by the sun in summer).

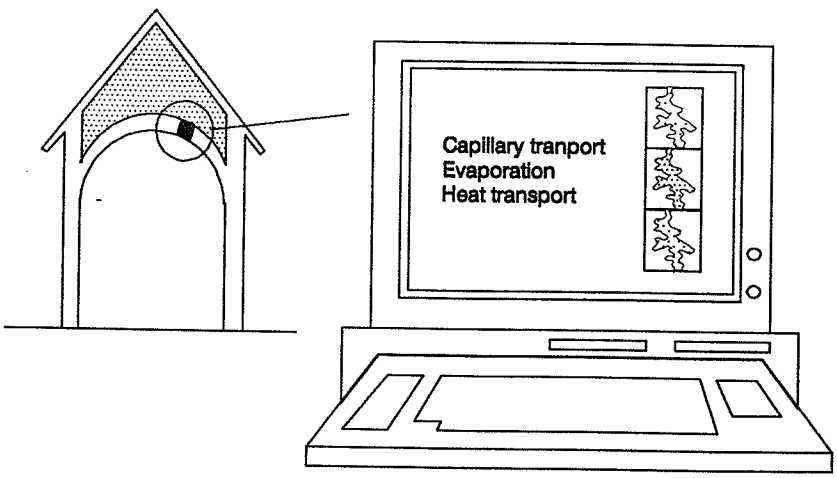

Data used in calculations are as follows

STRUCTURE

1)	ρ_d	=	1870 kg/m^3
	p	=	0.29 m^3/m^3
	r_k	=	$3.0 \cdot 10^{-8}$ m
2) - 6)	ρ_d	=	1750 kg/m^3
	p	=	0.34 m^3/m^3
	r_k	=	$3.0 \cdot 10^{-8}$ m

MOISTURE

1) - 6)

$$u_m = 0.0115 \exp\left[-0.210 \ln\left(1 - \frac{\ln\phi_k}{4.45 \cdot 10^{-4}}\right)\right]$$

	ß	=	$1.0 \cdot 10^{-8}$ m
	δ	=	$3.0 \cdot 10^{-11}$ kg/m s Pa
1)	u_{ssd}	=	0.12 kg/kg (distilled water)
		=	0.09 kg/kg (sodium chloride solution)
2) - 6)	u_{ssd}	=	0.14 kg/kg

SALT

1)	c	=	0.2278 kg/kg (water for capillary suction)
1) - 6)	ϕ_s	=	0.76
	c_s	=	0.2647 kg/kg

HEAT

1) - 6)	λ	=	0.6 J/m s K
	C_p	=	960 J/kg K
	$ß_T$	=	8 J/s K

Capillary suction of brick specimen

The brick specimen is divided up into 10 elements each 10 mm heigh. Moisture and salt content are recorded with increasing time intervals corresponding to experimenst in section 5.3. Mass content are given as function of time in figure 5.22-23 and sodium chloride distribution in specimen is given in figure 5.24.

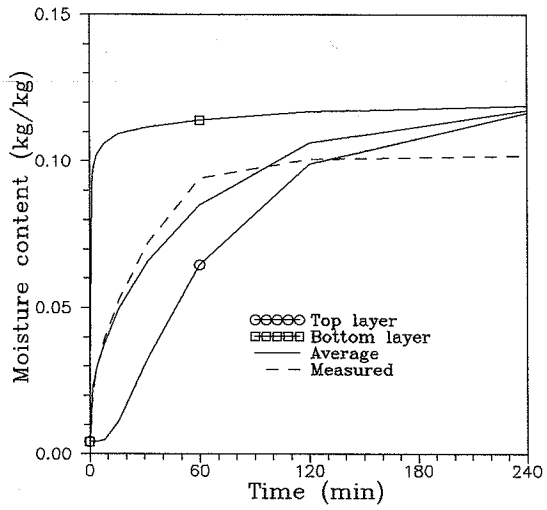

Figure 5.22. *Calculated mass content as function of time for brick specimen by capillary suction of distilled water corresponding to experiments in section 5.3.*

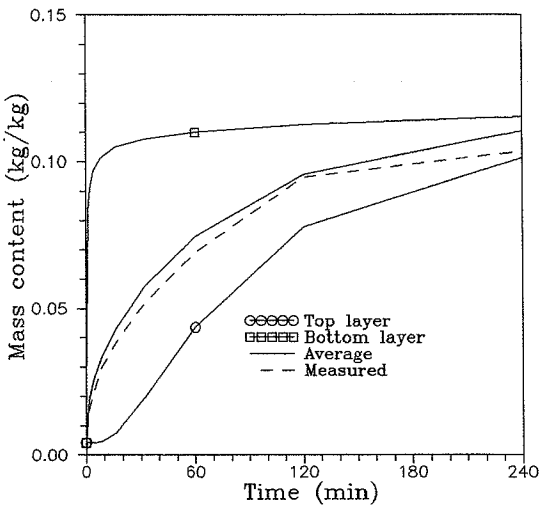

Figure 5.23. *Calculated mass content of brick specimen as function of time by capillary suction of NaCl-solution corresponding to experiments in section 5.3.*

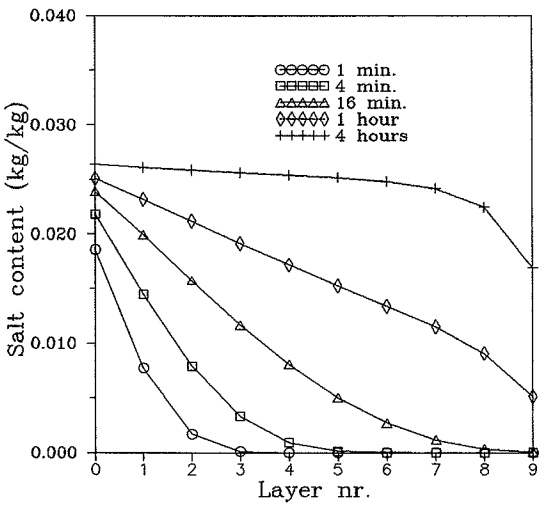

Figure 5.24. *Sodium chloride distribution in brick specimen by capillary suction of NaCl-solution (from left) corresponding to experiments in section 5.3.*

Capillary suction of church vault

To extract salts with a sacrificial layer of lime mortar, as described in section 5.4, it is necessary to wet the brick to give good adherence of the mortar and disolve the salts in the brick. The influence of capillary suction from the upper side of a vault on an even sodium chloride distribution in the brick is therefore calculated.

Before capillary suction an even distribution of sodium chloride of 0.4 wt% in the brick is assumed corresponding to the measured salt content in a vault in Odden church described in section 5.4. The moisture content is assumed to be 0.75 wt% evenly distributed so that the brick is in equilibrium at 70% relative humidity.

Each layer is assumed to be 16.25 mm high. In this way 8 layers corresponds to the thickness of the vault, and the remaining 2 layers to the thickness of the mortar layer. By capillary suction the moisture and salt content of the two bottom layers is neglected.

Results of calculations are given in figure 5.25-26 as moisture and salt distribution in the vault at diffetent times.

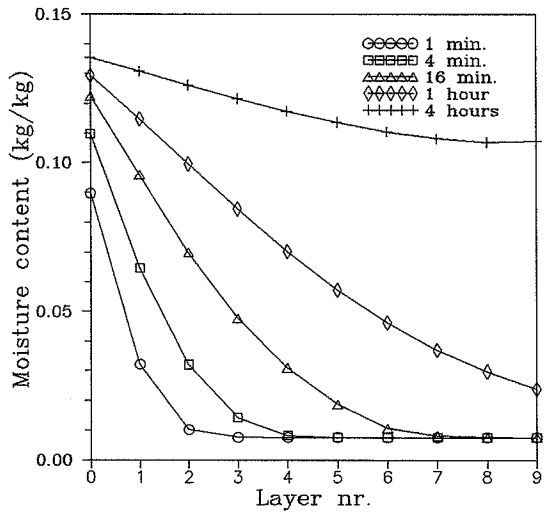

Figure 5.25. *Calculated distribution of moisture in church vault by capillary suction of distilled water from upper side (left). Each layer is 16.25 mm thick.*

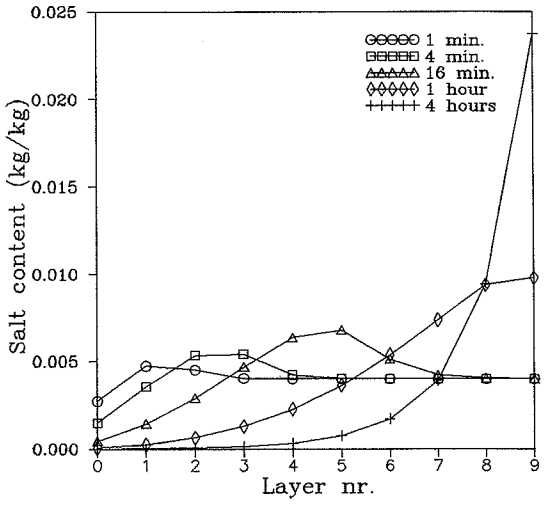

Figure 5.26. *Calculated distribution of NaCl in church vault by capillary suction of distilled water from upper side (left). Each layer is 16.25 mm thick.*

Drying of church vault after initial capillary suction

Moisture and salt distribution in the eight upper layers after 16 minutes of capillary suction, as calculated above, are used as starting point for calculations of salt and moisture transport by drying of church vault at 50% rh, 20°C above and 95% rh, 20°C below the vault. On top of the vault are placed two layers of lime mortar each 16.25 mm thick with 0.12 wt% moisture, without salt and, for simplicity, the same properties as brick. Moisture and salt distribution are given in figure 5.27-28.

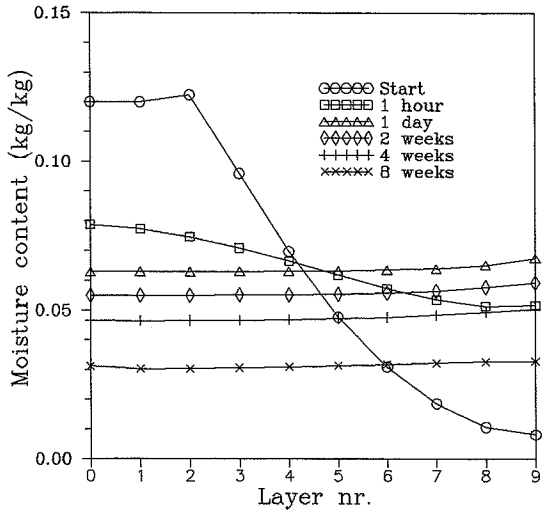

Figure 5.27. *Calculated distribution of moisture in church vault by drying at 50% rh above (left) and 95% rh above vault after capillary suction. Each layer is 16.25 mm thick.*

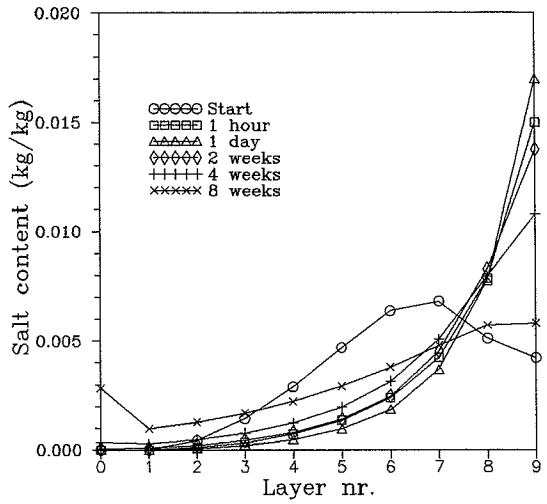

Figure 5.28. *Calculated distribution of NaCl in church vault by drying at 50% rh above (left) and 95% rh below vault after capillary suction. Each layer is 16.25 mm thick.*

Drying of church vault without initial capillary suction

The same even distribution of 0.4 wt% sodium chloride and moisture content corresponding to equilibrium at 70% rh, 20 °C as *before* capillary suction is used as starting point to calculate moisture and salt transport by drying of church vault at 50% rh, 20 °C above and 95% rh, 20 °C below the vault. Moisture and salt distribution are given in figure 5.29-30.

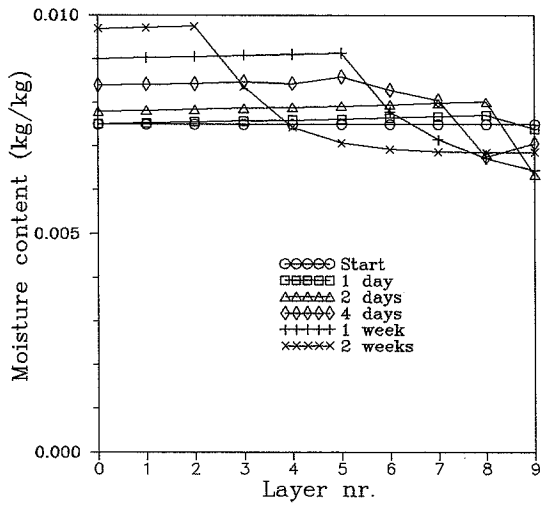

Figure 5.29. *Calculated distribution of moisture in church vault by drying at 50% rh above (left) and 95% rh below vault without initial capillary suction. Each layer is 16.25 mm thick.*

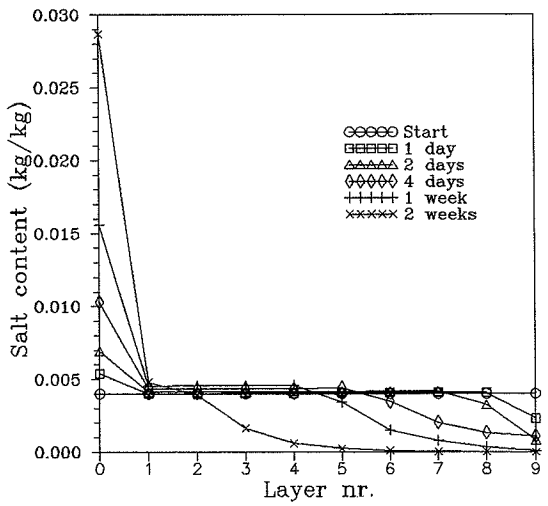

Figure 5.30. *Calculated distribution of NaCl in church vault by drying at 50% rh above (left) and 95% rh below without initial capillary suction. Each layer is 16.25 mm thick.*

Heating below church vault (winter)

An even distribution of 0.4 wt% sodium chloride and moisture content corresponding to equilibrium at 95% rh, 10 °C is used as starting point to calculate moisture and salt transport by heating in the church room in winter below the vault from 10 °C, 95% rh to 20 °C in two days and thereafter cooling at 10 °C for 5 days. Climate above church vault is constantly 10 °C, 95% rh. Salt and temperature distribution after heating and cooling is given in figure 5.31-32.

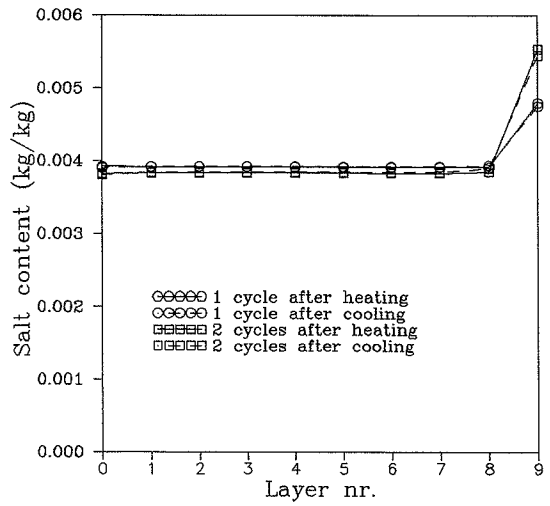

Figure 5.31. *Calculated distribution of NaCl in church vault by heating of lower side (right) from eliquibrium at 10 °C, 95% rh to 20 °C. One cycle consists of 2 days heating and 5 days cooling.*

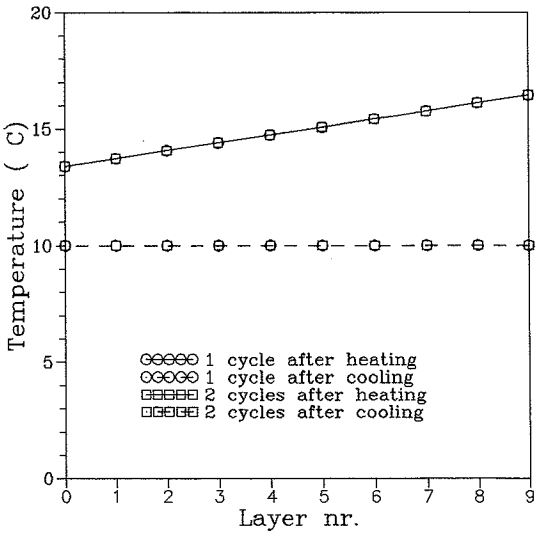

Figure 5.32. *Calculated temperature distribution in church vault by heating of lower side (right) from equlibrium at 10 °C, 95% rh to 20 °C. Each cycle consists of 2 days heating and 5 days cooling.*

Heating above church vault (summer)

An even distribution of 0.4 wt% sodium chloride and moisture content corresponding to equilibrium at 70% rh, 20 °C is used as starting point to calculate moisture and salt transport by heating of the church loft above the vault by the sun from 20 °C, 70% rh to 40 °C in 12 hours and thereafter cooling at 20 °C for 12 hours. Climate below church vault is constantly 20 °C, 70% rh.

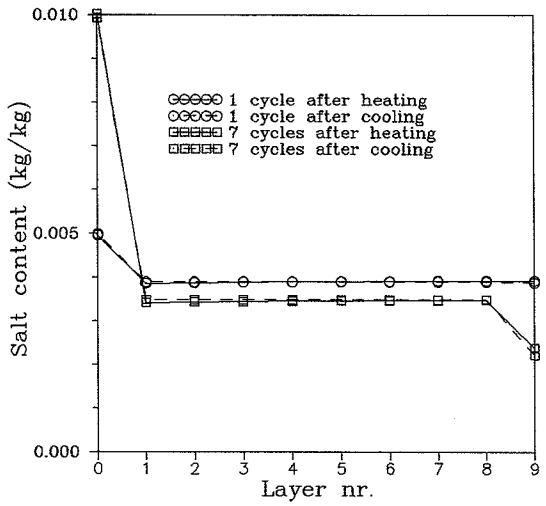

Figure 5.33. *Calculated distribution of NaCl in church vault by heating of upper side (left) from eliquibrium at 20 °C, 70% rh to 40 °C. Each cycle consists of 12 hours heating and 12 hours cooling.*

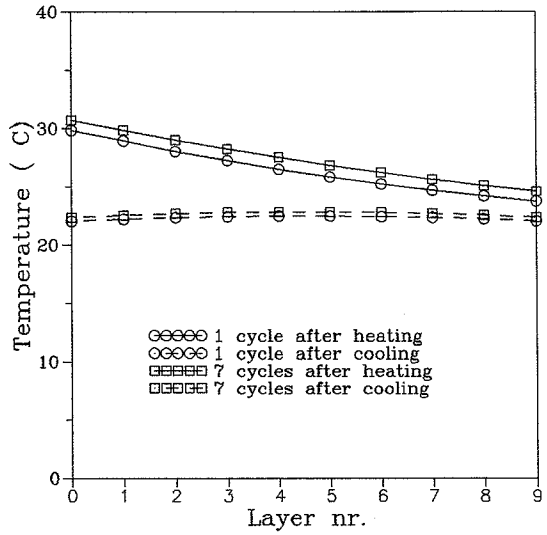

Figure 5.34. *Calculated temperature distribution in church vault by heating of upper side (left) from equilibrium at 20 °C, 70% rh to 40 °C. Each cycle consists of 12 hours heating and 12 hours cooling.*

Discussion of capillary suction

The calculated moisture content by capillary suction of distilled water is close to measured data. Calculated moisture capacity is above and calculated moisture content in the time interval 30 to 90 minutes below the measured vaule. It seems difficult to obtain the abrupt increase in moisture content in this time interval without obtaining a too large moisture capacity.

In the model there are three ways to control moisture uptake by capillary suction

1) Size of characteristic pore size, r_k
2) Size of moisture content at saturation, u_{ssd}
3) Size of suction pressure at the free liquid surface, P_{suc}

Theese three parameters are varied to obtain a best fit to measured data. The characteristic pore size is selected a little larger than the value $r_k=2.9 \cdot 10^{-8}$ m obtained from capillary suction experiments in section 5.3. The geometric pore size obtained in chapter 4 is not to be used, as the model does not take considerations to the influence of pore shape and connectivity on moisture transport. As stated in section 5.3, the characteristic pore size does include theese parameters, and therefore it can be used directly.

Moisture content at saturation is assumed less than the actual vaule 0.16 kg/kg which can be calculated from porosity and density. This is done to fit water capacity at the expence of capillary suction rate in the time interval 30 to 90 minutes. The problem seems to be, that it is attempted to fit measured data with a model with only one pore size and therefore all pores are filled in the same way. In practice, brick has very large pores which are filled by diffusion. This can only be described in a model with several pore sizes (pore size distribution). But the simplicity of the present model is estimated to overrise the advantage of a more precise and with that more complex description.

The suction pressure at the free liquid surface is selected as small as possible without giving numerical instabillity due to large amounts of moisture taken up in the surface element. This is done by selecting $u/u_{ssd}=0.995$ in (3.26) and (3.27). (3.27) determines the magnitude of transport coefficient by transport from the free surface into the surface element, as suction pressure at the surface always is the smallest.

By capillary suction of sodium chloride solution moisture content at saturation is selected smaller than by capillary suction of distilled water, because due to the salt content moisture content is smaller by capillary suction of sodium chloride solution. At the selected moisture content at saturation calculated data seems to fit measured data very well.

As stated in section 5.3, the lower moisture content by capillary suction of sodium chloride solution might be due to larger contact angles, but the dependence of contact angle on salt content is uncertain and therefore it seems better to fit measured data by decreasing moisture content at saturation. In figure 5.21 it is seen how salt content increases through the specimen with time. In 4 hours the specimen is almost saturated with salt solution through the entire specimen.

Discussion of extraction of salt in church vault

Moisture content at saturation for medieval brick is selected higher than above due to the higher porosity. The characteristic pore size and suction pressure at the surface is not changed.

The salt content in the vault is selected as evenly distributed from measured data from Odden church given in section 5.4. This distribution is used as reference to compare extraction by initial capillary suction followed by drying and salt extraction only by drying without initial capillary suction, corresponding to experiments in Odden church. The same salt distribution is used to calculate salt transport by one-sited heating of the church vault.

From figure 5.22 and 5.23 it is clearly seen, that sodium chloride is washed to the opposite side of that, where capillary suction takes place. After 4 hours most of the salt is situated at the opposite side. Before plastering, the vault is wetted to give better adherence and to solute salts. The amount of water used for this is normally less than needed to saturate the vault. If extraction of salts is attempted to the same side as from where the vault is wetted, wetting is a ballance between the amount of disolved salt and the distance salts are transported from the extraction surface. If the vault is saturated, the salt might precipitate by drying at the opposite side, and it would be very hard to extract salts.

If the amount of disolved salt is weighted by the distance from the opposite side, the maximum value is obtained after about 10 minutes of capillary suction. The salt and moisture distribution at the optimum time for plastering is therefore assumed to be as after 16 minutes of capillary suction. This corresponds to almost saturation of the surface, with decreasing moisture content against the middle of the vault, and with the highest salt content in the middle of the vault.

The optimum selected is only apparent, because moisture content is equalized due to the steap decrease in moisture content immediately after capillary suction has stopped, and salt is transported to the opposite side. This is seen from figure 5.24 and 5.25. After about one day moisture content is equalized giving an average moisture content of 0.06 kg/kg and a salt content of 0.017 kg/kg at the opposite side of the extraction layer.

This rather high salt content is only controlled, and precipitation prevented, by a high relative humidity at the opposite side. By 95% rh the salt content is only slowly reduced and after 8 weeks an increase in salt content is seen on the side of extraction. The calculated average salt content of 0.25 wt% in the upper half of the vault after 56 days is of the same order of magnitude as that measured in Odden church after 52 days of extraction in spring. But as climate was not measured below the vault in the first period, it can not be established if extraction in Odden church was caused by high relative humidity below the vault. The relative humidity measured in autumn below the vault was approximately 95%. With time the salt content in the upper half of the vault therefore is expected to increase additionally, as indicated by calculations indicate. This is in aggrement with observations.

By drying of the church vault at the same conditions without initial capillary suction, it is seen from figure 5.27 that salt is transported very fast from the side with high relative humidity to the side with low relative humidity. Salt is transported at low moisture contents, approximately only one tenth of moisture content by extraction after capillary suction. Only salt content at the surface with low relative humidity increases. After two weeks the lower half of the vault is salt free and salt is concentrated in the upper half.

From the start a saturated salt solution exists through the entire vault. By increasing relative humidity at one side, the salt solution is diluted and because the vault is dry, the solution is quickly transported due to high suction pressures through the vault to the other side, where salts precipitate. Due to decreasing salt content, moisture content decreases at the side with high relative humidity. At the side with low relative humidity moisture content increases due to increasing salt content.

This extraction method seems much more efficient than extraction by capillary suction. However, this behaviour is not observed in the reference field in Odden church which indicates, that either the outlined transport mechanism is wrong or the climate was not as assumed in calculations. Calculations of extraction by initial capillary suction assuming high relative humidity below the vault aggreed well with measured data in Odden church as stated above, but this might be due to another initial distribution of moisture and salt, than assumed. Especially a higher initial moisture content might give another extraction rate. Observed extraction of salts into the church wall indicates that the initial moisture content was high.

From calculations in figure 5.28 to 5.31 it is seen that one-sided heating is expected to cause an increase in salt content at the heated surface, and a decrease in salt content at the oppsite side. The heating does not affect salt distribution in the middle of the vault, only salt content decreases evenly corresponding to the increase in salt content at the surfaces.

In calculations it is assumed, that relative humidity in the material does not change with temperature. In practice, relative humidity is observed to increase with temperature for a given moisture content. Saturation vapour pressure increases with temperature, and therefore at constant relative humidity vapour pressure in the material increases. Vapour pressure of the ambient air is constant, and therefore relative humidity decreases with temperature. When the surface of the material is heated, the vapour pressure in the material increases giving evaporation to the ambient air and into the vault. Here moisture dissolves salts, and by capillary suction salt solution is transported to the surface where salt precipitate. In the middle of the vault the difference between salt transport to an element and salt transport from the element at a given time is constant through the vault giving no change in salt distribution only a general decrease in salt content. At the surface with the lowest temperature salt content decreases, becauses there is no supply of salt solution.

Thus, by heating there is a vapour transport from areas with high temperatures to areas with low temperatures, and capillary transport of salt solution in the opposite direction, which transports salts towards the surface with the highest temperature. By cooling the direction of vapour and capillary transport changes, but calculations indicate that only minor capillary transport takes place as salt concentration at the surface does not change. This might be due to differences in salt concentration. The high salt concentration at the surface after heating gives a high suction pressure, and therefore prevents capillary transport. This also indicates, that extraction by heating is not possible, if salt content from the start is higher at the opposite side. Capillary transport by heating thus is one-way and only the heating time is of importance.

The transport of salts by one-sided heating can explain the observed overall transport of salts towards the upper side of the vault in Odden church in summer due to the suns heating of the church loft, and the overall transport of salts towards the lower side of the vault in winter due to the heating of the church room. But as stated above this mechanism alone is not enough, because when the salt content is high at the lower side of the vault after the winter period, the one-sided heating of the upper side during summer is not able to transport salts upwards due to the high salt content at the lower side. But the mechanism might work in combination with changes in relative humidity.

One very important assumption for the outlined salt transport by one-sided humidifieing or heating is, that capillary transport can take place at low moisture contents. For salt free materials this is generally not the case, but for saline materials the capillary transport might take place as transport in a thin salt film as suggested by Pühringer (1983). However, for the model it is not decisive for calculations if transport is due to capillary transport in pores or in a salt film. The important property is the rate of transport at low moisture contents, which has to be measured and related to calculations in the outlined model. Results in this work from Odden church and laboratory experiments indicates that salts are transported hygroscopically at relative humidities above the deliquescence point of the salt.

Diffusion is neglected in the outlined model. Experiments with electro-chemical extraction of salts in section 5.5 indicates that diffusion is not without significance at large differences in salt content when the material is saturated with salt solution. The increases in salt concentrations calculated above might be reduced by diffusion, which tends to smoothen out very high salt contents at the surface. In the model high salt concentrations is hard to reduce, because suction pressure is high and therefore attracts additional salt solution. This effect would be reduced if considerations was taken to diffusion.

Generally it seems, that extraction of salts to the same side as initial capillary suction followed by drying is not very efficient in thin constructions like vaults, because salts are washed to the opposite side, and only high relative humidities over a long period prevents precipitation here. On the contrary, extraction by capillary suction from one side and collecting salts on the other side seems very efficient. If this is not possible, extraction by one-sided humidifieing or heating as stated above might be possible. This demands a close control of the climate on both sides. As this was not carried out in Odden, it is difficult to estimate the effect in practice.

As described in section 5.4, the lower side of a vault in Alslev church was washed with water, which was observed to decrease the salt content in the lower side. At the same time the upper side of the vault was plastered and the loft over the vault was heated and dried. In this case, the order of washing, plastering and climate control is very important. The correct order is first to plaster the upper side, as this washes salts to the lower side. After this the lower side should be cleaned by washing, as this moves the salt to the upper side where they are collected in the mortar, and after this the loft should be dried and heated, as this extracts salts into the mortar. In practice, the order was not controlled, and the extraction seemed to have failed as spalling continued a few months after cleaning. This indicates how important it is to coordinate several repair methods.

Extraction of salts in bulk constructions is similar to extraction of salts from vaults, only extraction takes much longer time due to very slow drying and capillary suction, and it might be complicated by rising ground water and two-dimensional moisture and salt transport.

6. HYGRIC DEFORMATIONS

In this chapter the subject is to measure the length changes of saline brick and sandstone by wetting and drying (hygric deformations). Theese deformations are assumed to rupture the material. The model proposed in section 3.3 is used to estimate shrinkage and swelling for hygroscopic materials and results are compared with experimental results.

6.1 INTRODUCTION

Brick and calcareuos sandstone have only small length changes by adsorption of moisture from the ambient air (hygroscopic strain). Meanwhile, during repeated wet-dry cycles a thin crust is formed at the surface. This crust contains salts, and the cementing is decomposed, so that swelling and shrinkage of the crust differs from the underlaying unexposed stone. All salts are hygroscopic, especially NaCl, and this increases the amount of water in the material above the deliquescence point of the salt. This increase in moisture content is assumed to cause larger hygroscopic movements.

In the present work hygric strain is measured as a function of time for brick and calcareous sandstone with different salts at rather low concentrations. The dependence on time seems important as surface deterioration is an interaction between the rate of water uptake and the rate of climate changes. The low salt content is close to salt contents in real structures. There is only made one measurement with each salts rather than several measurements with the same salt. In this way measurements for one salt only represent a tendency rather than a statistic prove, and repeated measurements are necessary to aprove the tendency. Thus, it is the purpose of these experiments to show the effect of different salts on hygric movements of brick and calcareous sandstone by short time climate changes.

Only few investigations has been made to show the influence of salts on moisture movements in brick and sandstone. Searls and Thomasen (1990) describes the deterioration mechanisms in sandstone as the formation of a hard crust and a decomposed zone behind the crust. The expansion of the crust in contact with water results in separation of the crust from the underlaying stone. This is in agreement with what is found by Kiessl (1989). Wendler, Klemm and Snethlage (1990) finds that hygroscopic strain for "Sander Schilfsandstein" is proportional to the water uptake. It is shown that silicon-organic hydrophobing chemicals do not prevent the swelling and shrinking due to changes in humidity. Shuh, Klemm and Snethlage (1986) have determined strength and deformation properties of 6 Bavarian sandstones, and finds that swelling is multiplied by accumulation of gypsum in the pore volume. Shayan and Ritchie (1985) has measured the influence of sodium and potassium cations on the dimensional stability of rock prisms in wetting/drying cycles. It is found that sodium causes a greater dimensional movement in all rock types, which is attributed to the interaction with the clay minerals contained in the rocks. Felix (1983) has measured the linear swelling of sandstone due to isothermal water sorption. Water sensitivity appeared as a complex combination of mineralogical (clay minerals) and micro structural factors.

6.2 EXPERIMENTAL PROCEDURES

Materials

9 specimens of approximate size 160 by 50 by 20 mm were made out of modern brick, described in section 5.1. 9 specimens of approximate size 160 by 75 by 20 mm were made out of exposed calcareous sandstone, described in section 5.1. The specimens were taken from the inner of the stone, so that no exposed surface was included in the specimens.

Equipment

Strain was measured with Linear Displacement Transducers (LDT). The transducer is a linear variable differential transformer which has a single primary winding, two secondary windings and a movable core. The core is made of hydrogen annealed mumetal and mounted on non-magnetic stainless steel core rod. The output voltage is proportional to core displacement from electrical center and the linear range is $\pm$ 5 mm. The transducers were connected to a AC-amplifier giving output voltage 5 V DC/mm displacement. The transducers were fixed to a stainless steel frame, 300 mm long with a maximum number of 10 transducers, 5 in each end of the frame.

Brass plates ø 10 mm with internal thread was fixed to the specimens with epoxy and cores was then screwed in the brass plates. One core was fixed at each end of the specimen. In the frame specimens was supported on teflon tape. During measurements, there was no contact between cores and transducers. Equipment for strain measurements is seen on figure 6.1.

Displacements was recorded by a computer with one hour intervals. From displacement measurements and calibration data for the two transducers strain was calculated for the specimen.

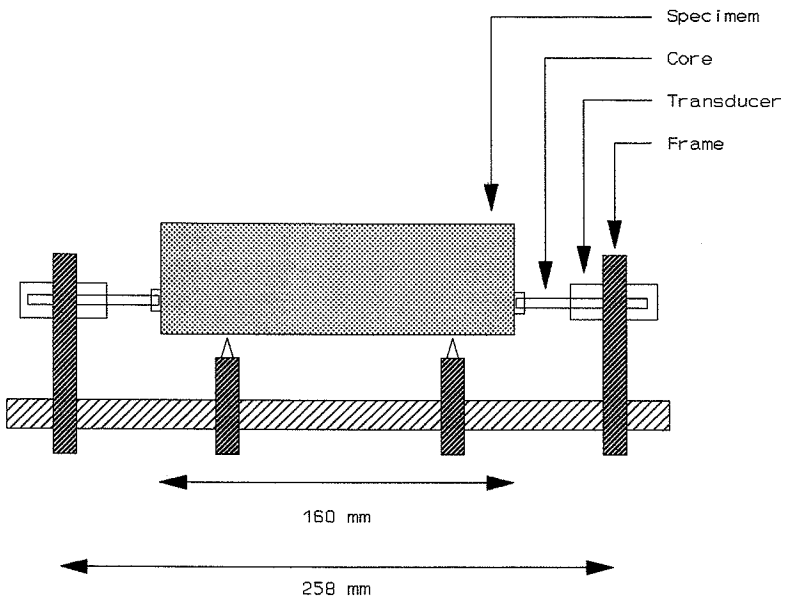

Figure 6.1. *Equipment for strain measurements.*

Procedure

All strain measurements was carried out at constant temperature, 20 °C. Hygroscopic strain was measured for salt free specimens in a one week cycle with varying relative humidity. The specimens were then saturated by capillary suction immersed in different salt solutions for 4 hours. Strain was measured for specimens containing salt, while they were drying in a week. Again, hygroscopic strain was measured for specimens with salt in a one week cycle with varying relative humidity. Finally, strain was measured while the saline specimens were absorbing distilled water by capillary suction. The measuring frame was left in a tray with specimens immersed a few mm in distilled water. After about 2 days capillary contact was lost due to capillary suction of specimens and evaporation from the water surface, and specimens were then left with water underneath for about 5 days. During all measurements a 154 mm long stainless steel rod ø 16 mm was used as reference, to ensure that only hygric movements took place.

The nine different salt solutions used for capillary suction and the resulting salt content of the specimens are given in table 6.1. The salt content is calculated from the mass content of the specimen saturated with salt solution, assuming that the concentration of the salt solution in the pores are the same as that of the free salt solution

(6.1)
$$s = 100 \frac{(m_{ssd} - m_d)}{m_d} c_k$$

Where

s	=	salt content in specimen [wgt%]
m_{ssd}	=	mass of specimen saturated with salt solution [kg]
m_d	=	dry mass of specimen [kg]
c_k	=	concentration of salt solution for capillary suction [kg/kg]

Table 6.1. *Salt solutions for capillary suction and salt content of specimens for strain measurements. B=brick, S=sandstone.*

Nr.	Salt in 1000 g water	Specimen nr.	Salt content (wgt%)	
1	Distilled water	B2	-	
		S2	-	
2	100 g NaCl	S8	0.63	
3	20 g Na_2SO_4	S4	0.12	
4	40 g Na_2SO_4	B6	0.41	
		S6	0.26	
5	50 g $MgSO_4 \cdot 7H_2O$	S1	0.32	
6	100 g $MgSO_4 \cdot 7H_2O$	B5	0.87	
		S5	0.60	
Two salts			a	b
7	a: 20 g Na_2SO_4 b: 100 g NaCl	B9	0.19	0.95
		S9	0.12	0.60
8	a: 50 g $MgSO_4 \cdot 7H_2O$ b: 100 g NaCl	B8	0.45	0.90
		S3	0.30	0.61
9	a: 20 g Na_2SO_4 b: 50 g $MgSO_4 \cdot 7H_2O$	B4	0.22	0.54
		S7	0.12	0.30

Climate

The frame was placed in a climate chamber. Temperature and relative humidity (RH) was controlled by a computer, measured by a NOVASINA transmitter with an electrolytic measuring cell and recorded by the computer with one hour intervals. The climate was varied in a four week cycle. Standard deviation for temperature and relative humidity are 0.5 °C and 2.0 % rh.

Table 6.2. *Climate during strain measurements in a four week cycle.*

Measurement	Time (days)	Temp. (°C)	ϕ (%)
Hygroscopic strain of salt free specimens (Drying at 105 °C before measurements)	2	20	80
	2		30
	2		80
	1		30
Capillary suction 4 hours in salt solution at 20 °C			
Strain during drying	4	20	50
	3		30
Hygroscopic strain of specimens with salt	2	20	80
	2		30
	2		80
	1		30
Strain during capillary suction of distilled water	7	20	50

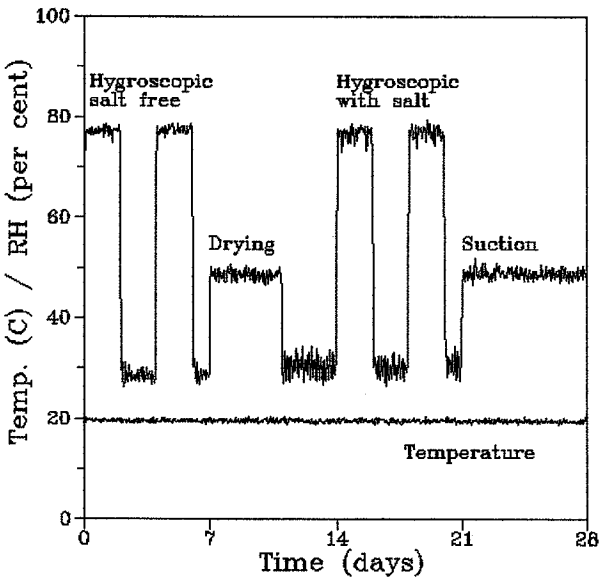

Figure 6.2. *Measured climate during strain measurements in a four week cycle.*

6.3 RESULTS

Strain at a given time is calculated as an average value in a 5-hour interval i.e. two values before and two values after the actual time (running average value). In this way the strain curve is smoothened to eliminate small fluctuations due to uncertainty of the measurements.

Hygroscopic strain of salt free specimens

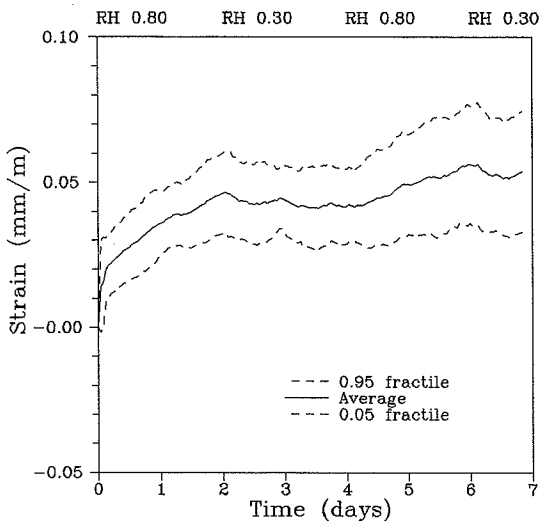

Figure 6.3. *Hygroscopic strain of salt free brick. Average values for 6 specimens.*

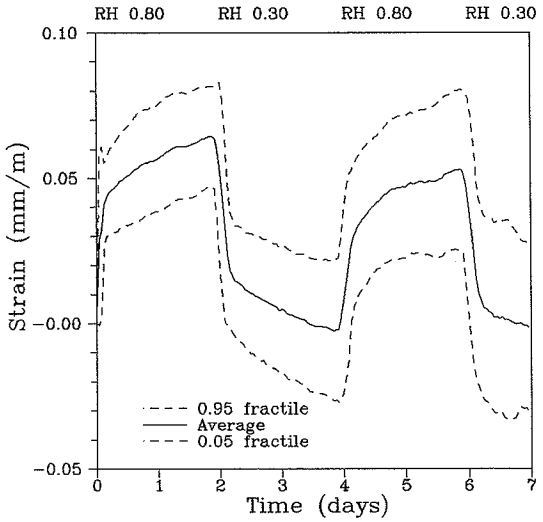

Figure 6.4. *Hygroscopic strain of salt free calcareous sandstone. Average values for 9 specimens.*

Strain by drying of specimens with salt

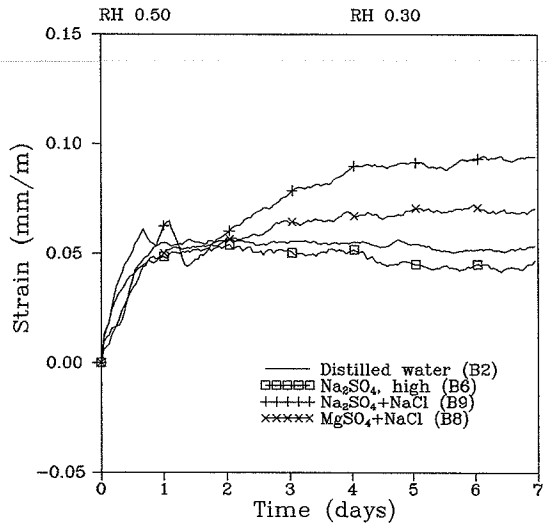

Figure 6.5. *Strain by drying of brick with salt.*

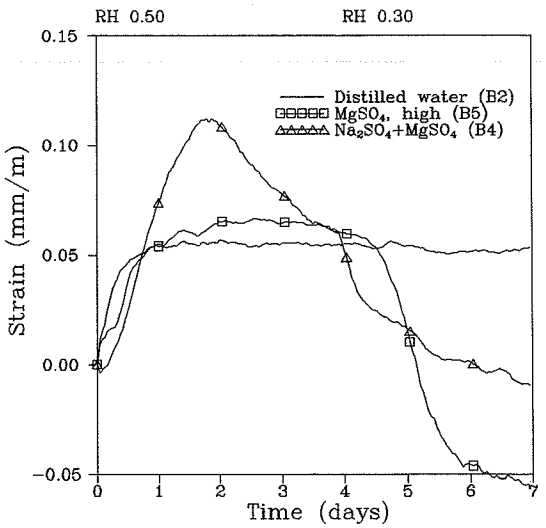

Figure 6.6. *Strain by drying of brick with salt.*

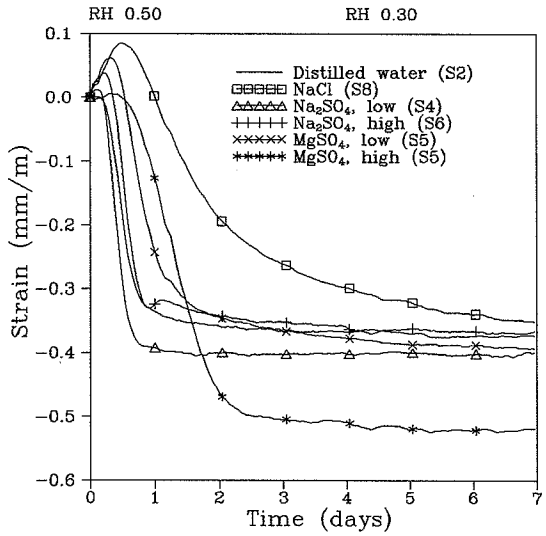

Figure 6.7. *Strain by drying of calcareous sandstone with salt.*

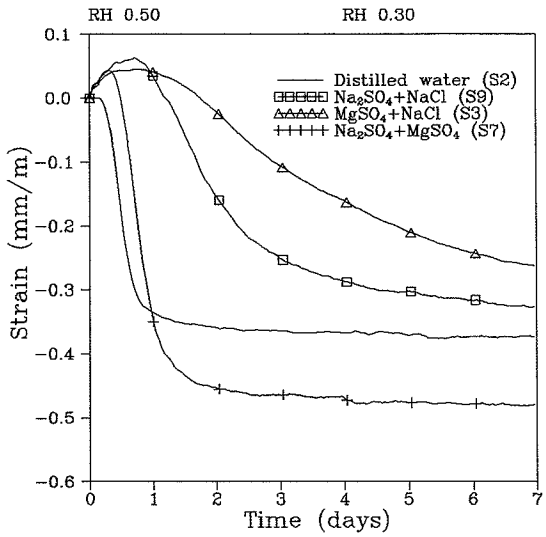

Figure 6.8. *Strain by drying of calcaraous sandstone with salt.*

Hygroscopic strain of specimens with salt

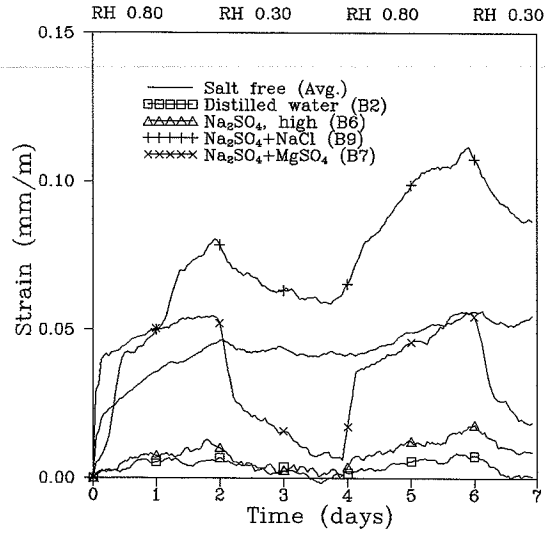

Figure 6.9. *Hygroscopic strain of brick with salt.*

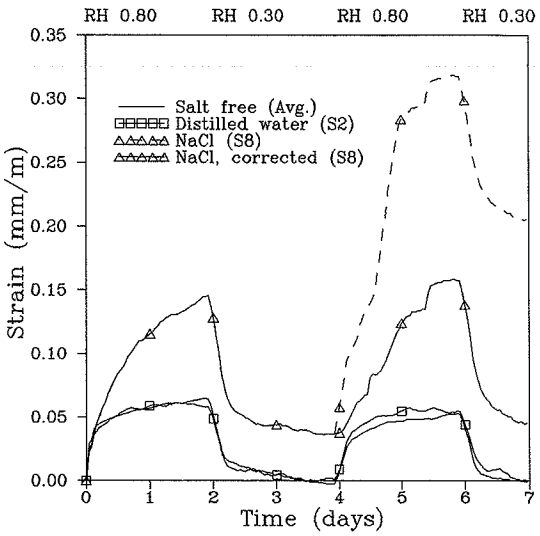

Figure 6.10. *Hygroscopic strain of calcareous sandstone with salt.*

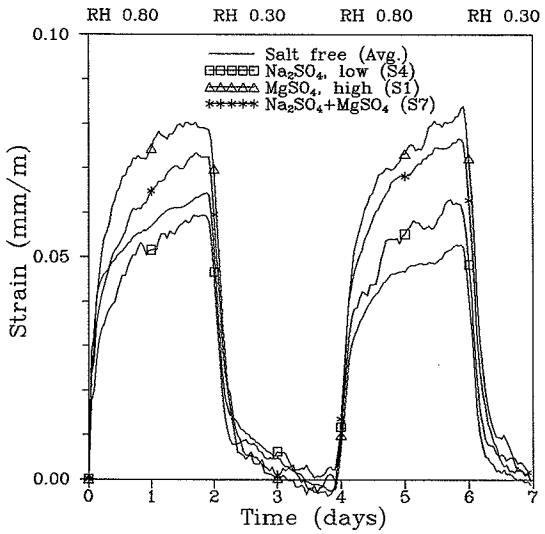

Figure 6.11. *Hygroscopic strain of calcareous sandstone with salt.*

Strain by capillary suction for specimens with salt

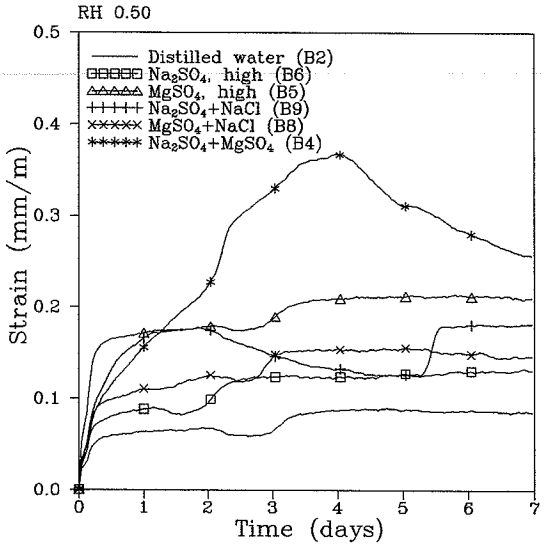

Figure 6.12. *Strain by capillary suction for brick with salt.*

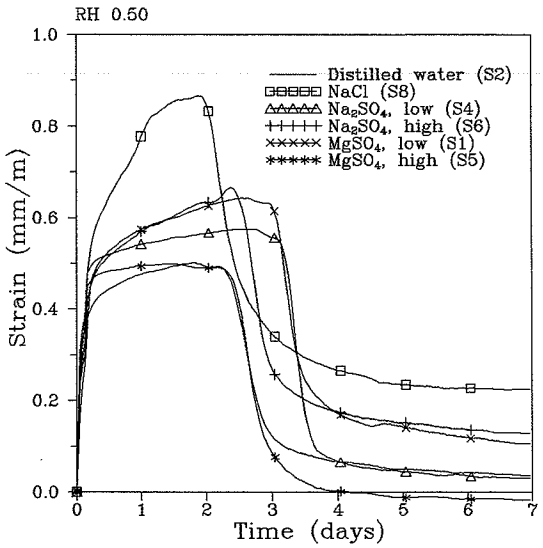

Figure 6.13. *Strain by capillary suction for calcareous sandstone with salt.*

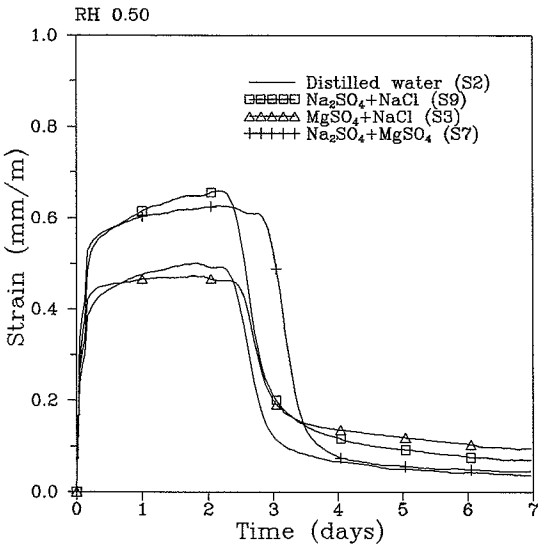

Figure 6.14. *Strain by capillary suction for calcareous sandstone with salt.*

6.4 CALCULATIONS OF STRAIN

As stated in section 3.3 the shrinkage and swelling can be calculated from two mechanisms; the Gibbs Bangham shrinkage due to adsorption of liquid on inner surfaces and the capillary shrinkage due to tension in the pore liquid. Strain by both mechanisms are calculated from the sorption isotherm for the material. In the calculations below two sorption isotherms from Hansen (1986) therefore are used, one for brick and one for red sandstone. For brick porosity is set to 0.29 m^3/m^3 and dry density 1870 kg/m^3 corresponding to brick used in chapter 5. For the sandstone porosity is set to 0.21 m^3/m^3 and dry density 2120 kg/m^3 likewise corresponding to the sandstone used in chapter 5. The elastic modulus for solid material and solid density are for both brick and sandstone set to respectively 20 GPa and 2650 kg/m^3. The poissons ratios are all set to 0.2. The sorption isotherms are given by Hansen (1986) by the equations

Brick

(6.2)
$$u_m = 0.0115 \exp\left[-0.210 \ln\left(1 - \frac{\ln\phi}{4.45 \cdot 10^{-4}}\right)\right]$$

Sandstone

(6.3)
$$u_m = 0.29 \exp\left[-0.671 \ln\left(1 - \frac{\ln\phi}{9.42 \cdot 10^{-4}}\right)\right]$$

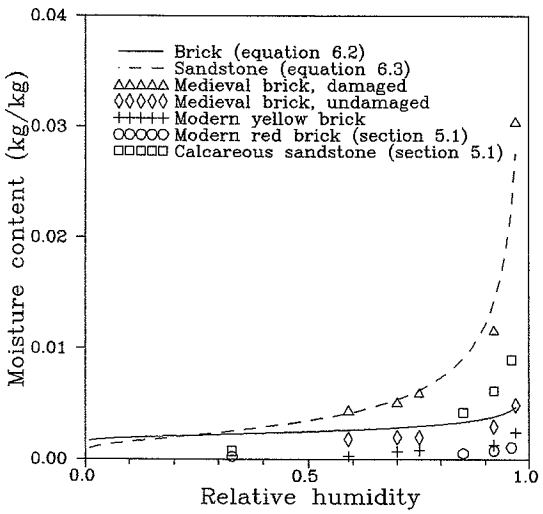

Figure 6.15. *Sorption isotherms for medieval and modern brick and sandstone. Larsen (1987). Hansen (1986).*

Larsen (1987) gives sorption isotherms for damaged and undamaged medieval brick from Alslev church washed out for salts and for a modern yellow brick. Theese are in figure 6.15 compared to sorption isotherms for salt free brick and sandstone given in section 5.2, and sorption isotherms given by (6.2) and (6.3) above.

Gibbs-Bangham shrinkage

The Gibbs-Bangham shrinkage is only important for materials like cement paste with a large inner surface and corresponding adsorption of water. The adsorption of water at low relative humidities for salt free brick and calcareuos sandstone used in theese experiments is low as found in section 5.2. The inner BET-surface found from sorption isotherms given above and the BET-equation is 6000 m^2/kg for brick and 6500 m^2/kg for sandstone. This is very low compared to cement paste, in which the inner BET-surface is of the magnitude 10^5 m^2/kg.

The change in surface free energy is calculated from the sorption isotherms above in the relative humidity range 30-80 % from V-t pore analysis as described in section 3.3. The inner surface found is 800 m^2/kg for brick and 5400 m^2/kg for sandstone. The change in surface free energy is 0.017 N/m for brick and 0.029 N/m for sandstone giving the linear strain 0.0016 mm/m for brick and 0.018 mm/m for sandstone.

If the V-t pore analysis was used without changes for saline materials, the change in surface free energy would be considerably larger due to adsorption of moisture of the salt. But this is under the assumption that all water is adsorped on inner surfaces, which is not necessarily the case as stated above. The change in surface free energy certainly will be different for a saline material due to the content of ions affecting especially clay minerals, but the magnitude of this change is difficult to estimate. Therefore, in this work, the Gibbs-Bangham shrinkage is not discussed further.

Capillary shrinkage

Shrinkage due to tension in the pore liquid can be calculated from (3.41) using the partial relative humidity ϕ_k. This is done for brick and sandstone with different contents of sodium chloride.

First the sorption isotherms are calculated from (6.2-3) as described in section 2.2. Sorption isotherms are given in figure 6.16-17. In figure 6.18 is given the degree of liquid saturation of brick. For low salt content and for highly hygroscopic materials the deliquescence point is below saturation humidity for the free salt, as stated in section 2.2. In figure 6.19 is calculated the deliquescence point for brick and calcareous sandstone at low salt contents. Capillary shrinkage is calculated for brick and sandstone. The results are given in figure 6.20-21.

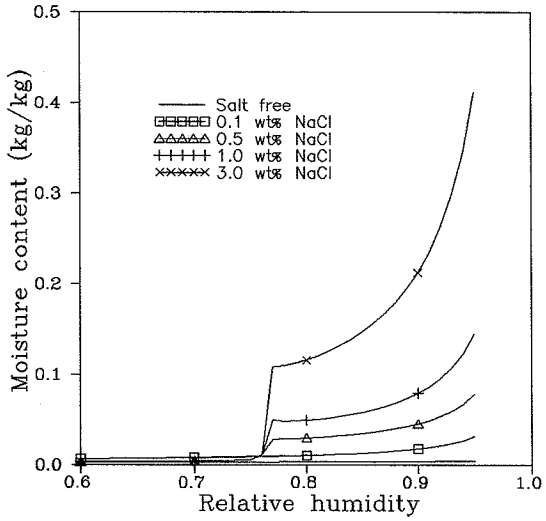

Figure 6.16. *Calculated sorption isotherms for brick with different contents of NaCl.*

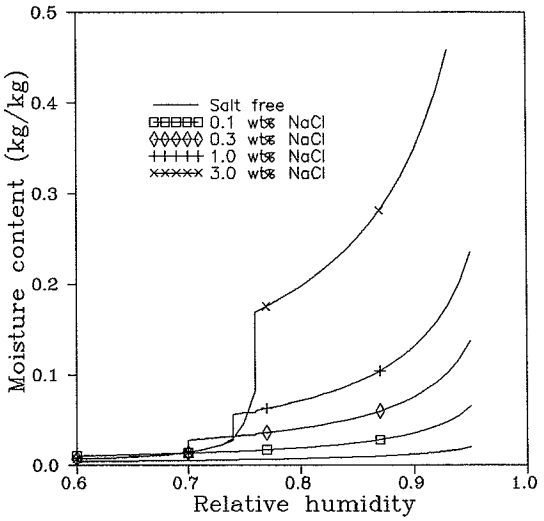

Figure 6.17. *Calculated sorption isotherms for sandstone with different contents of NaCl.*

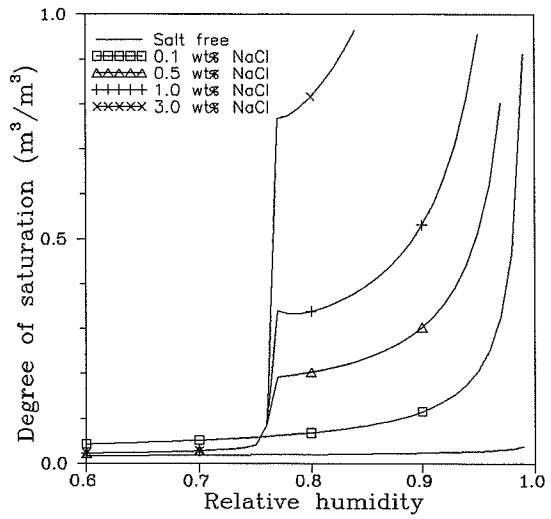

Figure 6.18. *Degree of saturation for brick with different content of NaCl.*

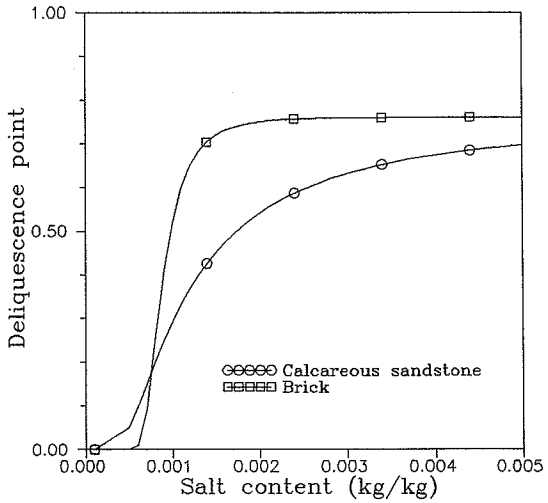

Figure 6.19. *Deliquescence point for brick and calcareous sandstone at low salt contents.*

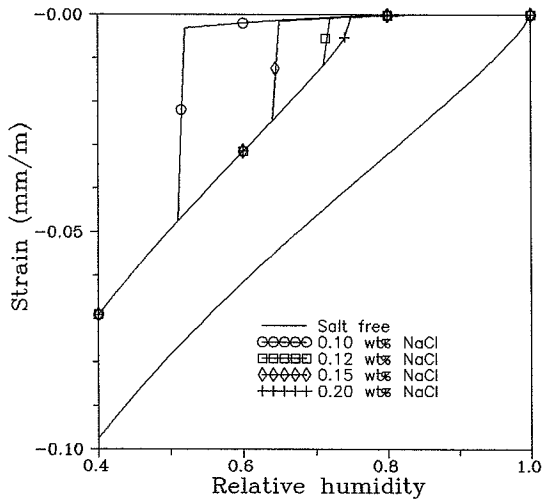

Figure 6.20. *Calculated strain for brick with different contents of NaCl as function of relative humidity.*

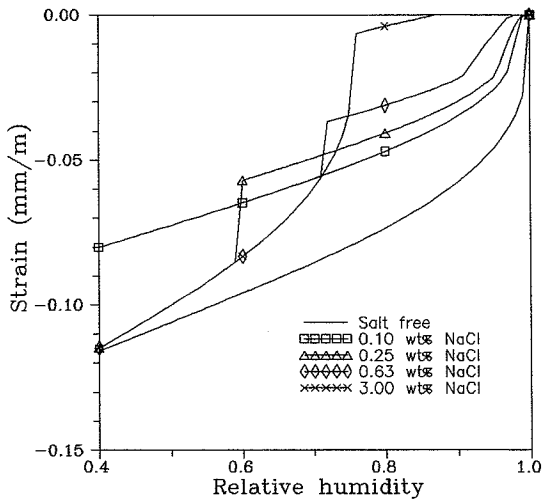

Figure 6.21. *Calculated capillary strain for sandstone with different contents of NaCl as function of relative humidity.*

6.5 DISCUSSION

Hygroscopic strain of salt free specimens

For brick the average hygroscopic strain in the relative humidity range 50-80 % is 0.05 mm/m with standard deviation 0.01 mm/m. From the shape of the curve it is seen that strain is not in equilibrium after two days. Strain by desorption is very small and strain by the next absorption less than by the first. It seems that strain is slightly irreversible.

For calcareous sandstone the average hygroscopic strain in two day cycles in the relative humidity range 30-80 % is 0.06 mm/m and standard deviation 0.015 mm/m. Strain develops as a quick initial strain and a slower subsequent strain. It seems that equilibrium almost is obtained after two days. There is no significant difference between strain by absorption and desorption.

Hygroscopic strain for brick and calcareous sandstone is of the same order of magnitude, but brick reacts much slower to climate changes than sandstone. This might be due to differences in rate of hygroscopic water uptake or differences in mineral composition and pore sizes.

Strain by drying of specimens with salt

For brick it is remarkable that specimens expand by drying the first 24 hours almost independently of salt content, and after this only slowly shrink. Expansions are of the same order of magnitude as hygroscopic strain for salt free specimens. The reason for this behaviour could be that brick is so coarse porous that capillary tensions is relased at the time where measurements starts, about one hour after specimens has left the immersion. This is in agreement with prior observations by Larsen and Nielsen (1990), who has observed expansions of drying brick after about one hour. Another almost contrary explanation is that the expansions is caused by late internal distribution of moisture from corse pores into fine pores releasing capillary or other internal tensions.

Specimens with sodium chloride and sulphates (B8 and B9) even expand after the first 24 hours. Specimens with Na_2SO_4 and $MgSO_4$ (B4 and B5) shrink after respectively 2 and 4 days. This might be due to loss of crystal water at relative humidity around 80 %. This does not take place when NaCl is present (B8 and B9), because NaCl forms a solution at relative humidity above 76 % which prevents the loss of crystal water.

Calcareous sandstone with salt expand by drying the first 12 hours, contrary to salt free sandstone (S2). The largest expansion is observed for NaCl (S8). Expansion is of the same order of magnitude as that for brick. After expansion a much larger shrinkage is observed, and therefore the expansion could not be caused by released capillary tensions. As for brick expansion might be caused by released internal tensions. After one week all specimens seem to have reached equilibrium, most of them even after 2 days. Specimens with NaCl (S3, S8 and S9) shrinks slower than the others. This might be caused by slower drying of saline materials, as observed in section 5.3. Shrinkage is of the same order of magnitude for all specimens when the expansion in the beginning of the drying phase is excluded. Specimens with $MgSO_4$ (S5 and S7) seems to have larger shrinkage. Shrinkage by drying is 6-7 times larger than hygroscopic expansion of salt free sandstone.

Hygroscopic strain of specimens with salt

For brick the first hygroscopic movement in the relative humidity range 30-80 % of the specimen with distilled water (B2) is much smaller than the average hygroscopic movement for all 6 specimens measured before capillary suction. This might be caused by the way specimens were dried. Before measuring the hygroscopic strain of the salt free specimens, they were dried at 105 °C and conditioned at 20 °C, 50% rh. This might have caused internal tensions which were released at high relative humidities by the first adsorption. Specimen (B2) was dried at 20 °C, 50% rh changing to 30% rh after 3 days. This much slower drying might not have induced tensions in the brick, and therefore strain by first adsorption is much smaller. Strain by the following changes in relative humidity is of the same order of magnitude as the average strain.

Sodium sulphate does not influence hygroscopic strain compared to salt free specimens at the present content (0.41 wt%). Strain caused by change in crystal water content from thenardite

to mirabilite at 70% rh is not observed. But when sodium sulphate is mixed with either sodium chloride or magnesium sulphate a large increase in strain is observed compared to strain for salt free specimens. This might be caused by either volume change of crystal water, change in capillary forces or change in surface free energy due to the ion content in the pore liquid.

For the mixture of sodium sulphate with magnesium sulphate the strain is almost entirely reversible but for the mixture of sodium sulphate with sodium chloride strain seems to be partly irreversible.

Whereas strain for brick is somewhat diffuse, the strain for calcareous sandstone very sharply increases and decreases with relative humdity. From the course of strain curves specimens seem to be in equilibrium within two days. The initial capillary suction of distilled water does not affect the hygroscopic strain in the relative humidity range 30-80 %, but initial capillary suction of salt solution clearly does.

Sodium chloride (0.63 wt%) increases strain with a factor of 3. In the second humidity cycle a very large increase in strain was measured, but strain occured in abrupt leaps, and this might have been caused by the measuring equipment. If the abrupt leaps are removed, a corrected strain curve occurs as indicated in figure 6.10, with an increase in strain similar to the first humidity cycle.

Sodium sulphate (0.26 wt%) alone does not affect hygroscopic strain, but mixed with magnesium sulphate it does. This might be caused by magnesium sulphate, that alone (0.60 wt%) affects strain. The effect on strain of sodium sulphate might be caused by volume change from crystal water.

In theese experiments strain could be caused by temperature change of the specimens due to heat of evaporation by adsorption and desorption of moisture. With a thermal expansion coefficient of $5\text{-}10 \cdot 10^{-6}$ pr. °C it would demand a temperature change of 5-10 °C for the entire specimen to give a strain of 0.05 mm/m, which is unlikely. But the influence on hygroscopic strain of surface temperature change caused e.g. through evaporation can not be excluded.

Strain by capillary suction for specimens with salt

Capillary contact between specimens and distilled water lasted about two days, and after this specimens were drying at 50 % rh above distilled water, which means that relative humidity must have been close to 1 on the lower side, close to 50 % at the upper side and something in between at the specimen sides. During the week a lot of efflorescence was observed on the upper half of the specimens with salt. This was clearly caused by the upwards transport of salt by capillary suction and the differences in relative humidity.

Strain curves for brick look very much like capillary suction curves (comparing figure 6.12-14 and figure 5.9-10) only strain curves are a little delayed. The point of capillary saturation of

the specimen is clearly recognized. Strain is about 4 times of that in the relative humidity range 30-80 %. Specimens with salt clearly has a larger strain than the salt free specimens. After the loss of capillary contact, after about two days, a slight expansion corresponding to the expansion by drying in figure 6.5 is observed and the rest of the strain curve is similar to figure 6.5. The expansion could be caused by differences in strain between the lower side (where the measure points were placed) with high relative humidity and the upper side with lower relative humidity.

If expansion was caused by releasing capillary tensions, as suggested above, shrinkage before expansion should be observed, but only very small shrinkages is observed. Expansion caused by delaied internal distribution of moisture is unlikely, as this would have taken place within 2 days of capillary suction. It seems that brick always tends to expand rather than shrink. This might be caused by internal tensions in the brick released by drying as a reaction to the compressive forces by capillary water. Release of these tensions, which possibly arise during firing of the brick, is irreversibel.

It is remarkable that specimen with sodium sulphate mixed with magnesium sulphate has a very large expansion, even after capillary suction has stopped, and hereafter shrinks. The same was observed by drying and hygroscopic strain as stated above. The expansion is not observed for the two salts individually.

As for brick, strain curves for calcareous sandstone look like capillary suction curves for sandstone. Specimens with salt have larger expansion than the salt free specimens, especially with sodium chloride. Expansion is about 10 times larger than hygroscopic strain, but is of the same order of magnitude as drying shrinkage, as seen in figure 6.7-8. Drying shrinkage when capillary suction stops is clearly seen and is of the same order of magnitude as that previous measured.

Calculations of strain

Strain is calculated for brick and sandstone, as representative for a slightly hygroscopic and a hygroscopic material, to show how different salt contents influence sorption isotherm and strain. Sodium chloride is selected as salt, because it is very hygroscopic and does not take up crystal water, which would complicate calculations.

The model is based on definition of the two partial relative humidities ϕ_k and ϕ_c, and the course of theese is decisive for strain calculations. Below the deliquescence point, a saturated salt solution exists in the pores, and therefore the assumption that ϕ_c equals saturation humidity seems reasonable. Above the deliquescence point ϕ_c is assumed to increase proportionally with relative humidity from the deliquescence point, which by adsorption seems reasonable as the simplest assumption. By desorption from liquid saturation of the material, the result of the above assumption is that the rate of change in ϕ_c decreases with salt content. In other words, the rate of concentration decreases with salt content in the material. This is due to the hygroscopicity of the material and therefore, the assumption seems reasonable.

In figure 6.16 is clearly seen that a slightly hygroscopic material with a high salt content has a sharp leap at the deliquescence point. The small amount of hygroscopic water from the material does not affect the deliquescence of the salt, which is mainly controled by the hygroscopic water uptake of the salt itself. For low salt concentrations the deliquescence point will be a little affected by the material.

In figure 6.17 is seen that contrary to the slightly hygroscopic material, a hygroscopic material decreases the deliquescence point even for moderate salt concentrations. The hygroscopic moisture from the material is for moderate salt contents able to dissolve all the salt below saturation humidity of the free salt, and therefore the salt starts to act hygroscopically. Below the deliquescence point, the material is seen to increase moisture uptake due to the salt.

The influence of material hygroscopicity on deliquescence point is outlined in figure 6.18. For a slightly hygroscopic material like brick, deliquescence point is only lowered for very low salt contents, but for a hygroscopic material like sandstone it is lowered even for moderate salt contents. For very low salt contents the effect of lowering the deliquescence point is minor, because the ammount of salt is small, and the moisture uptake by the salt therefore is small.

The sorption isotherm for a saline material is a ballance between the hygroscopicity of the material and the amount of salt in the material. The moisture content in a saline material is always higher than in a salt free material, even below the deliquescence point, because a saturated salt solution is formed in the pores, which at a given relative humidity makes the partial relative humidity ϕ_k corresponding to the Kelvin equation higher, so that the saline material increases moisture adsorption. To add sorption isotherms for salt and for a slightly hygroscopic material to get the sorption isotherm for the saline material only causes a minor error, but for highly hygroscopic materials it would cause considerably errors.

The degree of saturation of the material caused by the hygroscopicity of the salt is outlined in figure 6.17. Below the deliquescence point only low degrees of saturation is obtained, but above a considerably degree of saturation can be obtained for high salt contents. Again, the hygroscopicity of the material influence the degree of saturation compared to the salt free material.

The model described to calculate hygroscopic strain contains two opposite mechanisms. The partial relative humidity corresponding to the Kelvin equation determines the compression force of the material. For a given moisture content an increase in partial relative humidity would cause an decrease in capillary tension and therefore a decrease in shrinkage. The moisture content determines the compression surface of the material. For a given partial relative humidity an increase in moisture content would cause an increase in compression surface and therefore an increase in shrinkage. By adsorption of moisture the first mechanism thus makes the material expand, and the second mechanism makes it shrink. The ballance between the two mechanisms, how much moisture is taken up at a given relative humidity, is determinded by the sorption isotherm.

For a salt free material the expansive mechanism is the strongest, the material expand by adsorption of moisture. For a slightly hygroscopic material like brick the ballance is nearly constant, the expansion for a given change in relative humidity is constant throughout the entire relative humidity range, as seen on figure 6.20. For a hygroscopic material like sandstone the expansive mechanism gets stronger as relative humidity increases, as seen on figure 6.21.

Due to the formation of a saturated salt solution in the pores by adsorption of moisture for saline materials, the increase in partial relative humidity ϕ_k corresponding to the Kelvin equation always is higher than the increase in relative humidity. This means, that the expansive mechanism from the start of adsorption is stronger than for a salt free material.

The deliquescence point of a salt in a hygroscopic material is lowered as stated above. Below the deliquescence point the capillary strain is identical for different salt contents because in all cases a saturated salt solution exists in the pores. At the deliquescence point, the salt becomes hygroscopic and takes up moisture as given by (2.4). It is assumed that all pores up to a given size is filled with liquid and that larger pores are empty. Capillary strain is dependent on the volume filled with liquid and the pore size limit between filled and empty pores, as this poresize determines the capillary force. The poresize corresponding to ϕ_k can not be used, as this corresponds to the poresize filled with liquid only due to the material. Instead, the sorption isotherm for the salt free material is used to determine the relative humidity (and consequently the pore size) corresponding to the total moisture content of the saline material. In this way the pore size distribution for the material is used to determine the pore size limit. This limit is the pore size limit between filled and empty pores for the total liquid content.

As seen on figure 6.20-21, the result is that the material swell by adsorption as the salt becomes hygroscopic, which seems quite reasonable. If the corrected pore size limit was not used, the material would shrink as the salt became hygroscopic, because the water filled porosity would increase without changing the pore size limit. But this would demand an increase in volume fraction of pores at the pore size limit, which is not reasonable, as pore size distribution does not change.

Above the deliquescence point, the partial relative humidity ϕ_c corresponding to the salt increases from saturation humidity, as the salt solution is diluted. Therefore, the rate of change in partial relative humidity ϕ_k corresponding to the Kelvin equation decreases, as outlined in figure 2.1, which means that the expansive mechanism by adsorption decreases. As the salt becomes hygroscopic, and in this way increases liquid filled porosity, the shrinkage mechanism as described above increases. But here again, the corrected pore size limit between filled and empty pores has to be used. The total effect is that the rate of swelling by adsorption decreases above the deliquescence point.

This is seen on figure 6.20-21. The top line is the strain curve for the material with a saturated salt solution. Below is the similar strain curve for the salt free material. In between are strain curves for the material with a diluted salt solution above the deliquescence point. It is seen that the material swell by adsorption below the deliquescence point, at the

deliquescence point the material suddenly swell as the salt becomes hygroscopic, and above the deliquescence point the rate of swelling decreases. The rate of swelling finally increases when all the pores are filled with salt solution. The increase is caused by elimination of the shrinkage mechanism (pore filling) while salt solution in the saturated material is diluted.

The capillary shrinkage model does not predict any change in the overall magnitude of strain by salts, but the course of strain is changed. Below the deliquecence point, the rate of strain increases compared to a salt free material, and above the rate of strain decreases with a sudden change at the deliquescence point. The rate of strain below the deliquescence point for a slightly hygroscopic material almost equals the rate of strain for a salt free material, and there is almost no strain above the deliquescence point. The partial relative humidity ϕ_k corresponding to the Kelvin equation is close to unity at the deliquescence point, and therefore almost no strain occurs above. For a hygroscopic material, the rate of strain below the deliquescence is larger than for a salt free material, and for moderate salt contents the material still swell by adsorption above the deliquescence point.

For high salt contents there will be no change in strain course by increasing the salt content as the deliquescence point equals saturation humidity of the salt. Below there wil be a saturated salt solution in the pores corresponding to the top line, and above no strain occurs because the material is not able to adsorb more moisture.

From figure 6.15 it is seen that sorption isotherm for a undamaged medieval brick corresponds to sorption isotherm given by (6.2) for brik, and that sorption isotherm for a damaged mediveal brick corresponds to sorption isotherm given by (6.3) for sandstone. Although porosity and density is a little different, this does not change the course of strain given in figure 6.20 and 6.21, and therefore the comparrison above between a slightly hygroscopic and a hygroscopic material also is true for an undamaged and a damaged brick.

Comparison of measured and calculated strain

The calculated strain is one out of three strain mechanisms

1) capillary strain
2) change of surface free energy by adsorption of moisture and ions
3) strain by uptake and loss af crystal water

Therefore only some properties of the strain measurements can be explained from calculations in the present model. These properties will be pointed out below.

- According to the model the hygroscopic strain for salt free specimens in the relative humidity range 30-80% is estimated to 0.09 mm/m for brick and 0.05 mm/m for sandstone. This agrees well with measured strain for sandstone, but for brick it is overestimated. This might be due to relaxation of internal tensions in brick by drying as stated above.

- For sandstone with 0.63 wt% NaCl the hygroscopic strain in the relative humidity range 30-80 % is estimated to 0.1 mm/m which is of the same order of magnitude as the strain measured.

- The initial swelling by drying of specimens with salt can not be estimated by the model.

- Strain by drying and capillary suction is estimated to 0.12 mm/m for sandstone. The measured vaule is almost three times the estimated value. The slower shrinkage of saline materials is explained by the model. The model estimates saline materials to shrink at lower relative humidities than salt free materials.

- By capillary suction the specimen with NaCl swell more than the salt free specimen. This is not explained by the model.

It seems that the model gives a reasonable estimate for strain in the hygroscopic range for hygroscopic materials (sandstone), especially the difference in hygroscopic strain for salt free materials and saline materials is explained. This difference might be due to the different course of strain rather than an overall difference in the magnitude of strain.

Above the hygroscopic range, the model generally underestimates strain. The reason for this might be that the elastic properties change with moisture content. Further strain from change in surface free energy might influence measurements.

7. DISCUSSION

The study of decay mechanisms of porous building materials by salts is in this work concentrated on three subjects

- Equilibrium state of salt and moisture in the pores
- Moisture and salt movement in structures
- Hygroscopic length changes of saline materials

A new theory to estimate the effect of changing climate on saline structures is proposed and experimentally verified. The theory is based on two theeses describing the equilibrium state and this is the basis for the two other subjects; the equilibrium state of salt and moisture determines the vapour pressure and liquid properties in the micro structure, and therefore determines how moisture and salt are transported inside the material. Also, the equilibrium state determines the size of capillary tensions, and therefore hygroscopic movements and the way the material mechanically is deteriorated.

The equilibrium state therefore is very important, and the two theeses proposed in chapter 2 is decisive for the rest of the theoretical work. The way the theeses are deduced is basicly an engineering extrapolation of a known model and equation (the Kelvin equation assuming meniscus formation and cylindrical pores) to a wider area (lower relative humidities). It is an attempt to combine two known areas (material properties and salt properties) and obtain information in a new area (saline materials).

The experimental results in this work indicates that the theory gives the right answers for coarse porous materials like brick and sandstone infected with sodium chloride. For other materials and other salts the theory has to be evaluated from experimental data and observations, and it might be necessary to correct the assumptions slightly, but as an engineering tool the theory seems to be quite promising. The concept of partial relative humidities is quite workable. Though the course of partial relative humidities as outlined in figure 2.3 might not be correct, the concept may still be used by changing the course, especially at low relative humidities. In this way considerations can be taken to the ability of adsorbed water to dissolve salt.

First of all, and this is the most important result, with this theory it is possible to estimate the effect of changing climate on saline structures and the effect of specific stone conservation (salt extraction). Secondly, one gets an understanding of the mechanisms of stone deterioration on the basis of the micro structure of the material.

In this work it was observed that hygric movements change, when the material is infected with salts. At the same time hygroscopic and capillary moisture uptake and evaporation rate are changed. On the basis of experiments in this work it is proposed that the decay of porous materials by salts is caused by difference in hygric movement between the surface and the material behind. The mechanism is explained considering a damp wall with salts, for instance from rising groundwater.

When the wall is dried out from the surface, salts are transported towards the surface as observed in laboratory experiments described in section 5.3, in the vault in Odden church described in section 5.4 and as calculated in section 5.7. Above the deliquescence point of the salt the higher salt content at the surface decreases capillary shrinkage by drying compared to salt free material and increases shrinkage below the deliquescence point, as calculated in section 6.4 and rendered by experiments described in section 6.3.

The surface material therefore shrink less than the material behind in the beginning of the drying phase, even though relative humidity in the material behind is higher than relative humidity in the surface material. This causes compression in the surface material or, if the adherence is bad as for crust layers, forms a distinct bubble on the surface. Later in the drying phase, below the deliquescence point, the surface material shrink more than the material behind causing tension in the surface material or even cracks, as observed for crust layers.

The difference in calculated strain between sandstone with 3 wt% sodium chloride and salt free sandstone in the relative himidity range 70-75 % is 0.05 mm/m. In calculations elasticity of solid sandstone is assumed to be 20 GPa, corresponding 13 GPa for the porous material with porosity 0.21 m^3/m^2. Tension in the surface material by drying therefore is 0.7 MPa. This is normally less than tension strength of sandstone, but repeated drying/wetting causes fatigue and strength might be reduced by chemical dissolution of the cementation. The difference in hygroscopic strain due to the salt content therefore may explain the decay of sandstone.

In the same humidity range, there is no significant difference in strain between brick with moderate salt content and salt free brick as seen in figure 6.20. This means that there will be no tension in a saline surface layer, and therefore there will be no decay of the surface.

The mechanism is also valid for a partly damp wall or vault, which is wetted by an increase in relative humidity of the ambient air or by rain water. A high salt content at the surface increases hygroscopic moisture uptake, and makes the surface material swell more than the material behind causing compression parallel to the surface and tension perpendicular to the surface, which might form a distinct bubble on the surface if the adherence is bad as for crust layers. This will happen more often for a surface material with salts than for a salt free material, because a saline material starts swelling at lower relative humidities than a salt free material, as calculated in section 6.4.

By heating the surface of a saline material, the salts is transported towards the surface as calculated and discussed in section 5.7. Heating dries out the surface, and in the same way as explained above for a damp wall, causes compression and tension in the surface material. Thermal expansion by heating counteracts hygric movements, but temperature change of the surface by heating of for instance a church room is normally only about 10 °C, which is further reduced due to heat of evaporation. By a thermal expansion coefficient of $10 \cdot 10^{-6}$ K^{-1} thermal expansion is of the same order of magnitude as hygric movement, and no decay of the surface in brick and sandstone is expected.

Whereas heating does not seem to cause decay of the surface for brick and sandstone, changes of relative humidity around the deliquescence point without temperature changes is expected to cause decay of the surface for a hygroscopic material, because the difference in hygroscopic strain between the surface with high salt content and the material behind with a lower salt content is particularly large in this range, as seen from figure 6.21. This is in agreement with observations of dust fall in Alslev church (figure 5.13), which is at its maximum when the weekly average relative humidity is around 75 %. Modern brick is only slightly hygroscopic, and therefore has hygroscopic strain as calculated in figure 6.20, but Larsen (1987) observed medieval brick to be hygroscopic (figure 6.15), corresponding to sandstone as given by equation (6.3), and therefore hygroscopic strain is as calculated in figure 6.21.

As stated in section 6.6, from sorption isotherms given in figure 6.15 it is concluded that calculated strain for brick corresponds to strain for undamaged, medieval brick, and calculated strain for sandstone corresponds to strain for damaged medieval brick. From the discussion above it is concluded that the difference in decay of the two medieval bricks is due to difference in sorption isotherms or hygroscopicity. The brick is hygroscopic because it is fine porous due to burning at low temperature, and therefore the difference in rate of decay is related to pore size distribution. This difference is not seen on SEM-backscatter images, but it is detected in MIP and from the sorption isotherm.

Hygroscopic bricks take up more moisture, dry slower and have larger suction potentials, as stated in section 3.2 and 5.3, and therefore salts are transported into hygroscopic bricks from slightly hygroscopic bricks. Due to burning at low temperature hygroscopic bricks are weaker, and as hygroscopic strain is larger and is different for saline and salt free material in a narrow range around the deliquescence point, a hygroscopic brick decay, and a slightly hygroscopic brick does not.

Efflorescence on the surface was observed to increase evaporation from the surface during capillary suction in laboratory experiments described in section 5.3. This was concluded from the increase in salt content during capillary suction after saturation. Efflorescence thus results in an increased capillary suction, which again, in the case of rising groundwater in a wall, further increases salt content in the wall. Concluding the other way round, efflorescence increases the rate of hygroscopic water uptake due to the increased surface area, which might increase hygroscopic strain and with that decay of the surface.

The effect of several salts in a material is very complex, because new salts may be formed depending on relative humidity, temperature and salt contents. In brick it was observed that sodium sulphate mixed with sodium chloride or magnesium sulphate caused a large increase in strain (figure (6.6),(6.9) and (6.12)). Sodium chloride was observed to prevent shrinkage by drying in brick with magnesium or sodium sulphate (figure 6.5). Theese effects might be caused by change of relative humidity over salt solutions and change in deliquescence points due to interactions of the salts. Detailed thermodynamic measurements on theese multi-salt systems has to be carried out to establish a certain basis for further conclusions.

Stone conservation

The most efficient way to do stone conservation is to extract the salts.

Calcualtions in section 5.7 and observations from Odden church described in section 5.5 indicates that the most efficient way to extract salts are by capillary suction of distilled water. Before extraction it has to be established where the saline water will be transported, and therefore has to be collected. In a church vault with capillary suction from one side the salt might be collected in a sacrificial layer on the other side. The surface of bulk walls might be cleaned by running water which, as indicated by accelerated weathering experiments in section 5.6, seems to be quite efficient. But in doing this one should be aware that salts are transported into the wall or into other parts of the construction, and therefore might return at the surface or cause problems in other parts of the construction some time after the cleaning has stopped.

In many cases, the use of large amounts of water is not possible or acceptable as this will cause damage in other parts of the construction or the furniture. Another way to extract salts therefore is to make use of the hygroscopicity of the salts by controlling the climate at the surfaces of the material. Calculations and observations in this work indicates that for constructions like thin vaults it might be possible to extract salts with a high relative humidity on one side of the construction, and a low relative humidity on the other side, using a sacrificial layer on the side with low relative humidity. This demands a carefull controll of the climate close to the vault, and the climate must be adjusted from the deliquescence point of the present salts and the hygroscopicity of the material.

Electro-chemical extraction of salts from brick was observed to be very efficient in laboratory experiments, as described in section 5.5, and it might be used to extract salts in bulk walls, as described by Friese (1984), but laboratory experiments indicated that complex reaction products might be formed, which would cause other problems. The electro-chemical extraction has to be tested on a large scale and under close observation, before it seems safe.

8. CONCLUSIONS

A new theory to estimate the effect of changing climate on saline structures is proposed and experimentally verified. The following conclusions can be drawn:

- The deliquescence point in a hygroscopic material with low salt content is below saturation humidity over a free salt solution, and moisture content is higher than in a salt free material, even below the deliquescence point. Salts are observed to decrease capillary suction and evaporation in a porous material.

- A model to calculate moisture and salt transport in porous materials is proposed. The model agrees with observations from capillary suction experiments and large-scale extraction of chlorides in a church vault.

- A model to calculate capillary shrinkage and swelling of saline, hygroscopic materials is proposed. The model gives a reasonable estimate for strain in the hygroscopic range, but seems to underestimate strain in the over hygroscopic range. The course of strain rather than the overall magnitude of strain is changed by salts.

- Pore size distributions was determinded for brick, sandstone and lime mortar using digital image processing on images of polished sections. Although not complete comparable Mercury Intrusion Porosimetry and digital image processeing seems to complement each other, especially for materials with two distinct pore size ranges.

- Experiments and calculations indicate that decay of hygroscopic, porous materials by salts might be caused by differences in hygric movement due to increased shrinkage at relative humidities close to the deliquescence point of the salt. The increase depends on hygroscopicity of the material. This might explain why a hygroscopic brick decay contrary to a less hygroscopic brick, as observed in the vaults in Alslev church.

- Measured chloride content in a vault in Odden church shows that approximately one fourth of the original chloride content is extracted in 6 months by a 35 mm lime mortar layer on top of the vault. Calculations indicate that salts are extracted much more efficiently by capillary suction from one side of the vault and collecting salts in a mortar layer on the other side. It seems possible to extract salts by maintaining a high relative humidity on one side of the vault and a low relative humidity on the other side.

9. ACKNOWLEDGEMENTS

The author wishes to thank tekn.dr. Anders Nielsen, Building Materials Laboratory, The Technical University of Denmark and Mr Tim Padfield, The National Museum of Denmark, Departement of Conservation, for their support and guidance during this project.

Thanks to the staff at the Building Materials Laboratory for invaluable help in experimental work, especially Mrs Britta Roll in laboratory work, and to Mr Morten Hjorslev Hansen for fruitful discussions of theoretical work. I would also like to thank all the students who helped me in experimental work during their courses at the Building Materials Laboratory.

Thanks to the Danish Building Research Institute for help by accelerated weathering, especially Mr Erik Stoklund Larsen for invaluabel help and company during two study tours in Germany and the United States.

Thanks to Kalk- og Teglværkslaboratoriet in Aarhus for delivery of materials and help in weathering experiments and to the church council in Odden for financial support and collaboration during extraction experiments.

I would like to thank the following institutes at the Technical University of Denmark for assistance in experimental work; Instituttet for Mineralindustri; Instituttet for Metallære; Instituttet for Teknisk Geologi, Laboratoriet for Teknisk Hygiejne.

The study has been possible thanks to a grant from the Technical University of Denmark and financial support by the Danish Technical Research Council.

10. REFERENCES

1. Arnold, A. and Zehnder, K. (1988):"Decay of stony materials by salts on humid atmosphere". in the 6th International Congress on Deterioration and Conservation of Stone. Torun.

2. Arnold, A. (1984):"Determination of salts from monuments". Studies in Conservation, 1984, **29**, 129-138.

3. Beltrán, V., Escardino, A., Feliu, C. and Rodrigo, D. (1988): "Liquid Suction by Porous Ceramic Materials". Br. Ceram. Trans. J., **87**, 1988.

4. Berryman, J.G. and Blair, S.C. (1986):"Use of digital image analysis to estimate fluid permeability of porous materials: Application of two-point correlation functions". J.Appl.Phys. **60** (6), september 1986 pp. 1930-1938.

5. Bowler, G.K. and Fisher, K. (1989):"Soluble Salt Analysis and Indexation of Sulphation Risk". Masonry International vol. 3, No. 2, 1989.

6. Bowley, M.J. (1975):"Desalination of stone: a case study". CP 46/75 Building Research Establishment, Garston Watford.

7. Butterworth, B. (1964):"Laboratory Tests and the Durability of Bricks". Transaction of the British Ceramic Society, Vol. 63, pp 615-703, 1964.

8. Chan, L.S. (1987):"Applications of stereological and image analytical methods for concrete testing", in Pore Structure and Construction Materials Properties, Proceedings of the first International Congress held by RILEM, edited by J.C. Maso, Versailles, France, 1987. Chapman and Hall.

9. CRC (1984):"Handbook of Chemistry and physics", 64TH edition.

10. Devitofrancesco, G., Conte, C. and Petronio, B.M. (1987):"Deterioration of Structure Surfaces Caused by Particulate Matter". Durability of Building Materials, 4 (1987) pp. 301-308.

11. DS 1127 (1985):"Metode til at udsætte bygningskomponenter og byggematerialer for accelereret klimapåvirkning i vertikal stilling". Dansk Standiseringsråd, 1985.

12. Fagerlund, G. (1972):"Conections between porosity and mechanical properties of materials". Report 26, Division of Building Technology, The Lund Institute of Technology, Lund, Sweden. (In swedish).

13. Fagerlund, G. (1975):"General method for calculations of equilibrium shrinkage of porous and brittle materials". Report 18:75, Swedish Research Institute for Cement and Concrete, Stockholm, 1975.

14. Felix, C. (1983):"Sandstone linear swelling due to isothermal water sorption", in Werkstoffwissenschaften und Bausaniering, edited by F.H.Wittmann, Technische Akademie Esslingen pp. 305-310.

15. Friese, P. (1984): "Elektrochemische Entsalzung von Mauerwerk. Teil I: Notwendigkeit und theoretische Grundlagen". Bauphysik 6/1984, pp. 94-97.

16. Friese, P. and Birkenhofer, H. (1985): "Elektrochemische Entsalzung von Mauerwerk. Teil II: Praktische Ausführing, Entsalzung und Trocknung". Bayphysik 4/1985, pp. 105-109.

17. Garrecht, H., Hilsdorf, H.K. and Kropp, J. (1991): "Hygroscopic salts - influence on the moisture behaviour of structural elements" in Durability of Building Materials and Components. Conference, Nov., 7-9 1990. Chapman and Hall, London.

18. Gregg, S.J. and Sing, K.S.W. (1967):"Adsorption, Surface Area and Porosity", Academic Press, London & New York, 1967.

19. Gundersen, H.J.G. (1988): "The nucleator", Journal of Microscopy, Vol. 151, Part 1, July 1988, pp. 3-21.

20. Hansen, K.K (1986):"Sorption isotherms - A Catalogue". Technical Report 162/86, Building Materials Laboratory, The Technical University of Denmark.

21. Hansen, T.C (1967):"Drying shrinkage due to capillary action". Technical Report 1/1967, Dept. Civ. Eng., The Technical University of Denmark.

22. Hansen, W. (1987):"Drying Shrinkage Mechamisms in Portland Cement Paste". J. Am. Ceram. Soc. **70** [5] (1987), pp. 323-28.

23. Holten, L.M. and Stein, H.N. (1988):"Influence of surfactants on contact angles of ceramic brick-aqueous solution-air and sand lime brick-aqueous solution-air". Am. Ceram. Soc. Bull., **67** [8] 1399-1402.

24. Kiessl, K.:"Bauphysikalische Einflüsse bei der Krustenbildung am Gestein alter Bauwerke", Bauphysik 11(1989), H.1 pp. 44-49.

25. Knöfel, D.K., Hoffmann, D. and Snethlage, R. (1987): "Physico-chemical weathering reactions as a formulary for time-lapsing ageing tests". TC 58-VPM RILEM COMMITTEE, Materials and Structures, vol. 20 nr. 116.

26. Konow, T. (1989):"Saltvittring i tegel - saltvittringsmekanismer [Deterioration in bricks due to salts - mechanisms of salt deterioration]". Technical Research Centre of Finland, Research Notes 1003. Espoo 1989. (In swedish).

27. Larsen, E.S. (1988):"Mursalte". Technical report 181/88, Building Materials Laboratory, The Technical University of Denmark. (In danish).

28. Larsen, E.S. and Nielsen, C.B. (1990):"Decay of bricks due to salt", Materials and Structures, 1990, **23**, 16-25

29. Lewin, S.Z. (1981):"The mechanism of masonry decay through crystallization" in Conservation of Historic Stones, Buildings and Monuments. Conference , Feb., 2-4 1981. National Academy of Sciences, Washington.

30. Litvan, G.G. (1973):"Phase Transitions of Adsorbates - V. Aqueous Sodium Chloride Solutions Adsorbed of Porous Silica Glass". Journal of Colloid Interface Science, Vol. 45, No. 1, October 1973, pp. 154-168.

31. Livingston, R.A. (1988):"Geochemical methods applied to the reproduction of handmolded brick". Proceedings, 8th International Brick/Block Masonry Conference , J.de Courcy ed., Elsevier, New York, 1988.

32. Niblack, W.:"Digital Image Processing". Prentice/Hall International 2nd edition 1986.

33. Nielsen, A. and Trudsø, E. (1978):"Tegl, Gasbeton og andre silikatbygningsmaterialer". Polyteknisk Forlag, København. (In danish).

34. Nielsen, C.B. (1988):"Thermisk deformation og svind af saltholdige teglsten". Techical Report 182/88, Building Materials Laboratory, The Technical University of Denmark. (In Danish).

35. Nielsen, C.B. (1991):"Udtrækning af salte - Odden kirke [Extraction of salts - Odden Church]". Technical report 225/91, Building Materials Laboratory, The Technical University of Denmark. (In Danish).

36. Padfield, T. and Erhardt, D. (1987):"The spontaneous transfer to glass of an image of Joan of Arc", in ICOM Committee for Conservation, Procedings of the Sydney Conference 1987, vol III, Working Group 17, p. 909-913.

37. Powers, T.C. (1965):"Mechanisms of shrinkage and reversible creep of hardened cement paste" in The Structure of Concrete and its behaviour under load, edited by A.E. Brooks and K. Newman. Proceedings of an International Conference. London, September 1965.

38. Pühringer, J. (1983):"Saltvittring, Saltvandring och saltnedbrytning - en hypotes". Rapport R22:1983, Statens råd för byggnadsforskning, Stockholm. (In swedish)

39. Quiblier, J. (1984):"A new Three-dimensional Modeling Technique for Studying Porous Media". Journal of Colloid and Interface Science, Vol. 98, No. 1, march 1984 pp. 84-102.

40. Robinson and Stokes (1955):"Electrolyte Solutions". Butterworth, London.

41. Scrivener, K.L. and Pratt, P.L. (1987):"The characterization and quantification of cement and concrete microstructures" in Pore Structure and Construction Materials Properties, Proceedings of the first International Congress held by RILEM, edited by J.C. Maso, Versailles, France 7-11, 1987. Chapman and Hall.

42. Searls, C.L. and Thomasen S.E. (1990):"Deterioration mechanisms in sandstone", in Durability of Building Materials and Components, edited by J.M. Baker et al pp. 87-96.

43. Serra, J. (1982):"Mathematical Morphology and Image Analysis", Academic Press.

44. Shayan, A. and Ritchie, D.J. (1985):"Influence of sodium and potassium cations on the dimensional stability of rock prisms". Durability of Building Materials, 2 365-378.

45. Shuh, H., Klemm, D. and Snethlage, R. (1986):"Festigheits- und Verformungseigenschaften ausgewählter Sandsteine", in Werkstoffwissenschaften und Bausaniering, edited by F.H. Wittmann pp. 403-408.

46. Suenson, E. (1942):"Byggematerialer III, Natursten". 3. udgave. Jul. Gjellerups Forlag, København 1942.

47. Vale, J. and Martin, A. "Deterioration of sandstone in simuylated atmospheres". Durability of Building Materials **3** (1986), pp. 183-196 and 197-212.

48. Weber, H. (1983):"Steinkonservierung - Der Leitfaden zur Konservierung und Restaurierung von Natursteinen". 2. Auflage, Kontakt & Studium, Band 59, Expert Verlag, Grafenau.

49. Wendler, E.,Klemm, D.D. and Snethlage, R. (1990):"Consolidation and hydrophobic treatment of natural stone", in Durability of Building Materials and Components, edited by J.M. Baker et al pp. 203-224.

50. Winkler, E.M (1973):"Stone: Properties, Durability in Man's Environment". Applied Mineralogy (4) 1973, Springer-Verlag Wien New York.

51. Winslow, D.N. and Shi, D. (1988):"Automatic image segmentation using fuzzy probability". Civ. Engng. Syst. 1988, vol. 5, June pp. 104-108.

52. Wittmann, F.H. and Boekwijt W.O.:" Grundlage und Anwendbarkeit der Elektroosmose zum Trocknen durchfeuchteten Mauerwerks". Bayphysik 4/1982 pp. 123-127.